DYNAMICS AND ANALYSIS OF MODELS FOR CHRONIC HEPATITIS B VIRUS INFECTION

by

Kalyan Manna

DEPARTMENT OF MATHEMATICS

INDIAN INSTITUTE OF TECHNOLOGY GUWAHATI

GUWAHATI-781039, INDIA

June, 2016

DYNAMICS AND ANALYSIS OF MODELS FOR CHRONIC HEPATITIS B VIRUS INFECTION

A Thesis submitted

in partial fulfillment of the requirements

for the degree of

DOCTOR OF PHILOSOPHY

by

Kalyan Manna

(Roll Number: 10612309)

to the

DEPARTMENT OF MATHEMATICS

INDIAN INSTITUTE OF TECHNOLOGY GUWAHATI

June, 2016

Declaration

I hereby declare that the work contained in this thesis entitled **"Dynamics and analysis of models for chronic hepatitis B virus infection"** was done by me, under the supervision of **Dr. Siddhartha Pratim Chakrabarty**, Associate Professor, Department of Mathematics, Indian Institute of Technology Guwahati for the award of the degree of Doctor of Philosophy and this work has not been submitted elsewhere for a degree.

June, 2016

Kalyan Manna
Roll No. 10612309
Department of Mathematics
Indian Institute of Technology Guwahati

Certificate

It is certified that the work contained in this thesis entitled **"Dynamics and analysis of models for chronic hepatitis B virus infection"** by **Kalyan Manna,** a student in Department of Mathematics, Indian Institute of Technology Guwahati, for the award of the degree of Doctor of Philosophy has been carried out under my supervision and this work has not been submitted elsewhere for a degree.

June, 2016

Dr. Siddhartha Pratim Chakrabarty
Associate Professor
Department of Mathematics
Indian Institute of Technology Guwahati

To

My Mother

Acknowledgements

Every great experience requires the help and support of many people. I would like to take the opportunity to thank all those who have extended their helping hand whenever I needed. In the first place, I would like to express my deepest gratitude to my Ph.D Supervisor, Dr. Siddhartha P. Chakrabarty, for introducing me to Mathematical Biology. This thesis would not have been possible without his extraordinary support, patient guidance, enthusiastic encouragement and useful critiques during the progress of this research work.

I would like to express my deepest appreciation to my doctoral committee chair, Professor Rajen K. Sinha, for his valuable suggestions and support during my research work. I want to convey my sincere thanks to my other committee members Professor Jiten C. Kalita and Dr. Arabin K. Dey for reviewing my research work and giving valuable suggestions to improve my research work. I sincerely acknowledge Indian Institute of Technology Guwahati for providing me with the various necessary facilities and financial assistance to carry out my research.

I offer my heartiest gratitude to all the faculties of the Department of Mathematics, IIT Guwahati for rendering me a very good and friendly environment to work. I thank all the staff members of the Department of Mathematics, IIT Guwahati for their assistance in official and technical matters.

I am also thankful to all my research scholar friends of the Department of Mathematics, IIT Guwahati for their love and company during my stay in the IIT Guwahati campus. Especially, I want to thank those friends of mine who made my stay pleasant and lively at campus: Dr. Santu Das, Dr. Kaushik Mondal, Arnab Ghosh, Himadri Nayak, Dr. Barun Gorain, Debopam Chakraborty, Anirban Majumdar, Abhishek Das, Hiranmoy Pal, Purnendu Mandal and Niladri Sett.

I do not have enough words to adequately thank my loving parents and my sweet sister for everything they have done to enable me to fulfill my dreams. Thanks for being proud of me even without knowing very well about what I have been working on during these years. A very special thank to my dear wife Aparna. I wouldn't have made it without her selfless love, emotional support and tolerance for the long periods of being neglected during preparation of this thesis.

IIT Guwahati — Kalyan Manna

Abstract

This thesis investigates several models for hepatitis B virus (HBV) infection including the incorporation of the dynamics of intracellular HBV DNA-containing capsids. Firstly, we analyze a model for infected hepatocytes, capsids and virions along with the homeostatic mechanism of the liver and incorporating a discrete time delay in the production of mature capsids. We then present and analyze a modified model where the dynamics of both uninfected hepatocytes and capsids (along with infected hepatocytes and virions) are included. This is followed by the incorporation of one and two discrete delays in this modified model and its dynamical analysis. A pharmacokinetic model with the combination therapy of pegylated interferon and lamivudine is proposed and a critical drug efficacy in terms of model parameters is derived. A control problem is also formulated and solved numerically to obtain the optimal therapeutic regimen, accounting for both the biomedical goals and cost constraints. Finally, a diffusion driven HBV infection model is presented taking into account the spatial mobility of both capsids and virions. The analysis is carried out for global stability as well as on a discretized version of the model. A non-standard finite difference scheme for this model is introduced and the dynamic consistency of this scheme is analyzed.

Contents

List of Figures

Chapter 1

Introduction and Thesis Outline

1.1 Introduction

Hepatitis B virus (HBV) infection has emerged as a critical concern for public health at a global level. HBV infection is a hepatological problem affecting the hepatocytes (or the liver cells) [1]. In most cases, the infection is initially acute in nature with the short term clinical implications being minimal. The acute phase lasts for several weeks during which the viral load of HBV could reach up to 10^{10} HBV DNA copies/ml [2, 3] followed by a clearance rate of $85-95\%$ in case of adult patients. The persistence of infection in the form of chronic flares [4] of hepatitis is observed in $1-10\%$ of adult infected cases, which goes up to 95% in case of newly born infants, making them a very high-risk group. The long term implications in case of chronically infected patients are more severe and may lead to a range of new complications like chronic active hepatitis as well as liver cirrhosis and hepatocellular carcinoma (HCC) [4]. The prevalence of HBV is seen to be much more alarming in regions of Asia and Africa as compared to the United States and western Europe [4].

The process of replication of HBV is fairly complex and has been elucidated in detail by Rebeiro et al. [4] and Lewin et al. [5]. A prototype of the hepadnaviridae family of viruses, the HBV is an enveloped virus which contains a 3.2 kilobase (kb) partially double stranded (ds) open circular DNA genome, that is enclosed in a nucleocapsid. The process of infectivity of the hepatocytes results in the DNA genome being transformed to covalently closed circular DNA (cccDNA). The cccDNA, with potentially multiple copies is located in the nucleus of the infected cells and acts as a template for the production of mRNA and the consequent HBV transcription. The pre-genomic mRNA then undergoes reverse transcription into the DNA by the virally encoded polymerase which leads to the formation of HBV using the reverse transcriptase function. The persistence of virus for chronic HBV patients is contingent on the availability of the cccDNA copies, which is a major cause of post therapeutic relapse.

Several approved therapies such as interferon alpha (IFN) and nucleoside analogs (NAs) which act as inhibitors of reverse transcription, exist for treatment of chronic HBV cases [6]. Reverse tran-

scription inhibitors, particularly lamivudine (LMV) and adefovir dipivoxil, achieve partial blocking of conversion of capsids (which contain HBV RNA) to DNA-containing HBV capsids [7]. Interferon (IFN) alpha-2b and pegylated interferon (PEG IFN) alpha-2a are approved therapies for chronic HBV infection. IFN has been observed to have limited therapeutic effect in chronic HBV patients and is often accompanied by side effects beyond tolerable limits [8, 9]. On the other hand, treatment using PEG IFN has been proven to have greater efficacy [8]. IFNs typically have a direct role in inhibiting the synthesis of viral DNA as well as boosting of immune response against infected hepatocytes. As already mentioned, the efficacy of IFN has been improved by the usage of PEG IFN instead of IFN. This changeover of therapeutic protocol has reduced the dosage of three times per week to once a week [8] thereby reducing the side effects. LMV inhibits the elongation of viral minus strand DNA as well as polymerase activity for second-strand DNA synthesis [7, 10]. Adefovir, in addition to inhibiting the elongation of viral minus strand DNA, also blocks the priming of reverse transcription [7, 11]. Studies have shown that a combination treatment of LMV with IFN or PEG IFN [9] leads to greater therapeutic response as compared to monotherapy (of either PEG IFN or LMV), due to the additive effect of combination therapy.

In many cases, the decay observed in HBV patients under therapy is biphasic [6] in nature with a more rapid decline over the first few weeks followed by a slower decline. In other cases, this decay is triphasic or stepwise. In many other cases, however, the behavior of HBV load is unpredictable [5] or even prolonged periods with more or less static viral load [6]. There are instances of failure of primary treatment in the first six months or failure in secondary treatment preceded by a response in the primary treatment [6].

Analysis of viral dynamics using mathematical models have helped gain insights into the understanding of viral infections such as human immunodeficiency virus (HIV), hepatitis C virus (HCV) and HBV [1]. Nowak et al. [12] presented one of the earliest quantitative analysis for HBV by way of a simple ODE driven model comprising of uninfected and infected hepatocytes and HBV. The classical model of viral infection was amended by Min et al. [13] by replacing the mass action term of the uninfected hepatocytes and HBV, by a standard incidence function. They argued that the inclusion of the mass action term in case of HBV infection is not appropriate since it indicates that an individual with a smaller liver is less prone to infection than somebody with a larger liver. Wang et al. [14] discussed the global properties of an improved HBV model. Gourley et al. [15] also considered a standard incidence function and included the time delay observed during the process of production of the virions by including delay differential equation. Hews et al. [16] presented a modified model by replacing the constant source term for uninfected hepatocytes by a logistic growth term accompanied by a standard incidence function. A logistic proliferation (for uninfected hepatocytes) driven model, in addition to the stability of uninfected and infected steady states could also lead to Hopf bifurcation [17]. The dynamics under delay in the mass action

term along with a logistic proliferation of uninfected hepatocytes was presented by Eikenberry et al. [18]. While most models for chronic HBV lead to convergence towards either the uninfected or the infected steady state, the introduction of delay in model considered in [18] captures the possibility of sustained oscillatory dynamics. The dynamics of acute infection in chimpanzees is captured through a standard incidence function driven model in [19]. Yu et al. [20] considered a basic viral infection model used for the study of viral diseases such as HBV, HCV and HIV and constructed a nonlinear infection rate (instead of a mass-action term) for this model. The influence of chronic HBV on superimposed hepatitis E virus (HEV) infection was examined by Cheng et al. [21]. They considered two groups of patients, one with co-infection of HBV and HEV and the other with only HEV, and performed a comparative statistical analysis for the two groups. Zoulim [22] discussed the role of occult HBV infection on the clinical evolution of chronic hepatitis C patients. Nowak and Bangham [23] extended the basic virus infection model by incorporating the cytotoxic T lymphocytes (CTLs) immune responses for HIV, HBV, human T cell leukemia virus-1 (HTLV-1) infections. Some other HBV infection models with CTL immune responses and their analysis can be found in [24, 25].

Qualitative representation of HBV pharmacokinetics are somewhat limited. Lewin et al. [26] used a basic ordinary differential equation (ODE) driven model involving the uninfected and infected hepatocytes as well as HBV to experimental data to analyze the decline in HBV load for twelve weeks after initiation of treatment of either LMV monotherapy or combination therapy of LMV and fanciclovir (FCV). Ribeiro et al. [4] in their review article, among other things, included treatment involving NAs as a part of their mathematical model for HBV dynamics. A similar model involving combination therapy was used to analyze experimental data in [5]. An extended therapeutic model was presented by Dahari et al. [6] to model the complex decay in HBV profile while administering antiviral therapy. The model was drawn from their previous work incorporating the proliferation of hepatocytes in hepatitis C virus (HCV) infection [27, 28]. They introduced the notion of critical efficacy and hepatocyte proliferation in a HBV pharmacokinetic model to capture complex decay profiles (such as flat, triphasic and stepwise) of HBV, in addition to the usual biphasic decline patterns.

Optimal control theory as a tool has been widely used in biomedical problems [29]. One of the key applications of control theory is in the determination of the optimal therapeutic protocols subject to various biomedical constraints and considerations. These applications are wide ranging and include cancer, epidemics, diabetes, leukemia, virological diseases like HIV, HCV, HBV, to name a few.

Optimal control theory has had a long standing application in cancer therapy. This topic had been extensively discussed by Swan in his review article [30], where he considered three kinds of models, namely, growth kinetics, cell cycle and miscellaneous models. He used deterministic control

theory with applications in the design of more effective chemotherapy strategies. Murray examined the optimal control problems for cancer chemotherapy with toxicity limits (by imposing bounds on the drug usage) [31] and on models with general growth and loss functions [32]. de Pillis et al. [33] analyzed a model for chemotherapy for tumor immune interaction with the goal of minimizing the tumor burden and side effects using both quadratic and linear controls. Fister and Panetta [34] studied three different cell-kill models to determine the optimal strategy for chemotherapy characterized by the goal of minimizing the cancer cells as well as the cost of therapy.

Optimal control theory is also applied for various epidemic models, for example, SEIR model, seeking to minimize the cost of administering a vaccination program aimed at restricting the number of infected individuals in the affected population [29]. In order to achieve the fall of glucose levels below a desired set threshold, in the case of diabetic patients, one can use the injected insulin levels as the control variable and hence determine the optimal levels of insulin to be administered, as was done by Chavez et al. [35] for type 1 diabetic patients. Optimal treatment regimens that seek to minimize the cancer cell count and side effects of drugs were studied by Nanda et al. [36] for targeted as well as broad cytotoxic therapy for individuals with chronic myelogenous leukemia (CML).

Optimal control theory has been studied with great interest in case of virus borne diseases such as HIV and HCV. Krischner et al. [37] using an objective functional based on maximizing the T-cell count and minimizing the systemic cost of therapy, determined the optimal therapy (like protease inhibitor) for HIV infected patients. Joshi [38] considered a similar problem for HIV patients but with combination therapy of immune boosting and viral suppressing drugs. Adams et al. [39] studied the modeling, data analysis and optimal therapy for HIV patients. Stengel [40] considered a drug resistant strain of HIV which resulted in rapid viral replication and determined that a continued optimal treatment is the key to sustained virological response in this case.

In case of HCV infection, Chakrabarty and Joshi [41] considered a pharmacokinetic model to determine the optimal combination therapy of interferon and ribavirin. Chakrabarty [42] considered a similar model, with a known clinical functional form for IFN to determine the optimal ribavirin efficacy. Pachpute and Chakrabarty [43] determined the optimal therapy (both monotherapy with IFN and combination therapy of IFN and ribavirin). They generated samples for patient scenarios and applied this optimal therapy to determine the short term responses in case of these samples. In another recent paper, Martin et al. [44] explored an optimal program aimed at patients who contract HCV by being injecting drug users (IDUs), subject to policy objectives and budget constraints.

Most models on viral dynamics do not take into account the spatial mobility of both cells and viruses [45] despite such motions being modeled in biological processes [46]. These models are based on the assumption that cell and virus populations are well mixed [45, 47]. However, the occurrence of many such infections in solid tissues results in the relaxation of this assumption

through the inclusion of the spatial structure. Two models for virus-immune dynamics through locally occurring dispersal of viruses and immune effector cells were analyzed through the inclusion of a spatial structure [47]. Wang and Wang [45] considered a basic HBV model where the HBV was assumed to move freely through the liver but there is no mobility on the part of the uninfected and infected hepatocytes. Accordingly, a Fickian diffusion process was assumed for the viral motion, where the population flux of the virus is proportional to the concentration gradient [45, 48]. In a subsequent work, this model was relaxed through the inclusion of delay in addition to diffusion and the effects of both were encapsulated through in-silico simulations [49]. A similar diffusion-delay model with a saturation response term for infectivity was analyzed in [50]. Shaoli et al. [51] proposed a diffusive HBV model taking into account CTL immune response. Hattaf and Yousfi [52] studied the global stability properties of several diffusion equations arising in biology, through construction of Lyapunov functions. A description of the method was followed by illustrations through various applications of viral dynamics models and SIR epidemic models. In a recent paper, Hattaf and Yousfi [53] considered a fairly general HBV model, consisting of spatial diffusion, a general incidence rate and two time delays. Qin et al. [54] in their recent work considered the HBV model due to Wang and Wang [45] and constructed an non-standard finite difference (NSFD) scheme for this model. They established the (grid independent) positivity of the solution using M-matrices as well as the (grid independent) global stability of the discrete system in terms of the basic reproduction number, using discrete Lyapunov functions. In several recent works, the application of NSFD scheme in biological models have been demonstrated in case of predator-prey [55], LotkaVolterra competition [56], epidemic [57, 58] and dengue [59] models.

1.2 Thesis Outline

In this thesis, we present and analyze the dynamics of the mathematical models for HBV infection in vivo. The organization of the thesis is as follows.

In Chapter 2, we examine a mathematical model for HBV infection, which incorporates the dynamics of infected hepatocytes, the number of intracellular HBV DNA-containing capsids and the virions. We analyze the stability of the uninfected and infected steady states and obtain the basic reproduction number R_0 in terms of the model parameters. If $R_0 \leq 1$ then the uninfected steady state is stable and the patient will be cleared of infection. On the other hand, if $R_0 > 1$ then the infected steady state is stable and the infection persists. The model is then modified to incorporate a delay in the production of intracellular HBV DNA-containing capsids from infected hepatocytes. It is shown that this delay does not affect the local stability of the system. Finally, the results obtained are numerically illustrated for various scenarios.

In Chapter 3, we analyze the dynamics of chronic HBV infection taking into account both

uninfected and infected hepatocytes along with the intracellular HBV DNA-containing capsids and the virions. While previous HBV models have included either the uninfected hepatocytes or the intracellular HBV DNA-containing capsids, our model accounts for both these two populations. We prove the conditions for local and global stability of both the uninfected and infected steady states in terms of the basic reproduction number. The results for the model are finally numerically illustrated.

In Chapter 4, we incorporate time lags in the model to encompass the intracellular delay in the production of the productively infected hepatocytes and in the production of the matured capsids to determine whether these delays have any effect on the overall dynamics of the system. Two models, one with one-delay and the other with two-delays are analyzed for global properties in terms of the basic reproduction number. By constructing the appropriate Lyapunov functions, it is shown that the uninfected (infected) steady state is globally asymptotically stable when the basic reproduction number is less than or equal to (more than) one for both the one-delay and two-delay models. Finally, illustrative numerical simulations are presented.

In Chapter 5, a model for combination therapy of pegylated interferon and lamivudine is presented. A critical drug efficacy in terms of the parameters of the model comprising of coupled ordinary differential equations is obtained. The dynamics of viral load is greatly impacted by the relation of the efficacies of the individual drugs vis-a-vis the critical efficacy. A control problem is formulated and solved numerically to obtain the optimal therapeutic regimen keeping in mind both biomedical goals and cost constraints.

In Chapter 6, a diffusion driven model for HBV infection, taking into account the spatial mobility of both the HBV and the HBV DNA-containing capsids is presented. The global stability for the continuous model is discussed in terms of the basic reproduction number. The analysis is further carried out on a discretized version of the model. Since the standard finite difference (SFD) approximation could potentially lead to numerical instability, it has to be restricted or eliminated through dynamic consistency. The latter is accomplished by using a non-standard finite difference (NSFD) scheme and the global stability properties of the discretized model were studied. The results are numerically illustrated for the dynamics and stability of the various populations in addition to demonstrating the advantages of the usage of NSFD method over the SFD scheme.

Finally, Chapter 7 concludes and outlines the future directions of the thesis. All the numerical simulations incorporated in this thesis were carried out using MatLab™ .

Chapter 2

The HBV Infection Model with Capsids

In this chapter, we analyze a HBV infection model proposed by Murray et al. [7]. We show the existence of the steady states and obtain the conditions for the local and global stability in terms of the basic reproduction number. Further, we extend the model by incorporating one discrete delay and then analyzing for local stability. Finally, numerical simulations are presented to support the theoretical results.

2.1 Mathematical Model

We consider a mathematical model for chronic HBV infection proposed by Murray et al. [7]. The model takes into account three types of population: $I(t)$, the number of infected hepatocytes, $D(t)$, the number of intracellular HBV DNA-containing capsids and $V(t)$, the number of virions in plasma all at time t. The model is described by three coupled ordinary differential equations (ODEs) as

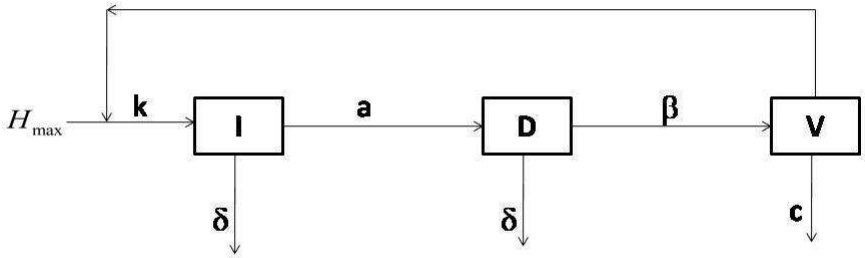

Figure 2.1: Schematic representation of the model (2.1.1).

follows:

$$\begin{aligned} \frac{dI(t)}{dt} &= kH(t)V(t) - \delta I(t), \\ \frac{dD(t)}{dt} &= aI(t) - \beta D(t) - \delta D(t), \\ \frac{dV(t)}{dt} &= \beta D(t) - cV(t). \end{aligned} \tag{2.1.1}$$

Here $H(t)$ represents the number of uninfected hepatocytes. The uninfected hepatocytes are assumed to be infected by the HBV at a rate k, thereby producing infected hepatocytes, which in turn have a clearance rate of δ. Intracellular HBV DNA-containing capsids are produced at a rate of a per infected hepatocyte and undergo clearance at rate δ and β is the rate at which the capsids are exported to the blood producing the virions. The rate of clearance of virions in the plasma is taken to be c. The homeostatic mechanism of the liver is taken into account by assuming that the sum of the uninfected and infected hepatocytes maintain a constant level of $H_{\max}$. As such, the number of uninfected hepatocytes can be determined by subtracting the number of infected hepatocytes I from the total of $H_{\max}$ [7]. All the parameters of the model are positive. A schematic representation of the model (2.1.1) is given in Figure 2.1.

It can be shown that the solutions to the system (2.1.1) subject to positive initial condition remains positive. We now prove the boundedness of the solution trajectories with positive initial conditions (on the lines of [60, 61]). For this purpose let us define the variable, $T(t) = D(t) + V(t)$. Then, adding the last two equations of (2.1.1) we get

$$\frac{dT}{dt} = aI - \delta D - cV.$$

Using $I = H_{\max} - H$ and defining $\gamma_1 = aH_{\max}$ and $\gamma_2 = \min\{\delta, c\}$, we obtain

$$\frac{dT}{dt} \leq \gamma_1 - \gamma_2 T.$$

It can be easily shown that

$$T(t) \leq T(0)\exp(-\gamma_2 t) + \frac{\gamma_1}{\gamma_2}\left(1 - \exp(-\gamma_2 t)\right).$$

Hence,

$$\limsup_{t\to\infty} T(t) \leq \frac{\gamma_1}{\gamma_2}.$$

This gives $\limsup_{t\to\infty} D(t) \leq \frac{\gamma_1}{\gamma_2}$ and $\limsup_{t\to\infty} V(t) \leq \frac{\gamma_1}{\gamma_2}$. Therefore, $D(t) \leq \frac{\gamma_1}{\gamma_2}$ and $V(t) \leq \frac{\gamma_1}{\gamma_2}$. Now, from the first equation of (2.1.1), we get

$$\frac{dI}{dt} = kHV - \delta I \leq kH_{\max}\left(\frac{\gamma_1}{\gamma_2}\right) - \delta I.$$

Using the result derived for $T(t)$, we see that

$$\limsup_{t\to\infty} I(t) \leq \frac{kH_{\max}\gamma_1}{\delta\gamma_2}.$$

Thus the populations I, D and V are all bounded. Hence we have the closed and bounded, positively invariant set

$$\mathcal{D} = \left\{(I, D, V) \in \mathbb{R}^3_+ : 0 \leq D, V \leq \frac{\gamma_1}{\gamma_2}, 0 \leq I \leq \frac{kH_{\max}\gamma_1}{\delta\gamma_2}\right\}$$

with respect to (2.1.1), where $\mathbb{R}^3_+ = \{(I, D, V) : I \geq 0, D \geq 0, V \geq 0\}$.

The model (2.1.1) under consideration admits two steady states:

1. The uninfected steady state is given by $E_u = (0, 0, 0)$. This means that for this steady state we have $H = H_{\max}$.

2. The infected steady state given by $E_i = (I^*, D^*, V^*)$, where the following relations hold:

$$V^* = \left[\frac{a\beta kH_{\max}}{c(\beta+\delta)} - \delta\right]\frac{1}{k},\ D^* = \left[\frac{c}{\beta}\right]V^* \text{ and } I^* = \left[\frac{\beta+\delta}{a}\right]D^*.$$

The infected steady state exists whenever the basic reproduction number,

$$R_0 = \frac{a\beta kH_{\max}}{c\delta(\beta+\delta)} > 1.$$

2.2 Stability Analysis

We now derive the results for local and global stability of steady states E_u and E_i. For the purpose of local stability analysis, the Jacobian matrix of system (2.1.1) is given by:

$$J = \begin{bmatrix} -kV-\delta & 0 & k(H_{\max}-I) \\ a & -\beta-\delta & 0 \\ 0 & \beta & -c \end{bmatrix}.$$

Note that here we have made use of $H + I = H_{\max}$ and replaced H with $H_{\max} - I$.

Theorem 2.2.1. *The uninfected steady state is locally asymptotically stable when $R_0 < 1$ and becomes unstable when $R_0 > 1$.*

Proof. The characteristic equation for the uninfected steady state is given by

$$\lambda^3 + A\lambda^2 + B\lambda + C = 0,$$

where

$$A = (\beta + 2\delta + c),\ B = [\delta(\beta+\delta+c) + (\beta+\delta)c] \text{ and } C = [\delta(\beta+\delta)c - kH_{\max}a\beta].$$

The Routh-Hurwitz criterion for stability requires that $A > 0$,$C > 0$ and $AB - C > 0$. It is easy to see that $A > 0$. Now, $AB - C = (\beta + 2\delta + c)\left[\delta(\beta + \delta + c) + (\beta + \delta)c\right] - \delta(\beta + \delta)c + kH_{\max}a\beta > 0$. $C = \delta(\beta + \delta)c - kH_{\max}a\beta > 0$ means

$$\frac{a\beta kH_{\max}}{c\delta(\beta + \delta)} = R_0 < 1.$$

Thus the uninfected steady state is locally asymptotically stable whenever $R_0 < 1$. Further, when $R_0 > 1$, at least one of the roots of the characteristic equation becomes positive and hence, the uninfected steady state becomes unstable. □

Theorem 2.2.2. *The infected steady state is locally asymptotically stable when* $R_0 > 1$.

Proof. The characteristic equation for the infected steady state is given by

$$\lambda^3 + A\lambda^2 + B\lambda + C = 0, \tag{2.2.1}$$

where

$A = (kV^* + \beta + 2\delta + c)$, $B = (kV^* + \delta)(\beta + \delta + c) + (\beta + \delta)c$ and $C = (kV^* + \delta)(\beta + \delta)c - k(H_{\max} - I^*)a\beta$.

Since $R_0 > 1$ for the existence of infected steady state, we can easily see that $A > 0$. Now,

$$C = \left[\frac{a\beta kH_{\max}}{(\beta + \delta)c}\right](\beta + \delta)c - k(H_{\max} - I^*)a\beta = kH_{\max}a\beta - kH_{\max}a\beta + kI^*a\beta = ka\beta I^*.$$

Therefore $C > 0$, since $I^* > 0$ for $R_0 > 1$. Now we have to prove $AB - C > 0$ *i.e,* $k(H_{\max} - I^*)a\beta > 0$. This is true since,

$$\begin{aligned} & \delta > 0 \Rightarrow kV^* + \delta > kV^* \Rightarrow \frac{kH_{\max}a\beta}{(\beta + \delta)c} > kV^* \\ \Rightarrow \quad & kH_{\max} > \frac{k(\beta + \delta)c}{a\beta}V^* \\ \Rightarrow \quad & kH_{\max} > kI^* \Rightarrow k(H_{\max} - I^*) > 0. \end{aligned}$$

Thus the infected steady state is locally asymptotically stable whenever $R_0 > 1$. □

Theorem 2.2.3. *The uninfected steady state is globally asymptotically stable when* $R_0 \leq 1$.

Proof. Define a Lyapunov function $L(t)$ for the system (2.1.1) as

$$L(t) = \frac{a\beta}{\delta(\beta + \delta)}I(t) + \frac{\beta}{\beta + \delta}D(t) + V(t). \tag{2.2.2}$$

Its derivative along a solution of system (2.1.1) is

$$\frac{dL}{dt} = \left(\frac{a\beta kH}{c\delta(\beta + \delta)} - 1\right)cV. \tag{2.2.3}$$

Since $H \leq H_{\max}$, we have $\frac{dL}{dt} \leq \left(\frac{a\beta k H_{\max}}{c\delta(\beta+\delta)} - 1\right) cV = (R_0 - 1)cV$. Hence $\frac{dL}{dt} \leq 0$ for $R_0 \leq 1$. From the Lyapunov-LaSalle invariance principle [60, 61] all paths in $\mathcal{D}$ approach the largest invariant subset (as $t \to \infty$) of the set M for which $\frac{dL}{dt} = 0$. Now, $\frac{dL}{dt} = 0$ only when $R_0 < 1$ and $V = 0$ or when $R_0 = 1$ and $I = 0$. Hence the set $M = \{E_u\} = \{(0, 0, 0)\}$. Thus all solution paths in $\mathcal{D}$ approach $E_u = (0, 0, 0)$. Hence, the uninfected steady state is globally asymptotically stable when $R_0 \leq 1$. □

Theorem 2.2.4. *The infected steady state is globally asymptotically stable when* $R_0 > 1$.

Proof. In order to prove the theorem, we first show that the system (2.1.1) is uniformly persistent [62] in the interior of $\mathcal{D}$ (int $\mathcal{D}$) [61]. Consider the Lyapunov function (2.2.2). Whenever $R_0 > 1$, its derivative, $dL/dt > 0$ along a solution of system (2.1.1), provided I is sufficiently close to 0, except for the case when $V = 0$. This means that for the case $R_0 > 1$, all trajectories emanating from a neighborhood of the uninfected steady state E_u must leave it, except the one from the origin. As such E_u cannot be ω-limit point of any orbit starting in int $\mathcal{D}$. Note that the maximal invariant set on the boundary of $\mathcal{D}$ being the origin is isolated. Hence using the results of Freedman et al. [63] and Butler et al. [64] as in [61], the uninfected steady state E_u becomes unstable and the system is uniformly persistent in int $\mathcal{D}$.

We now use a theorem by Busenberg and van den Driessche [65] to show that the system (2.1.1) has no periodic solutions, homoclinic loops, or oriented phase polygons inside the invariant region $\mathcal{D}$. We first define a Lipschitz continuous vector field $\mathbf{f}$ on int $\mathcal{D}$ as

$$\mathbf{f}(I, D, V) = \langle f_1, f_2, f_3 \rangle, \tag{2.2.4}$$

where f_1, f_2 and f_3 are the right hand side of the system (2.1.1), *i.e.,*

$$\begin{aligned} f_1(I, D, V) &= kHV - \delta I, \\ f_2(I, D, V) &= aI - \beta D - \delta D, \\ f_3(I, D, V) &= \beta D - cV. \end{aligned}$$

Let us now define a vector field $\mathbf{g}$ as

$$\mathbf{g}(I, D, V) = \langle g_1, g_2, g_3 \rangle, \tag{2.2.5}$$

which is piecewise smooth on compact subsets contained in int $\mathcal{D}$ and satisfies the conditions $\mathbf{g} \cdot \mathbf{f} = 0$ and $\langle \text{curl } \mathbf{g} \rangle \cdot \langle 1, 1, 1 \rangle < 0$ in the interior of $\mathcal{D}$. If $\mathbf{g}$ is taken to be

$$\begin{aligned} \mathbf{g}(I, D, V) &= \langle (f_3 - f_2), (f_1 - f_3), (f_2 - f_1) \rangle \\ &= \langle (2\beta D - cV - aI + \delta D), (kVH - \delta I - \beta D + cV), (aI - \beta D - \delta D - kVH + \delta I) \rangle \end{aligned}$$

then it can be easily seen that the condition $\mathbf{g} \cdot \mathbf{f} = 0$ is satisfied. Also

$$\begin{aligned} \langle \text{curl } \mathbf{g} \rangle \cdot \langle 1,1,1 \rangle &= \langle (-\beta - \delta - kH - c), (-c - a - \delta), (-2\beta - 2\delta) \rangle \cdot \langle 1,1,1 \rangle \\ &= (-\beta - \delta - kH - c) + (-c - a - \delta) + (-2\beta - 2\delta) < 0. \end{aligned}$$

Thus the system (2.1.1) has no periodic solutions, homoclinic loops, or oriented phase polygons inside the invariant region $\mathcal{D}$. Hence the infected steady state E_i exists and is globally asymptotically stable when $R_0 > 1$. □

2.3 The Delay Model

The model used is based on the assumption that the production of the intracellular HBV DNA-containing capsids from infected hepatocytes is instantaneous in nature. This production in reality, however, is not immediate. In order to incorporate a time lag in the production of the intracellular HBV DNA-containing capsids from infected hepatocytes, we introduce a time delay of τ, to obtain the following modified model:

$$\begin{aligned} \frac{dI(t)}{dt} &= kH(t)V(t) - \delta I(t), \\ \frac{dD(t)}{dt} &= aI(t-\tau) - \beta D(t) - \delta D(t), \\ \frac{dV(t)}{dt} &= \beta D(t) - cV(t), \end{aligned} \tag{2.3.1}$$

with initial conditions $I(\theta) = I_0 \geq 0$, $D(\theta) = D_0 \geq 0$, and $V(\theta) = V_0 \geq 0$; where $\theta \in [-\tau, 0]$. The steady states for the delay model (2.3.1) remain unchanged from the original model (2.1.1). As a result the steady states of the delay model will be $E_u = (0,0,0)$ and $E_i = (I^*, D^*, V^*)$ as before.

2.4 Stability Analysis with Delay

The stability analysis for the uninfected steady state E_u is straight forward and it can be shown that it is locally asymptotically stable for $R_0 < 1$ and is unstable for $R_0 > 1$ for all values of τ. We will thus restrict ourselves to the stability analysis of the infected steady state E_i. We perturb the delay system about the infected steady state, E_i [66, 67] resulting in the following linearized system

$$\frac{dY(t)}{dt} = J_1 Y(t) + J_2 Y(t-\tau), \tag{2.4.1}$$

where

$$J_1 = \begin{bmatrix} -kV^* - \delta & 0 & kH^* \\ 0 & -\beta - \delta & 0 \\ 0 & \beta & -c \end{bmatrix}, J_2 = \begin{bmatrix} 0 & 0 & 0 \\ a & 0 & 0 \\ 0 & 0 & 0 \end{bmatrix},$$

$$Y(t) = \begin{bmatrix} I(t) \\ D(t) \\ V(t) \end{bmatrix} \text{ and } Y(t-\tau) = \begin{bmatrix} I(t-\tau) \\ D(t-\tau) \\ V(t-\tau) \end{bmatrix}.$$

Note that here we have used $H^* = H_{\max} - I^*$. The characteristic equation of the linearized system (2.4.1) is given by

$$A(\lambda) + B(\lambda)e^{-\lambda\tau} = (\lambda^3 + A_2\lambda^2 + A_1\lambda + A_0) + B_0 e^{-\lambda\tau} = 0, \tag{2.4.2}$$

where

$$\begin{aligned} A_2 &= \beta + 2\delta + c + kV^* > 0, \\ A_1 &= c(\beta+\delta) + (\beta+\delta+c)(\delta+kV^*) > 0, \\ A_0 &= c(\beta+\delta)(\delta+kV^*) > 0, \\ B_0 &= -a\beta k(H_{\max} - I^*) < 0. \end{aligned}$$

Note that when $\tau = 0$, this characteristic equation (2.4.2) reduces to the one for the original model (2.1.1). As such, in this case ($\tau = 0$), the real part of all the roots of (2.4.2) will be negative, since $R_0 > 1$ (necessary for existence of E_i). When $\tau > 0$, then equation (2.4.2) being transcendental, will have infinitely many roots. In order to determine the periodic solutions, the eigenvalues will have to be purely imaginary. Thus, substituting $\lambda = i\omega,\ \omega \in \mathbb{R}$ in equation (2.4.2) and separating the real and imaginary parts, we obtain

$$\omega^3 - A_1\omega = -B_0 \sin\omega\tau, \tag{2.4.3}$$

$$A_0 - A_2\omega^2 = -B_0 \cos\omega\tau. \tag{2.4.4}$$

Squaring and adding (2.4.3) and (2.4.4), we get

$$(\omega^3 - A_1\omega)^2 + (A_0 - A_2\omega^2)^2 = B_0^2. \tag{2.4.5}$$

Substituting $\omega^2 = \mu$ in (2.4.5), we get the following cubic equation in μ:

$$\mu^3 + C_2\mu^2 + C_1\mu + C_0 = 0, \tag{2.4.6}$$

where

$$C_2 = A_2^2 - 2A_1, C_1 = A_1^2 - 2A_0A_2, C_0 = A_0^2 - B_0^2.$$

The roots of the equation (2.4.6) will have negative real part if and only if the Routh-Hurwitz criterion is satisfied and consequently (2.4.2) will have no purely imaginary root. Now we note

that, in the above case, the conditions for Routh-Hurwitz criterion are satisfied, *i.e.,*

$$\begin{aligned} C_2 &= A_2^2 - 2A_1 = c^2 + (\beta+\delta)^2 + (\delta + kV^*)^2 > 0, \\ C_0 &= A_0^2 - B_0^2 = a\beta k I^*[c(\beta+\delta)(\delta+kV^*) + a\beta k(H_{\max} - I^*)] > 0, \\ C_2C_1 - C_0 &= c^4\left\{(\beta+\delta)^2 + (\delta+kV^*)^2\right\} + (\beta+\delta)^4\left\{c^2 + (\delta+kV^*)^2\right\} \\ &\quad +(\delta+kV^*)^4\left\{c^2+(\beta+\delta)^2\right\} + 3c^2\delta^2(\beta+\delta)^2 \\ &\quad +c^2(\beta+\delta)^2k^2V^{*2} + 4c^2(\beta+\delta)^2\delta kV^* + a\beta c(\beta+\delta)k^2I^*V^* > 0. \end{aligned}$$

Thus, all the roots of (2.4.6) will have negative real parts, resulting in equation (2.4.5) having no real roots. Therefore, we can conclude that for any value of $\tau > 0$, the roots of the characteristic equation (2.4.2) will always lie in the negative half plane. The results obtained above may now be summarized as:

Theorem 2.4.1. *The infected steady state E_i is locally asymptotically stable for the delay system (2.3.1) for all $\tau > 0$, provided $R_0 > 1$.*

2.5 Numerical Results

In this section, we present some numerical results to illustrate the theoretical results obtained for various scenarios. For this purpose, we take into account two sets of parameters corresponding to the cases of stability of the infected steady state ($R_0 > 1$) and uninfected steady state ($R_0 < 1$). The system under consideration being nonlinear is solved numerically.

We first choose the parameter values to be $H_{\max} = 2.4\times10^9$ cells, $k = 1.67\times10^{-12}$ day^{-1} virion^{-1}, $\delta = 0.053$ day^{-1}, $a = 150$ day^{-1}, $\beta = 0.87$ day^{-1} and $c = 3.8$ day^{-1}. Of these $H_{\max}$ was obtained from [68] while the other values are available in [7]. The value of R_0 in this case turns out to be $R_0 = 2.814 > 1$, thereby indicating that the infected steady state is asymptotically stable. To illustrate this we choose three different initial conditions of $0.4, 0.8$ and 1.4 times $E_i = (1.55\times10^9, 2.51\times10^{11}, 5.76\times10^{10})$. We ran the simulation for a period of 100 days and observe that the dynamics of the system eventually converges to E_i irrespective of the initial condition. This (as can be seen in Figure 2.2) supports the result that the infected steady state is stable, thereby indicating that the patient does not eventually recover. We also illustrate in the last figure of Figure 2.2, the dynamics of the three state variables for various initial conditions ranging from 0.1 to 1.9 times E_i in increments of 0.05, all of which show a convergence towards E_i. We now change one of the above parameter values k, to $k = 3\times10^{-13}$ day^{-1} virion^{-1} [1], which renders the value of R_0 to be $R_0 = 0.5055 < 1$. In this case, we would expect the uninfected steady state to be asymptotically stable. We again choose three different initial conditions and run the simulations for a period of 300 days and observe (Figure 2.3) that the three state variables converge towards

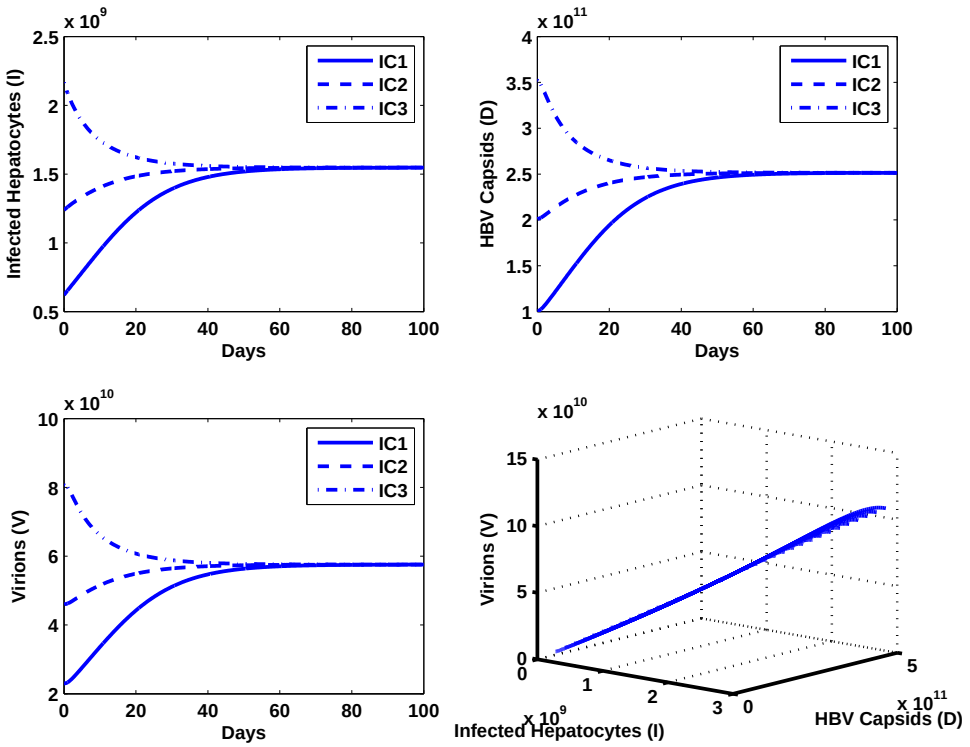

Figure 2.2: Dynamics of non-delay model for $R_0 = 2.814$. Here $IC1$, $IC2$ and $IC3$ represent three different initial conditions.

$E_u = (0, 0, 0)$, indicating the stability of the uninfected steady state. We further illustrate this with more initial conditions over a larger range in Figure 2.3.

We now illustrate the results for the delay model. We first make use of the parameter values for which $R_0 > 1$. It has already been shown that the stability of the infected steady state is unaffected by the delay and its length. We take the initial condition to be 1.4 times E_i. We however, now consider three different delays of $\tau = 1, 10$ and 50 days. We ran the simulations for a period of 300 days (Figure 2.4). For all the three delays, the dynamics of the system converges towards E_i, which is consistent with the theoretical results obtained. Results with multiple initial conditions and a delay of $\tau = 10$ days are also included in Figure 2.4. Similar simulations were carried out for the case with $R_0 < 1$. In this scenario also we consider an initial condition with three different delays as well as multiple initial conditions with one delay. The results are presented in Figure 2.5 and show an eventual approach of the trajectories towards the uninfected steady state E_u.

2.6 Conclusion

We considered a model for chronic HBV infection driven by three coupled ODEs. The model admits two steady states, namely the uninfected and the infected steady state. A parameter R_0 in terms of

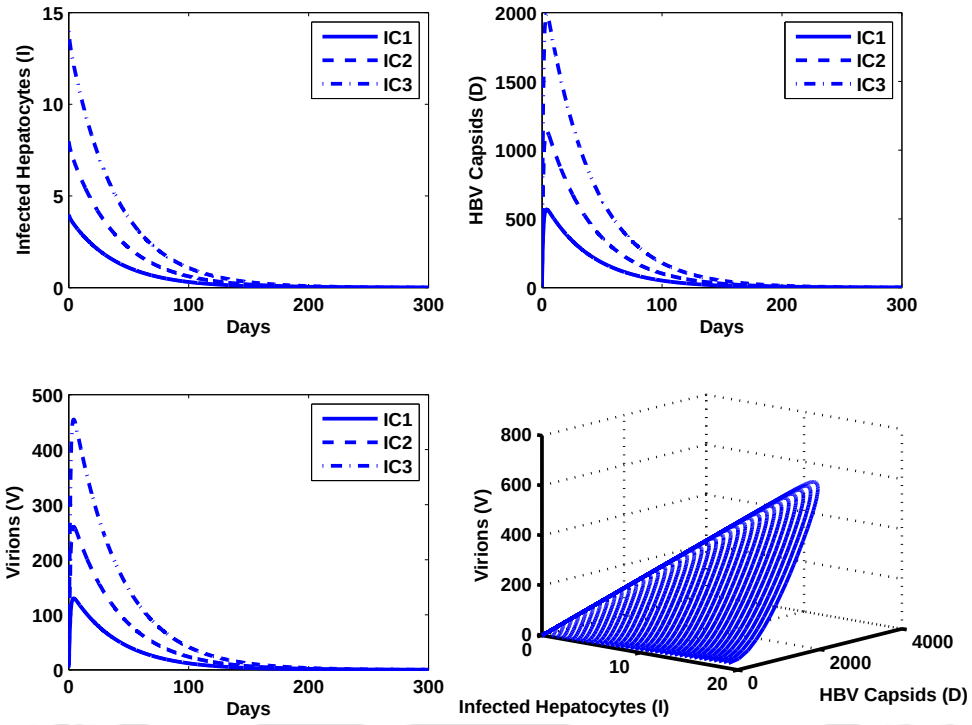

Figure 2.3: Dynamics of non-delay model for $R_0 = 0.5055$. Here $IC1$, $IC2$ and $IC3$ represent three different initial conditions.

the parameters of the model is obtained and the stability of the steady states are analyzed in terms of R_0. The uninfected steady state is proved to be stable for $R_0 \leq 1$ whereas the infected steady state is shown to be stable for $R_0 > 1$. A modified model incorporating the delay in the production of the intracellular HBV DNA-containing capsids from the infected hepatocytes is presented. It is shown that the nature of stability of the steady states remains unchanged even with the inclusion of the delay term. The results for both the cases are illustrated numerically for two parameter sets, one with $R_0 < 1$ and the other with $R_0 > 1$. The simulations for the non-delay case was done for several initial conditions, all of which showed convergence to the appropriate steady state depending on the value of R_0. In case of the delay, the results are presented for several delays as well as several initial conditions.

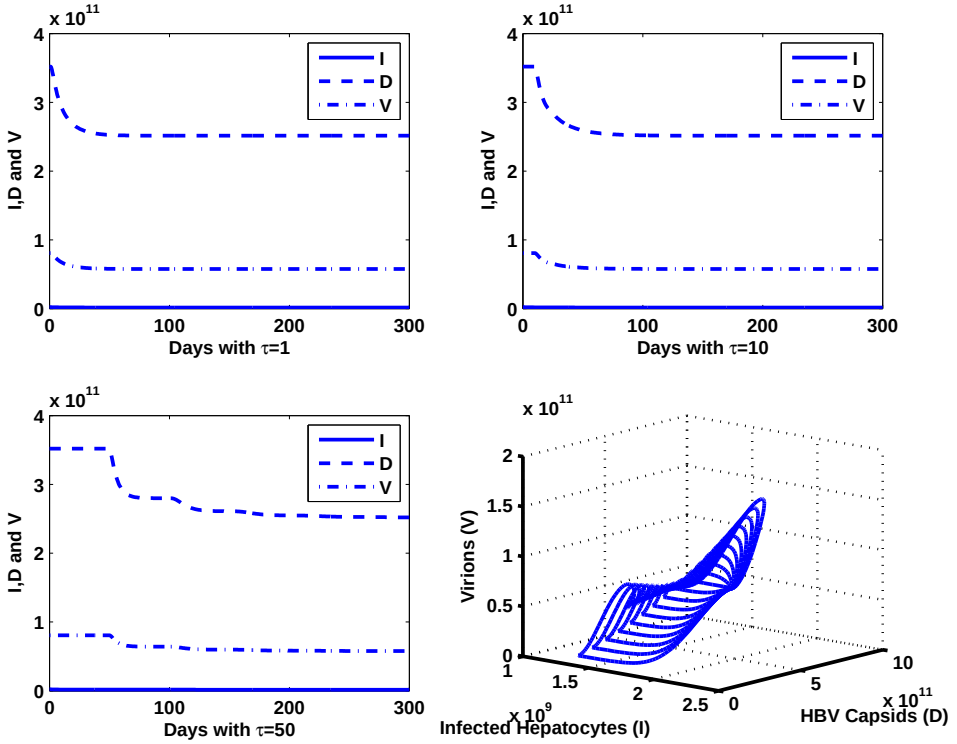

Figure 2.4: Dynamics of delay model for $R_0 = 2.814$

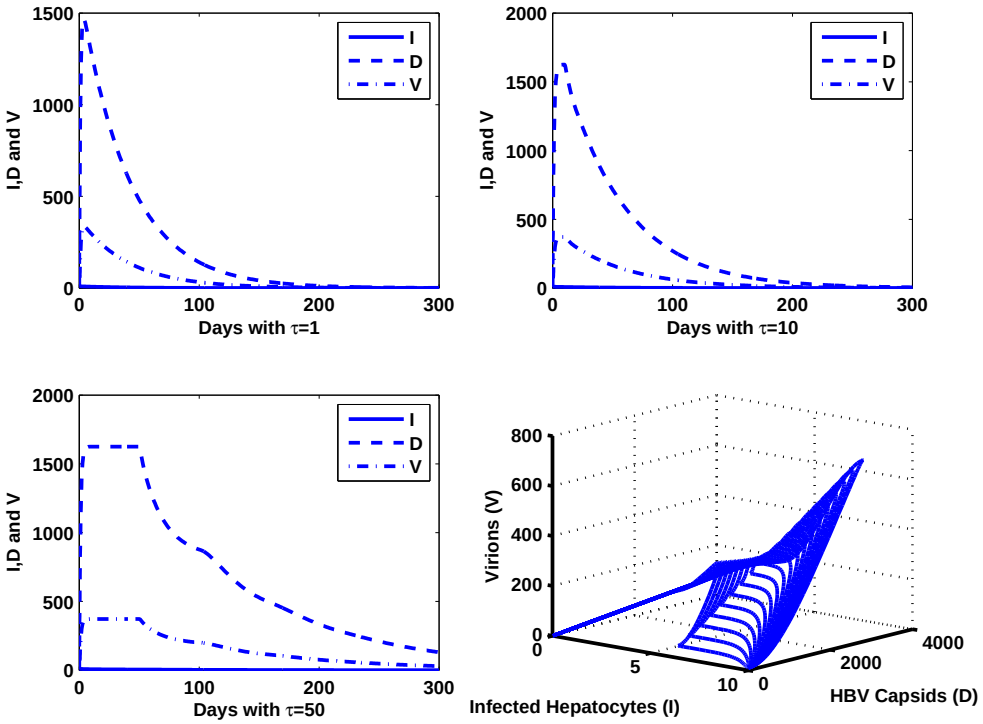

Figure 2.5: Dynamics of delay model for $R_0 = 0.5055$

Chapter 3

The Modified HBV Infection Model

In this chapter, we extend the model (2.1.1) by incorporating an equation for uninfected hepatocytes instead of using the homeostatic mechanism of the liver to obtain the dynamics of uninfected hepatocytes. We show the existence of the steady states and obtain the conditions for the local and global stability in terms of basic reproduction number. Further, numerical simulations are presented to support the theoretical results.

3.1 Mathematical Model

Most mathematical models for analyzing HBV dynamics incorporate the uninfected and infected hepatocytes as well as the virions. These models formulate the infection as a mass action process between the virions and the uninfected hepatocytes. Some models incorporate a constant source for the uninfected hepatocytes. All these models however do not include the intracellular HBV DNA-containing capsids. On the other hand, the mathematical model proposed by Murray et al. [7] does not include any equation for the uninfected hepatocytes. Instead, the homeostatic mechanism is incorporated via the relation that the sum of the uninfected and infected hepatocytes is maintained at a constant level $H_{\max}$. We therefore propose the following modified model which incorporates equations for both uninfected hepatocytes and the intracellular HBV DNA-containing capsids :

$$\begin{aligned} \frac{dH(t)}{dt} &= s - kH(t)V(t) - \mu H(t), \\ \frac{dI(t)}{dt} &= kH(t)V(t) - \delta I(t), \\ \frac{dD(t)}{dt} &= aI(t) - \beta D(t) - \delta D(t), \\ \frac{dV(t)}{dt} &= \beta D(t) - cV(t). \end{aligned} \tag{3.1.1}$$

The populations included in this model are the uninfected and the infected hepatocytes ($H(t)$ and $I(t)$ respectively), the intracellular HBV DNA-containing capsids ($D(t)$) and the virions in plasma ($V(t)$). The uninfected hepatocytes are produced at a constant rate s and have a natural death rate

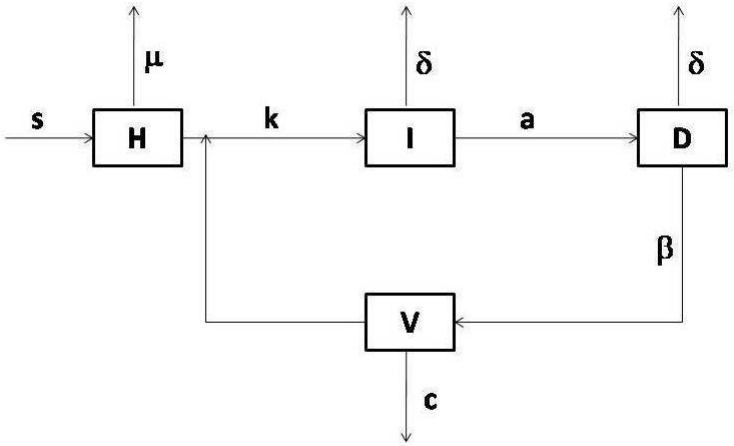

Figure 3.1: Schematic representation of the model (3.1.1).

of μ. The virions infect these uninfected hepatocytes at a rate k leading to the production of infected hepatocytes, which clear out at a rate δ. Also we assume that $\mu \leq \delta$. This is a reasonable assumption from the biomedical point of view, since a higher death rate for the uninfected hepatocytes as compared to that of infected hepatocytes, would result in a low chance of patient survival. The parameter a represents the rate of production of intracellular HBV DNA-containing capsids with β being the rate at which the capsids are transmitted to blood which then results in the growth of virion population. The capsids and the virions have a natural death rate of δ and c respectively. All the parameters of the model are positive. A schematic representation of the model (3.1.1) is given in Figure 3.1.

The solutions to the system (3.1.1) with positive initial conditions will remain positive. In order to prove the boundedness of the solution trajectories subject to positive initial conditions [60, 61, 69], we define a new variable, $T(t) = H(t) + I(t)$. From the first two equations of (3.1.1), we get

$$\frac{dT}{dt} = s - \mu H - \delta I.$$

Using the condition $\mu \leq \delta$, we obtain

$$\frac{dT}{dt} \leq s - \mu(H + I).$$

Hence,

$$\limsup_{t\to\infty} T(t) \leq \frac{s}{\mu}.$$

We thus have $\limsup_{t\to\infty} H(t) \leq \frac{s}{\mu}$ and $\limsup_{t\to\infty} I(t) \leq \frac{s}{\mu}$. Therefore, $H(t) \leq \frac{s}{\mu}$ and $I(t) \leq \frac{s}{\mu}$.

Now, from the third equation of (3.1.1) and using this bound for $I(t)$, we get

$$\frac{dD}{dt} \leq \frac{as}{\mu} - \beta D - \delta D.$$

Hence,

$$\limsup_{t\to\infty} D(t) \leq \frac{as}{\mu(\beta+\delta)}.$$

Similarly, from the fourth equation of (3.1.1) and using this bound for $D(t)$, we obtain

$$\frac{dV}{dt} \leq \frac{a\beta s}{\mu(\beta+\delta)} - cV,$$

which gives

$$\limsup_{t\to\infty} V(t) \leq \frac{a\beta s}{c\mu(\beta+\delta)}.$$

Thus all the model populations are bounded and we have the following closed and bounded, positively invariant set

$$\mathcal{D} = \left\{(H,I,D,V) \in \mathbb{R}^4_+ : 0 \leq H, I \leq \frac{s}{\mu}, 0 \leq D \leq \frac{as}{\mu(\beta+\delta)}, 0 \leq V \leq \frac{a\beta s}{c\mu(\beta+\delta)}\right\}$$

with respect to (3.1.1), where $\mathbb{R}^4_+ = \{(H,I,D,V) : H \geq 0, I \geq 0, D \geq 0, V \geq 0\}$. The model (3.1.1) has two steady states:

1. The uninfected steady state, $E_u = \left(\frac{s}{\mu}, 0, 0, 0\right)$.
2. The infected steady state, $E_i = (H^*, I^*, D^*, V^*)$ where,

$$H^* = \frac{c\delta(\beta+\delta)}{a\beta k},\ V^* = \left[\frac{a\beta s}{c\delta(\beta+\delta)} - \frac{\mu}{k}\right],\ D^* = \left[\frac{c}{\beta}\right] V^* \text{ and } I^* = \left[\frac{\beta+\delta}{a}\right] D^*.$$

The infected steady state, E_i, exists provided the basic reproduction number,

$$R_0 = \frac{a\beta sk}{c\delta\mu(\beta+\delta)} > 1.$$

3.2 Stability Analysis

For the purpose of stability analysis of both the steady states, we need the Jacobian matrix for the model (3.1.1), which is given by,

$$J = \begin{bmatrix} -kV-\mu & 0 & 0 & -kH \\ kV & -\delta & 0 & kH \\ 0 & a & -(\beta+\delta) & 0 \\ 0 & 0 & \beta & -c \end{bmatrix}.$$

Theorem 3.2.1. *The uninfected steady state E_u is locally asymptotically stable when $R_0 < 1$ and it becomes unstable when $R_0 > 1$.*

Proof. The characteristic equation for E_u is

$$(\lambda+\mu)\left[(\lambda+\delta)(\lambda+c)(\lambda+\beta+\delta)-\frac{a\beta sk}{\mu}\right]=0.$$

While one eigenvalue $\lambda=-\mu$ is negative, the other three eigenvalues are given by the solution of the following cubic equation,

$$\lambda^3+A\lambda^2+B\lambda+C=0,$$

where

$$A=(\beta+2\delta+c),\ B=[(\delta+c)(\beta+\delta)+c\delta] \text{ and } C=\left[\delta(\beta+\delta)c-\frac{a\beta sk}{\mu}\right].$$

One can easily see that $A>0$ and $AB-C=(\beta+2\delta+c)\left[(\delta+c)(\beta+\delta)+c\delta\right]-\delta(\beta+\delta)c+\frac{a\beta sk}{\mu}>0$. Also $C=\delta(\beta+\delta)c-\frac{a\beta sk}{\mu}>0$ means $R_0=\frac{a\beta sk}{c\delta\mu(\beta+\delta)}<1$. Thus the Routh-Hurwitz criterion is satisfied for the above cubic equation. Hence the uninfected steady state is locally asymptotically stable whenever $R_0<1$. Finally, whenever $R_0>1$, the characteristic equation has atleast one positive root and therefore E_u will become unstable. □

Theorem 3.2.2. *The infected steady state E_i is locally asymptotically stable when $R_0>1$.*

Proof. The characteristic equation for E_i is

$$\lambda^4+A_3\lambda^3+A_2\lambda^2+A_1\lambda+A_0=0,$$

where

$$A_3=(kV^*+\mu+\beta+2\delta+c),\ A_2=(\delta+c)(\beta+\delta)+c\delta+(kV^*+\mu)(c+\beta+2\delta),$$

$A_1=[(c+\delta)(\beta+\delta)+c\delta](kV^*+\mu)+c\delta(\beta+\delta)-a\beta kH^*$ and $A_0=c\delta(\beta+\delta)(kV^*+\mu)-a\beta\mu kH^*$.

The Routh-Hurwitz criterion, namely, $A_3>0$, $A_0>0$, $A_3A_2-A_1>0$ and $(A_3A_2-A_1)A_1-A_3^2A_0>0$ must be satisfied to ensure that all the roots of the above characteristic equation have negative real parts. It can be easily seen that all these conditions are indeed satisfied under the condition $R_0>1$. Hence E_i is locally asymptotically stable whenever $R_0>1$. □

Theorem 3.2.3. *The uninfected steady state E_u is globally asymptotically stable when $R_0\leq 1$.*

Proof. A Lyapunov function $L(t)$ for the system (3.1.1) is defined as,

$$L(t)=\frac{a\beta}{\delta(\beta+\delta)}I(t)+\frac{\beta}{\beta+\delta}D(t)+V(t). \tag{3.2.1}$$

The derivative of $L(t)$ along a solution of system (3.1.1) is

$$\frac{dL}{dt}=\left(\frac{a\beta kH}{c\delta(\beta+\delta)}-1\right)cV. \tag{3.2.2}$$

In $\mathcal{D}$, we have $\frac{dL}{dt} \leq \left(\frac{a\beta sk}{c\delta\mu(\beta+\delta)} - 1\right) cV = (R_0 - 1)cV$. Therefore, $\frac{dL}{dt} \leq 0$ for $R_0 \leq 1$. Using the Lyapunov-LaSalle invariance principle [60, 61], we conclude that all paths in $\mathcal{D}$ approach the largest invariant subset of the set M for which $\frac{dL}{dt} = 0$, as $t \to \infty$. Observe that, $\frac{dL}{dt} = 0$ when either $V = 0$ or $R_0 = 1$ and $H = \frac{s}{\mu}$. Thus the required set $M = \{(\frac{s}{\mu}, 0, 0, 0)\} = \{E_u\}$. Hence, E_u is globally asymptotically stable when $R_0 \leq 1$. □

Before proceeding with the global stability analysis for the infected steady state we prove the following result:

Lemma 3.2.4. *The system (3.1.1) is uniformly persistent in int $\mathcal{D}$ when $R_0 > 1$.*

Proof. The derivative of the above Lyapunov function (3.2.1), $\frac{dL}{dt} > 0$ (whenever $R_0 > 1$) along a solution of the system (3.1.1), subject to the condition that $H(t)$ is sufficiently close to $\frac{s}{\mu}$, except when $V = 0$. That is, for $R_0 > 1$ all solution trajectories emanating from a neighborhood of E_u, must leave the neighborhood, except those on the positively invariant H-axis. Thus, any orbit starting in int $\mathcal{D}$ cannot have E_u as ω-limit point. Hence using the results of Freedman et al. [63] and Butler et al. [64] as in [61], we conclude that E_u is unstable and the system is uniformly persistent in int $\mathcal{D}$. □

3.3 Global Stability of the Infected Steady State

We now discuss the global stability of the infected steady state E_i following the approach due to Li and Muldowney [70, 71]. We present the summary of the results to be used in this approach. Let the map $x \to f(x)$ from an open subset $\Omega \subset \mathbb{R}^n$ to $\mathbb{R}^n$ be such that each solution $x(t)$ to the differential equation

$$x' = f(x) \tag{3.3.1}$$

is uniquely determined by its initial value $x(0) = x_0$. Let this solution be denoted by $x(t, x_0)$. A set E is said to be *absorbing* in Ω for the system (3.3.1) if $x(t, E_1) \subset E$ for each compact set $E_1 \subset E$ for sufficiently large t. The following assumptions are made:

(H1) Ω is simply connected.

(H2) There is a compact absorbing set $E \subset \Omega$.

(H3) $\bar{x}$ is the only equilibrium point of (3.3.1) in Ω.

Let J be a $n \times n$ matrix, whose *second additive compound matrix* of size $\binom{n}{2} \times \binom{n}{2}$ is denoted by

$J^{[2]}$. If $J = (a_{ij})$ is a 4×4 matrix, then $J^{[2]}$ is given by [72, 73],

$$J^{[2]} = \begin{bmatrix} a_{11}+a_{22} & a_{23} & a_{24} & -a_{13} & -a_{14} & 0 \\ a_{32} & a_{11}+a_{33} & a_{34} & a_{12} & 0 & -a_{14} \\ a_{42} & a_{43} & a_{11}+a_{44} & 0 & a_{12} & a_{13} \\ -a_{31} & a_{21} & 0 & a_{22}+a_{33} & a_{34} & -a_{24} \\ -a_{41} & 0 & a_{21} & a_{43} & a_{22}+a_{44} & a_{23} \\ 0 & -a_{41} & a_{31} & -a_{42} & a_{32} & a_{33}+a_{44}. \end{bmatrix} \tag{3.3.2}$$

The *Lozinskiĭ* measure for an $n \times n$ matrix B with respect to the induced matrix norm $\|\cdot\|$ is defined as

$$\nu(B) = \lim_{h \to 0^+} \frac{\|I + hB\| - 1}{h}.$$

Let $Q \to Q(x)$ be an $\binom{n}{2} \times \binom{n}{2}$ matrix-valued function that is C^1 and $Q^{-1}(x)$ exists for $x \in \Omega$. The matrix B is defined as $B = Q_f Q^{-1} + QJ^{[2]}Q^{-1}$, where $Q_f$is obtained by replacing the entry q_{ij} of Q by its directional derivative along the direction of f and $J^{[2]}$ is the *second additive compound matrix* of the *Jacobian* J of the system (3.3.1). The quantity $\bar{q}_2$ is defined as

$$\bar{q}_2 = \limsup_{t \to \infty} \sup_{x_0 \in E} \frac{1}{t} \int_0^t \nu(B(x(s, x_0)))ds. \tag{3.3.3}$$

We present the following result due to Li and Muldowney [70]:

Theorem 3.3.1. *Under the assumptions (H1),(H2) and (H3), the unique equilibrium point $\bar{x}$ of (3.3.1) is globally asymptotically stable in Ω provided the quantity $\bar{q}_2 < 0$.*

We now prove the following theorem:

Theorem 3.3.2. *The infected steady state E_i is globally asymptotically stable in int $\mathcal{D}$ when $R_0 > 1$ and when $\overline{b} > 0$ ($\overline{b}$ is defined in the proof).*

Proof. Since the system (3.1.1) is uniformly persistent in int $\mathcal{D}$ when $R_0 > 1$, therefore there exists a compact absorbing set $\Gamma \subset$ int $\mathcal{D}$ [70]. Now, since the system (3.1.1) is uniformly persistent in int $\mathcal{D}$, then there exists a constant $m > 0$, independent of the initial data in int $\mathcal{D}$, such that, all solutions $(H(t), I(t), D(t), V(t))$ of (3.1.1) satisfy

$$\liminf_{t \to \infty} H(t) > m, \liminf_{t \to \infty} I(t) > m, \liminf_{t \to \infty} D(t) > m, \liminf_{t \to \infty} V(t) > m$$

provided $(H(0), I(0), D(0), V(0)) \in$ int $\mathcal{D}$.

The Jacobian matrix J associated with the system (3.1.1) is

$$J = \begin{bmatrix} -\mu - kV & 0 & 0 & -kH \\ kV & -\delta & 0 & kH \\ 0 & a & -\beta - \delta & 0 \\ 0 & 0 & \beta & -c \end{bmatrix}$$

and its corresponding *second additive compound matrix* $J^{[2]}$ is given by,

$$J^{[2]} = \begin{bmatrix} -\delta-\mu-kV & 0 & kH & 0 & kH & 0 \\ a & -\beta-\delta-\mu-kV & 0 & 0 & 0 & kH \\ 0 & \beta & -c-\mu-kV & 0 & 0 & 0 \\ 0 & kV & 0 & -\beta-2\delta & 0 & -kH \\ 0 & 0 & kV & \beta & -c-\delta & 0 \\ 0 & 0 & 0 & 0 & a & -c-\beta-\delta \end{bmatrix}.$$

We take the function $Q = Q(H, I, D, V) = \text{diag}(1, 1, 1, 1, D, D)$. Then we get

$$Q_f Q^{-1} = \text{diag}\left(0, 0, 0, 0, \frac{D'}{D}, \frac{D'}{D}\right),$$

and

$$B = Q_f Q^{-1} + Q J^{[2]} Q^{-1}.$$

Now following the approach in [74], we get

$$\begin{aligned} B &= \begin{bmatrix} -\delta-\mu-kV & 0 & kH & 0 & \frac{kH}{D} & 0 \\ a & -\beta-\delta-\mu-kV & 0 & 0 & 0 & \frac{kH}{D} \\ 0 & \beta & -c-\mu-kV & 0 & 0 & 0 \\ 0 & kV & 0 & -\beta-2\delta & 0 & \frac{-kH}{D} \\ 0 & 0 & kVD & \beta D & \frac{D'}{D}-c-\delta & 0 \\ 0 & 0 & 0 & 0 & a & \frac{D'}{D}-c-\beta-\delta \end{bmatrix} \\ &= \begin{bmatrix} B_{11} & B_{12} \\ B_{21} & B_{22} \end{bmatrix}, \end{aligned}$$

where $B_{11} = \begin{bmatrix} -\delta-\mu-kV \end{bmatrix}$, $B_{12} = \begin{bmatrix} 0 & kH & 0 & \frac{kH}{D} & 0 \end{bmatrix}$, $B_{21} = \begin{bmatrix} a & 0 & 0 & 0 & 0 \end{bmatrix}^\top$ and

$$B_{22} = \begin{bmatrix} -\beta-\delta-\mu-kV & 0 & 0 & 0 & \frac{kH}{D} \\ \beta & -c-\mu-kV & 0 & 0 & 0 \\ kV & 0 & -\beta-2\delta & 0 & \frac{-kH}{D} \\ 0 & kVD & \beta D & \frac{D'}{D}-c-\delta & 0 \\ 0 & 0 & 0 & a & \frac{D'}{D}-c-\beta-\delta \end{bmatrix}.$$

The *Lozinskiĭ* measure of matrix B is defined as follows:

$$\nu(B) \leq \max\{g_1, g_2\}, \tag{3.3.4}$$

where $g_1 = \nu(B_{11}) + \|B_{12}\|$ and $g_2 = \|B_{21}\| + \nu(B_{22})$. One can easily compute that $\nu(B_{11}) = -\delta-\mu-kV$, $\|B_{12}\| = \max\{kH, \frac{kH}{D}\} = kH$ and $\|B_{21}\| = a$. Then,

$$g_1 = -\delta-\mu-kV+kH, \tag{3.3.5}$$

$$g_2 = a+\nu(B_{22}). \tag{3.3.6}$$

The matrix B_{22} is now partitioned as,

$$B_{22} = C = \begin{bmatrix} C_{11} & C_{12} \\ C_{21} & C_{22} \end{bmatrix}$$

where, $C_{11} = \begin{bmatrix} -\beta - \delta - \mu - kV \end{bmatrix}$, $C_{12} = \begin{bmatrix} 0 & 0 & 0 & \frac{kH}{D} \end{bmatrix}$, $C_{21} = \begin{bmatrix} \beta & kV & 0 & 0 \end{bmatrix}^\top$ and

$$C_{22} = \begin{bmatrix} -c-\mu-kV & 0 & 0 & 0 \\ 0 & -\beta-2\delta & 0 & \frac{-kH}{D} \\ kVD & \beta D & \frac{D'}{D}-c-\delta & 0 \\ 0 & 0 & a & \frac{D'}{D}-c-\beta-\delta \end{bmatrix}.$$

Accordingly, we define the *Lozinskiĭ* measure of matrix C as follows:

$$\nu(C) \leq \max\{g_3, g_4\}, \tag{3.3.7}$$

where, $g_3 = \nu(C_{11}) + \|C_{12}\|$ and $g_4 = \|C_{21}\| + \nu(C_{22})$. Thus we have $\nu(C_{11}) = -\beta - \delta - \mu - kV$, $\|C_{12}\| = \frac{kH}{D}$ and $\|C_{21}\| = \beta + kV$. Therefore, we have

$$g_3 = -\beta - \delta - \mu - kV + \frac{kH}{D}, \tag{3.3.8}$$

$$g_4 = \beta + kV + \nu(C_{22}). \tag{3.3.9}$$

Again, the matrix C_{22} is partitioned as,

$$C_{22} = F = \begin{bmatrix} F_{11} & F_{12} \\ F_{21} & F_{22} \end{bmatrix}$$

where, $F_{11} = \begin{bmatrix} -c - \mu - kV \end{bmatrix}$, $F_{12} = \begin{bmatrix} 0 & 0 & 0 \end{bmatrix}$, $F_{21} = \begin{bmatrix} 0 & kVD & 0 \end{bmatrix}^\top$ and

$$F_{22} = \begin{bmatrix} -\beta-2\delta & 0 & \frac{-kH}{D} \\ \beta D & \frac{D'}{D}-c-\delta & 0 \\ 0 & a & \frac{D'}{D}-c-\beta-\delta \end{bmatrix}.$$

Now we define the *Lozinskiĭ* measure of matrix F as follows:

$$\nu(F) \leq \max\{g_5, g_6\}, \tag{3.3.10}$$

where, $g_5 = \nu(F_{11}) + \|F_{12}\|$ and $g_6 = \|F_{21}\| + \nu(F_{22})$. Now we have, $\nu(F_{11}) = -c - \mu - kV$, $\|F_{12}\| = 0$ and $\|F_{21}\| = kVD$.
Therefore,

$$g_5 = -c - \mu - kV, \tag{3.3.11}$$

$$g_6 = kVD + \nu(F_{22}). \tag{3.3.12}$$

Further, the matrix F_{22} is partitioned as,

$$F_{22} = G = \begin{bmatrix} G_{11} & G_{12} \\ G_{21} & G_{22} \end{bmatrix}$$

where, $G_{11} = \begin{bmatrix} -\beta - 2\delta \end{bmatrix}$, $G_{12} = \begin{bmatrix} 0 & \frac{-kH}{D} \end{bmatrix}$, $G_{21} = \begin{bmatrix} \beta D & 0 \end{bmatrix}^\top$ and

$$G_{22} = \begin{bmatrix} \frac{D'}{D}-c-\delta & 0 \\ a & \frac{D'}{D}-c-\beta-\delta \end{bmatrix}.$$

We now define the *Lozinskiĭ* measure of matrix G as follows:

$$\nu(G) \leq \max\{g_7, g_8\}, \tag{3.3.13}$$

where, $g_7 = \nu(G_{11}) + \|G_{12}\|$ and $g_8 = \|G_{21}\| + \nu(G_{22})$. This gives us, $\nu(G_{11}) = -\beta - 2\delta$, $\|G_{12}\| = \frac{kH}{D}$ and $\|G_{21}\| = \beta D$. Also,

$$\begin{aligned} \nu(G_{22}) &= \max\left\{\frac{D'}{D} - c - \delta + a, \frac{D'}{D} - c - \beta - \delta\right\} \\ &= \frac{D'}{D} - c - \delta + a. \end{aligned}$$

Thus,

$$g_7 = -\beta - 2\delta + \frac{kH}{D}, \tag{3.3.14}$$

$$g_8 = \frac{D'}{D} - c - \delta + a + \beta D. \tag{3.3.15}$$

Also from the third equation of the system (3.1.1), we have

$$\frac{D'}{D} = \frac{aI}{D} - \beta - \delta. \tag{3.3.16}$$

So, from equations (3.3.14) and (3.3.15) and inequality (3.3.13) and using equation (3.3.16), we get

$$\nu(G) \leq \frac{D'}{D} + \max\left\{-\delta - \frac{aI}{D} + \frac{kH}{D}, -c - \delta + a + \beta D\right\}. \tag{3.3.17}$$

Now from equations (3.3.11), (3.3.12) and inequalities (3.3.10) and (3.3.17) and using (3.3.16), we obtain

$$\begin{aligned} \nu(F) \leq\ & \frac{D'}{D} + \max\left\{-c - \mu - kV - \frac{aI}{D} + \beta + \delta, -\delta - \frac{aI}{D} + \frac{kH}{D} + kVD,\right. \\ & \left. -c - \delta + a + \beta D + kVD\right\}. \end{aligned} \tag{3.3.18}$$

Further, from equations (3.3.8), (3.3.9) and inequalities (3.3.7) and (3.3.18) and using (3.3.16), we obtain

$$\begin{aligned} \nu(C) \leq\ & \frac{D'}{D} + \max\left\{-\mu - kV - \frac{aI}{D} + \frac{kH}{D}, -c - \mu - \frac{aI}{D} + 2\beta + \delta,\right. \\ & \left. -\delta - \frac{aI}{D} + \frac{kH}{D} + \beta + kV + kVD, -c - \delta + a + \beta + \beta D + kV + kVD\right\}. \end{aligned} \tag{3.3.19}$$

Again, from equations (3.3.5), (3.3.6) and inequalities (3.3.4) and (3.3.19) and using (3.3.16), we

obtain

$$\begin{aligned}
\nu(B) &\leq \frac{D'}{D} + \max\Big\{-\mu - kV - \frac{aI}{D} + \beta + kH, -\mu - kV - \frac{aI}{D} + a + \frac{kH}{D},\\
&\quad -c - \mu - \frac{aI}{D} + a + 2\beta + \delta, -\delta - \frac{aI}{D} + a + \beta + kV + kVD + \frac{kH}{D},\\
&\quad -c - \delta + 2a + \beta + \beta D + kV + kVD\}\\
&= \frac{D'}{D} - \min\Big\{\mu + kV + \frac{aI}{D} - \beta - kH, \mu + kV + \frac{aI}{D} - a - \frac{kH}{D},\\
&\quad c + \mu + \frac{aI}{D} - a - 2\beta - \delta, \delta + \frac{aI}{D} - a - \beta - kV - kVD - \frac{kH}{D},\\
&\quad c + \delta - 2a - \beta - \beta D - kV - kVD\}\\
&< \frac{D'}{D} - \min\Big\{\mu + km + \frac{am\mu(\beta+\delta)}{as} - \beta - \frac{ks}{\mu}, \mu + km + \frac{am\mu(\beta+\delta)}{as} - a - \frac{ks}{m\mu},\\
&\quad c + \mu + \frac{am\mu(\beta+\delta)}{as} - a - 2\beta - \delta, \delta + \frac{am\mu(\beta+\delta)}{as} - a - \beta - \frac{ak\beta s}{c\mu(\beta+\delta)} - \frac{a^2k\beta s^2}{c\mu^2(\beta+\delta)^2}\\
&\quad -\frac{ks}{m\mu}, c + \delta - 2a - \beta - \frac{\beta as}{\mu(\beta+\delta)} - \frac{ak\beta s}{c\mu(\beta+\delta)} - \frac{a^2k\beta s^2}{c\mu^2(\beta+\delta)^2}\Big\}.
\end{aligned}$$

Therefore,

$$\nu(B) < \frac{D'}{D} - \overline{b}$$

for t sufficiently large, where

$$\begin{aligned}
\overline{b} &= \min\Big\{\mu + km + \frac{am\mu(\beta+\delta)}{as} - \beta - \frac{ks}{\mu}, \mu + km + \frac{am\mu(\beta+\delta)}{as} - a - \frac{ks}{m\mu},\\
&\quad c + \mu + \frac{am\mu(\beta+\delta)}{as} - a - 2\beta - \delta, \delta + \frac{am\mu(\beta+\delta)}{as} - a - \beta - \frac{ak\beta s}{c\mu(\beta+\delta)} - \frac{a^2k\beta s^2}{c\mu^2(\beta+\delta)^2}\\
&\quad -\frac{ks}{m\mu}, c + \delta - 2a - \beta - \frac{\beta as}{\mu(\beta+\delta)} - \frac{ak\beta s}{c\mu(\beta+\delta)} - \frac{a^2k\beta s^2}{c\mu^2(\beta+\delta)^2}\Big\} > 0.
\end{aligned}$$

Let us consider any solution $(H(t), I(t), D(t), V(t))$ emanating from the compact absorbing set $\Gamma \subset \mathcal{D}$. Let $\overline{t}$ be large enough such that the system is persistent and $(H(t), I(t), D(t), V(t)) \subset \Gamma$ for all $t \geq \overline{t}$. Then along each solution $(H(t), I(t), D(t), V(t))$ such that $(H(0), I(0), D(0), V(0)) \in \Gamma$ we have, for $t > \overline{t}$,

$$\frac{1}{t}\int_0^t \nu(B)\, ds < \frac{1}{t}\int_0^{\overline{t}} \nu(B)\, ds + \frac{1}{t}\ln\left(\frac{D(t)}{D(\overline{t})}\right) - \left(\frac{t-\overline{t}}{t}\right)\overline{b}.$$

The boundedness of $D(t)$ and the definition of $\overline{q}_2$ (as in (3.3.3)) imply $\overline{q}_2 < 0$. This completes the proof. □

3.4 Numerical Results

The results obtained for the stability of the uninfected and the infected steady states are numerically illustrated in this section. We use two sets of parameter values, one which gives $R_0 < 1$ (uninfected

steady state is stable) and the other which leads to $R_0 > 1$ (infected steady state is stable). Both the models are numerically solved.

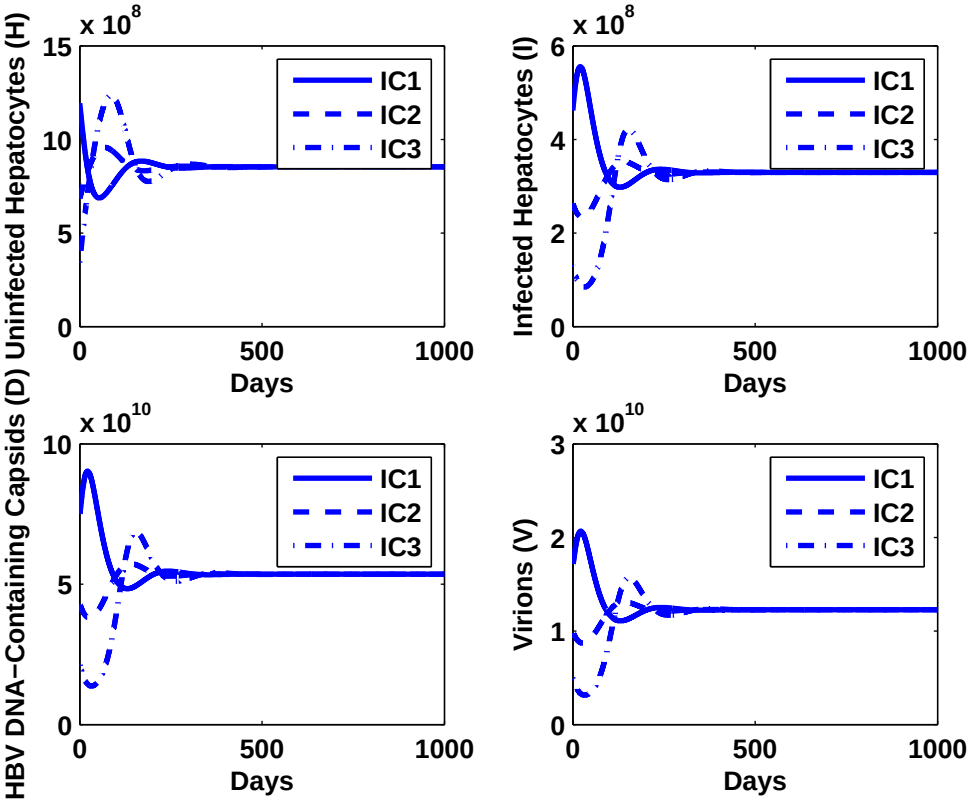

Figure 3.2: Dynamics of the model when $R_0 = 3.0482 > 1$ with three different initial conditions $IC1$, $IC2$ and $IC3$.

The first set of parameter values used are: $s = 2.6\times10^7$ cells day^{-1} $k = 1.67\times10^{-12}$ day^{-1} virion^{-1}, $\mu = 0.01$ day^{-1} $\delta = 0.053$ day^{-1}, $a = 150$ day^{-1}, $\beta = 0.87$ day^{-1} and $c = 3.8$ day^{-1}. While s and μ are chosen from [27], the rest of the parameter values are taken from [7]. For this set, the value of R_0 is $R_0 = 3.0482 > 1$. Thus in this case, the infected steady state is stable. The infected steady state is $E_i = (8.53 \times 10^8, 3.3 \times 10^8, 5.36 \times 10^{10}, 1.23 \times 10^{10})$. The evolution of the dynamics of the modified model for this scenario was observed for a duration of 1000 days. For this purpose, three different initial conditions, namely $IC_1 = 0.4 \times E_i$, $IC_2 = 0.8 \times E_i$ and $IC_3 = 1.4 \times E_i$ were chosen. The states of the system eventually converges to the infected steady state E_i for all the three initial condition. This is illustrated in Figure 3.2 which supports the result that the infected steady state, E_i is asymptotically stable whenever $R_0 > 1$.

In order to study the case when $R_0 < 1$, we now choose a different value of k, namely $k = 3 \times 10^{-13}$ day^{-1} virion^{-1} [1], while retaining the other parameter values. Then the value of R_0 becomes $R_0 = 0.5476 < 1$. Consequently, for this scenario, the uninfected steady state would have

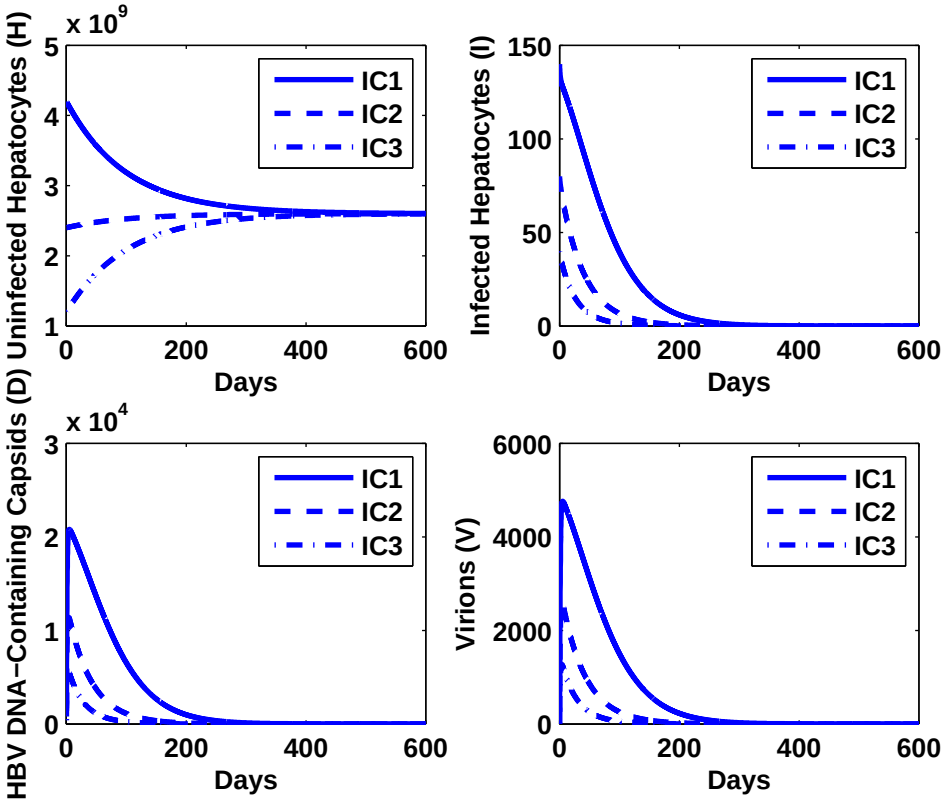

Figure 3.3: Dynamics of the model when $R_0 = 0.5476 < 1$ with three different initial conditions $IC1$, $IC2$ and $IC3$.

to be asymptotically stable. To illustrate we again choose three different initial conditions and ran the simulation for a duration of 600 days. It can be observed, from Figure 3.3, that all the state variables of the system eventually approach the uninfected steady state $E_u = (2.6 \times 10^9, 0, 0, 0)$, indicating the asymptotic stability of the uninfected steady state.

3.5 Conclusion

The previous models for HBV dynamics typically include the evolution of uninfected and infected hepatocytes along with the viral turnover. These models do not consider the virions produced from mature intracellular HBV DNA-containing capsids. While Murray et al. [7] consider the intracellular HBV DNA-containing capsids but do not consider the uninfected hepatocytes, the model presented here takes this into account and includes intracellular HBV DNA-containing capsids in addition to infected hepatocytes as well as HBV. The system (comprising of a system of four coupled ODEs) is seen to admit an uninfected and an infected steady state whose stability is analyzed in the context of the basic reproduction number R_0. It is shown that the uninfected steady state

is locally asymptotically stable whenever $R_0 < 1$, is stable when $R_0 = 1$ and is unstable whenever $R_0 > 1$. Further, its global asymptotic stability is shown for $R_0 \leq 1$, which gives the condition under which the patient is likely to recover as manifested by the decline of viral load below detection levels. The infected steady state is locally asymptotically stable when $R_0 > 1$. While the geometric approach for global stability due to Li and Muldowney [70] has found application in several other biomedical models, we use this approach for the HBV model. However, for the global stability, we arrive at another condition $\overline{b} > 0$ (where $\overline{b}$ has been defined in the proof of the global stability) in addition to R_0 being greater than 1.

Chapter 4

The Modified HBV Infection Model with Delays

In reality most biological processes are not instantaneous in nature, with delays happening for a number of events that take place during these processes. In this chapter, we present and analyze two models with one and two discrete delays. Several articles on the global properties of viral dynamics have appeared in literature [76, 77, 81]. Korobeinikov [81] discussed the global stability of basic virus dynamics models by constructing suitable Lyapunov functions. Huang et al. [77] showed the global stability for virus dynamics model with Beddington-DeAngelis functional response by constructing appropriate Lyapunov functions. Kajiwara et al. [76] presented a method for constructing Lyapunov functions for some delay differential equation driven models in virology and epidemiology. First, we include one delay (delay in production of productively infected hepatocytes) in the model (3.1.1) and analyze the local and global stability analysis in terms of basic reproduction number. The global stability analysis is accomplished by constructing suitable Lyapunov functions. The model is further extended by incorporating another delay in the production of the matured capsids. The global stability of the extended model is established. Finally, illustrative numerical simulations are presented.

4.1 The One-Delay Model

While most models incorporate the viral dynamics by way of a system of differential equations, they often do not account for the intracellular time delay between the process of infection of cells and the production of new virions [75]. For this purpose, we assume that there is a time delay of τ from the point where the uninfected hepatocytes are infected by HBV to the point where the productively infected hepatocytes are produced. This is modeled by incorporating a term $H(t-\tau)V(t-\tau)$. This implies that the density of hepatocytes that were infected at some time $t-\tau$ and have survived for the delay of τ give rise to infected hepatocyte population at time t. Therefore, we propose the

following delay model:

$$\begin{aligned}
\frac{dH(t)}{dt} &= s - kH(t)V(t) - \mu H(t), \\
\frac{dI(t)}{dt} &= kH(t-\tau)V(t-\tau) - \delta I(t), \\
\frac{dD(t)}{dt} &= aI(t) - \beta D(t) - \delta D(t), \\
\frac{dV(t)}{dt} &= \beta D(t) - cV(t),
\end{aligned} \tag{4.1.1}$$

with initial conditions $H(\theta) = H_0 > 0$, $I(\theta) = I_0 > 0$, $D(\theta) = D_0 > 0$ and $V(\theta) = V_0 > 0$ for $\theta \in [-\tau, 0]$. It can be shown that the solutions to the system (4.1.1) subject to positive initial conditions remain positive. We now prove the boundedness of the solution trajectories with non-negative initial conditions [69]. For this purpose, we define the variable, $T(t) = H(t) + I(t+\tau)$. Adding the first two equations of (4.1.1), we get

$$\frac{dT}{dt} = s - \mu H(t) - \delta I(t+\tau).$$

Using $\mu \leq \delta$, we obtain

$$\begin{aligned}
\frac{dT}{dt} &\leq s - \mu(H(t) + I(t+\tau)) \\
&= s - \mu T(t).
\end{aligned}$$

Hence,

$$\limsup_{t\to\infty} T(t) \leq \frac{s}{\mu}.$$

Without the loss of generality, this gives us, $\limsup_{t\to\infty} H(t) \leq \frac{s}{\mu}$ and $\limsup_{t\to\infty} I(t) \leq \frac{s}{\mu}$. Therefore, $H(t) \leq \frac{s}{\mu}$ and $I(t) \leq \frac{s}{\mu}$. Now using the bound for $I(t)$, we determine the bounds of $D(t)$ and $V(t)$. Thus we have the closed and bounded, positively invariant set

$$\mathcal{D} = \left\{ (H, I, D, V) \in \mathbb{R}^4_+ : 0 \leq H, I \leq \frac{s}{\mu}, 0 \leq D \leq \frac{as}{\mu(\beta+\delta)}, 0 \leq V \leq \frac{a\beta s}{c\mu(\beta+\delta)} \right\}$$

with respect to (4.1.1), where $\mathbb{R}^4_+ = \{(H, I, D, V) : H \geq 0, I \geq 0, D \geq 0, V \geq 0\}$. The delay model (4.1.1) has the same steady states as the ODE model (3.1.1), namely, the uninfected steady state $E_u = \left(\frac{s}{\mu}, 0, 0, 0\right)$ and the infected steady state $E_i = (H^*, I^*, D^*, V^*)$.

4.2 Stability Analysis of the One-Delay Model

It can be easily shown that the uninfected steady state E_u is locally asymptotically stable whenever $R_0 < 1$ and is unstable whenever $R_0 > 1$, for all $\tau > 0$. Now we undertake the local asymptotic

stability analysis for the infected steady state E_i of the delay system (4.1.1). The linearized system of (4.1.1) about E_i is given by [61, 67],

$$\frac{dY(t)}{dt} = J_1 Y(t) + J_2 Y(t-\tau), \tag{4.2.1}$$

where

$$J_1 = \begin{bmatrix} -\mu - kV^* & 0 & 0 & -kH^* \\ 0 & -\delta & 0 & 0 \\ 0 & a & -\beta-\delta & 0 \\ 0 & 0 & \beta & -c \end{bmatrix}, J_2 = \begin{bmatrix} 0 & 0 & 0 & 0 \\ kV^* & 0 & 0 & kH^* \\ 0 & 0 & 0 & 0 \\ 0 & 0 & 0 & 0 \end{bmatrix},$$

$$Y(t) = \begin{bmatrix} H(t) \\ I(t) \\ D(t) \\ V(t) \end{bmatrix} \text{ and } Y(t-\tau) = \begin{bmatrix} H(t-\tau) \\ I(t-\tau) \\ D(t-\tau) \\ V(t-\tau) \end{bmatrix}.$$

The corresponding characteristic equation of the linearized system (4.2.1) is given by

$$A(\lambda) + B(\lambda)e^{-\lambda\tau} = (\lambda^4 + A_3\lambda^3 + A_2\lambda^2 + A_1\lambda + A_0) + (B_1\lambda + B_0)e^{-\lambda\tau} = 0, \tag{4.2.2}$$

where

$$\begin{aligned} A_3 &= c + \beta + 2\delta + \mu + kV^* > 0, \\ A_2 &= (c+\delta)(\beta+\delta) + c\delta + (c+\beta+2\delta)(\mu+kV^*) > 0, \\ A_1 &= \{(c+\delta)(\beta+\delta) + c\delta\}(\mu+kV^*) + c\delta(\beta+\delta) > 0, \\ A_0 &= c\delta(\beta+\delta)(\mu+kV^*) > 0, \\ B_1 &= -a\beta kH^* < 0, \\ B_0 &= -a\beta\mu kH^* < 0. \end{aligned}$$

The characteristic equation for the original model (3.1.1) can be obtained from this characteristic equation (4.2.2), when $\tau = 0$. Since $R_0 > 1$ (when E_i exists), therefore the real parts of all roots of (4.2.2) will be negative whenever $\tau = 0$. For the case when $\tau > 0$, equation (4.2.2) becomes transcendental and thus has infinitely many roots. In order for the roots of (4.2.2) to have positive real part, it has to be purely imaginary for some value of $\tau > 0$. The real and imaginary parts obtained by substituting $\lambda = i\omega,\ \omega \in \mathbb{R}$ in (4.2.2) gives us

$$\omega^4 - A_2\omega^2 + A_0 = -(B_0\cos\omega\tau + B_1\omega\sin\omega\tau), \tag{4.2.3}$$

$$A_1\omega - A_3\omega^3 = B_0\sin\omega\tau - B_1\omega\cos\omega\tau. \tag{4.2.4}$$

Squaring and adding (4.2.3) and (4.2.4), we get

$$(\omega^4 - A_2\omega^2 + A_0)^2 + (A_1\omega - A_3\omega^3)^2 = B_0^2 + B_1^2\omega^2. \tag{4.2.5}$$

Substituting $\omega^2 = n$ in (4.2.5), we get the following quartic equation in n:

$$n^4 + C_3 n^3 + C_2 n^2 + C_1 n + C_0 = 0, \tag{4.2.6}$$

where

$$\begin{aligned} C_3 &= A_3^2 - 2A_2, \\ C_2 &= A_2^2 + 2A_0 - 2A_1 A_3, \\ C_1 &= A_1^2 - 2A_0 A_2 - B_1^2, \\ C_0 &= A_0^2 - B_0^2. \end{aligned}$$

The roots of the equation (4.2.6) will have negative real part if and only if the Routh-Hurwitz criterion is satisfied. In that case, (4.2.2) will have no purely imaginary root. It is verified below that the Routh-Hurwitz criterion in the above case is indeed satisfied.

$$\begin{aligned} C_3 &= c^2 + \delta^2 + (\beta+\delta)^2 + (\mu + kV^*)^2 > 0, \\ C_0 &= c^2\delta^2(\beta+\delta)^2(2\mu k V^* + k^2 (V^*)^2) > 0, \\ C_3C_2 - C_1 &= (c^2+\delta^2)^2\{(\beta+\delta)^2 + (\mu+kV^*)^2\} + c^2\delta^2\{(c^2+\delta^2) + (\beta+\delta)^2\} \\ &\quad +(\beta+\delta)^4\{(c^2+\delta^2) + (\mu+kV^*)^2\} + 2(c^2+\delta^2)(\beta+\delta)^2(\mu+kV^*)^2 \\ &\quad +\{(c^2+\delta^2) + (\beta+\delta)^2\}(\mu+kV^*)^4 > 0, \\ &\quad (C_3C_2 - C_1)C_1 - C_3^2 C_0 \\ &= (c^2+\delta^2)^3(\beta+\delta)^2\{(\beta+\delta)^2 + (\mu+kV^*)^2\}(\mu+kV^*)^2 + \\ &\quad c^2\delta^2(c^2+\delta^2)^2(\mu+kV^*)^4 + c^2\delta^2(c^2+\delta^2)^2(\beta+\delta)^2\mu^2 + \\ &\quad (c^2+\delta^2)(\beta+\delta)^2\{(c^2+\delta^2) + (\beta+\delta)^2\}(\mu+kV^*)^6 + c^2\delta^2(c^2+\delta^2)(\mu+kV^*)^6 \\ &\quad +c^2\delta^2(\beta+\delta)^2(\mu+kV^*)^4\mu^2 + 2(\beta+\delta)^4(\mu+kV^*)^4\{c^4+\delta^4+c^2\delta^2\} + \\ &\quad 2c^2\delta^2(\beta+\delta)^2(\mu+kV^*)^2\{(c^2+\delta^2) + (\beta+\delta)^2\}\mu^2 + c^2\delta^2(c^2+\delta^2)(\beta+\delta)^4\mu^2 \\ &\quad +c^2\delta^2(c^2+\delta^2)^2(\beta+\delta)^2(\mu+kV^*)^2 + c^4\delta^4\{(c^2+\delta^2) + (\beta+\delta)^2\}(\mu+kV^*)^2 \\ &\quad +\{c^4+\delta^4+c^2\delta^2\}(\beta+\delta)^6(\mu+kV^*)^2 + c^2\delta^2(\beta+\delta)^6\mu^2 + \\ &\quad (c^2+\delta^2)(\beta+\delta)^6(\mu+kV^*)^4 + c^2\delta^2(\beta+\delta)^4\{(\mu+kV^*)^4 + (c^2+\delta^2)\mu^2\} > 0. \end{aligned}$$

Hence, all the roots of (4.2.6) will have negative real parts which means that (4.2.5) has no real roots. Thus, we can conclude that for all values of $\tau > 0$, the roots of the characteristic equation (4.2.2) are always in the negative half plane. Therefore, we have the following result.

Theorem 4.2.1. *The infected steady state E_i is locally asymptotically stable for the delay system (4.1.1) for all $\tau > 0$, provided $R_0 > 1$.*

Before proceeding with the global stability analysis for the one-delay model (4.1.1) we present some inequalities [76] which will be used in the proofs. To begin with, we consider the function $G(x) = x - 1 - \ln x$ $(x > 0)$. Note that $G(x) \geq 0, \forall x$ and that $G(x) = 0$ if and only if $x = 1$. Let $x_1, x_2, \ldots, x_n$ be positive numbers. Then

$$1 - x_i + \ln x_i = -G(x_i) \leq 0, \forall i = 1 : n. \tag{4.2.7}$$

Summing (4.2.7) over $i = 1 : n$, we obtain

$$n - \sum_{i=1}^{n} x_i + \ln\left(\prod_{i=1}^{n} x_i\right) \leq 0. \tag{4.2.8}$$

Choosing $x_i = \frac{p_i}{q_i}$ where $p_i > 0, q_i > 0$ for $i = 1 : n$, it follows that

$$n - \sum_{i=1}^{n} \frac{p_i}{q_i} + \ln\left(\prod_{i=1}^{n} \frac{p_i}{q_i}\right) \leq 0. \tag{4.2.9}$$

If $p_1 p_2 \ldots p_n = q_1 q_2 \ldots q_n$, then $\prod_{i=1}^{n} \frac{p_i}{q_i} = 1$ which results in

$$n - \sum_{i=1}^{n} \frac{p_i}{q_i} \leq 0. \tag{4.2.10}$$

Theorem 4.2.2. *The uninfected steady state E_u is globally asymptotically stable when $R_0 \leq 1$.*

Proof. We define a Lyapunov function $L_1(t)$ as follows:

$$L_1(t) = H^0\left(\frac{H(t)}{H^0} - 1 - \ln\frac{H(t)}{H^0}\right) + I(t) + \frac{\delta}{a}D(t) + \frac{\delta(\beta+\delta)}{a\beta}V(t) + k\int_{t-\tau}^{t} H(\xi)V(\xi)d\xi.$$

The derivative of $L_1(t)$ along the solutions of the system (4.1.1) is

$$\begin{aligned}\frac{dL_1}{dt} &= \left(1 - \frac{H^0}{H}\right)[s - kHV - \mu H] + [kH(t-\tau)V(t-\tau) - \delta I] + \frac{\delta}{a}[aI - (\beta+\delta)D] \\ &\quad + \frac{\delta(\beta+\delta)}{a\beta}[\beta D - cV] + kHV - kH(t-\tau)V(t-\tau) \\ &= s\left[2 - \frac{H}{H^0} - \frac{H^0}{H}\right] + \frac{c\delta(\beta+\delta)}{a\beta}[R_0 - 1]V.\end{aligned}$$

Now, taking $p_1 = H, p_2 = H^0, q_1 = H^0, q_2 = H$ and using the inequality (4.2.10) for $n = 2$, we obtain

$$2 - \frac{H}{H^0} - \frac{H^0}{H} \leq 0.$$

Thus, when $R_0 \leq 1$ then $\frac{dL_1}{dt} \leq 0$. Let M be the largest invariant set in $\{(H, I, D, V) | \frac{dL_1}{dt} = 0\}$. We observe that $\frac{dL_1}{dt} = 0$ if and only if $H = H^0 = \frac{s}{\mu}, I = 0, D = 0$, and $V = 0$. Thus, $M = \{E_u\} = \{(\frac{s}{\mu}, 0, 0, 0)\}$. Therefore, by the Lyapunov-LaSalle invariance principle [25, 77], E_u is globally asymptotically stable whenever $R_0 \leq 1$. □

Theorem 4.2.3. *The infected steady state E_i is globally asymptotically stable when $R_0 > 1$.*

Proof. We define a Lyapunov function $L_2(t)$ as follows:

$$\begin{aligned} L_2(t) &= H^*\left(\frac{H(t)}{H^*} - 1 - \ln\frac{H(t)}{H^*}\right) + I^*\left(\frac{I(t)}{I^*} - 1 - \ln\frac{I(t)}{I^*}\right) + \frac{\delta}{a}D^*\left(\frac{D(t)}{D^*} - 1 - \ln\frac{D(t)}{D^*}\right) \\ &\quad + \frac{\delta(\beta+\delta)}{a\beta}V^*\left(\frac{V(t)}{V^*} - 1 - \ln\frac{V(t)}{V^*}\right) + kH^*V^*\int_{t-\tau}^{t} G\left(\frac{H(\xi)V(\xi)}{H^*V^*}\right)d\xi \\ &= L_2^1(t) + L_2^2(t), \end{aligned}$$

where

$$\begin{aligned} L_2^1(t) &= H^*\left(\frac{H(t)}{H^*} - 1 - \ln\frac{H(t)}{H^*}\right) + I^*\left(\frac{I(t)}{I^*} - 1 - \ln\frac{I(t)}{I^*}\right) + \frac{\delta}{a}D^*\left(\frac{D(t)}{D^*} - 1 - \ln\frac{D(t)}{D^*}\right) \\ &\quad + \frac{\delta(\beta+\delta)}{a\beta}V^*\left(\frac{V(t)}{V^*} - 1 - \ln\frac{V(t)}{V^*}\right), \\ L_2^2(t) &= kH^*V^*\int_{t-\tau}^{t} G\left(\frac{H(\xi)V(\xi)}{H^*V^*}\right)d\xi. \end{aligned}$$

The derivative of $L_2^1(t)$ along the solutions of the system (4.1.1) is

$$\begin{aligned} \frac{dL_2^1}{dt} &= \left(1 - \frac{H^*}{H}\right)\frac{dH}{dt} + \left(1 - \frac{I^*}{I}\right)\frac{dI}{dt} + \frac{\delta}{a}\left(1 - \frac{D^*}{D}\right)\frac{dD}{dt} + \frac{\delta(\beta+\delta)}{a\beta}\left(1 - \frac{V^*}{V}\right)\frac{dV}{dt} \\ &= \left(1 - \frac{H^*}{H}\right)[s - kHV - \mu H] + \left(1 - \frac{I^*}{I}\right)[kH(t-\tau)V(t-\tau) - \delta I] \\ &\quad + \frac{\delta}{a}\left(1 - \frac{D^*}{D}\right)[aI - (\beta+\delta)D] + \frac{\delta(\beta+\delta)}{a\beta}\left(1 - \frac{V^*}{V}\right)[\beta D - cV] \\ &= \left(1 - \frac{H^*}{H}\right)[s - kHV - \mu H] + \left(1 - \frac{I^*}{I}\right)[kHV - \delta I] \\ &\quad + \frac{\delta}{a}\left(1 - \frac{D^*}{D}\right)[aI - (\beta+\delta)D] + \frac{\delta(\beta+\delta)}{a\beta}\left(1 - \frac{V^*}{V}\right)[\beta D - cV] \\ &\quad + kH(t-\tau)V(t-\tau) - \frac{I^*}{I}kH(t-\tau)V(t-\tau) - kHV + \frac{I^*}{I}kHV \\ &= \mu H^*\left[2 - \frac{H}{H^*} - \frac{H^*}{H}\right] + \delta I^*\left[4 - \frac{H^*}{H} - \frac{I^*}{I}\frac{HV}{H^*V^*} - \frac{ID^*}{I^*D} - \frac{DV^*}{D^*V}\right] \\ &\quad + kH(t-\tau)V(t-\tau) - \frac{I^*}{I}kH(t-\tau)V(t-\tau) - kHV + \frac{I^*}{I}kHV. \end{aligned}$$

Now, using $\delta I^* = kH^*V^*$ from the second equation of (4.1.1), we get

$$\begin{aligned} \frac{dL_2^1}{dt} &= \mu H^*\left[2 - \frac{H}{H^*} - \frac{H^*}{H}\right] + \delta I^*\left[4 - \frac{H^*}{H} - \frac{I^*}{I}\frac{H(t-\tau)V(t-\tau)}{H^*V^*} - \frac{ID^*}{I^*D} - \frac{DV^*}{D^*V}\right] \\ &\quad + k[H(t-\tau)V(t-\tau) - HV]. \end{aligned}$$

Also, the derivative of $L_2^2(t)$ along the solutions of the system (4.1.1) is

$$\frac{dL_2^2}{dt} = kH^*V^*\left[\frac{HV}{H^*V^*} - \frac{H(t-\tau)V(t-\tau)}{H^*V^*} + \ln\frac{H(t-\tau)V(t-\tau)}{HV}\right].$$

Therefore, the derivative of $L_2(t)$ along the solutions of the system (4.1.1) is

$$\begin{aligned}\frac{dL_2}{dt} &= \frac{dL_2^1}{dt} + \frac{dL_2^2}{dt} \\ &= \mu H^* \left[2 - \frac{H}{H^*} - \frac{H^*}{H}\right] + \\ &\quad \delta I^* \left[4 - \frac{H^*}{H} - \frac{I^*}{I}\frac{H(t-\tau)V(t-\tau)}{H^*V^*} - \frac{ID^*}{I^*D} - \frac{DV^*}{D^*V} + \ln\frac{H(t-\tau)V(t-\tau)}{HV}\right].\end{aligned}$$

Using $n = 2$ in (4.2.10) it follows that

$$2 - \frac{H}{H^*} - \frac{H^*}{H} \leq 0.$$

Taking $p_1 = H^*, p_2 = I^*H(t-\tau)V(t-\tau), p_3 = ID^*, p_4 = DV^*, q_1 = H, q_2 = IH^*V^*, q_3 = I^*D, q_4 = D^*V$ and using (4.2.9) for $n = 4$, we obtain

$$4 - \frac{H^*}{H} - \frac{I^*}{I}\frac{H(t-\tau)V(t-\tau)}{H^*V^*} - \frac{ID^*}{I^*D} - \frac{DV^*}{D^*V} + \ln\frac{H(t-\tau)V(t-\tau)}{HV} \leq 0.$$

Thus, we have $\frac{dL_2}{dt} \leq 0$. Let M be the largest invariant set in $\left\{(H, I, D, V) | \frac{dL_2}{dt} = 0\right\}$. We observe that $\frac{dL_2}{dt} = 0$ if and only if $H = H^*, I = I^*, D = D^*, V = V^*$. Thus, $M = \{E_i\}$. Therefore, by the Lyapunov-LaSalle invariance principle [25, 77], E_i is globally asymptotic stable whenever $R_0 > 1$. □

4.3 The Two-Delay Model

Distributed and two-delay models have been previously reported in case of several viral dynamics models [78, 79, 80, 82, 83]. In [78], several delay differential equations based models for HIV-1 infection were analyzed. In particular, they allowed for a delay in the formation of the virus from the infected T-cells and considered a mathematical setup which could be applicable to hepatitis B and hepatitis C viral dynamics. Similar models of distributed delays were presented and analyzed in [79, 80]. Two-delay models for HIV infection appear in [82, 83]. In [82], a model for HIV infection was considered with time delays appearing in the infectivity of T-cells and the production of effector cells. Wang et al. [83] studied the global properties of a delayed HIV model with Cytotoxic T Lymphocytes (CTLs) immune response. They considered the first delay in the formation of infected T-cells from uninfected ones, akin to the first delay considered here. They incorporated a second delay in the formation of infected macrophages which eventually contributes to the production of the virus. In our case, the second delay, that can be attributed to the delay in the maturation process of the capsids during its life cycle [5, 7], is incorporated in the term for the production of the HBV DNA-containing capsids which in turn contributes to the production of the HBV.

Accordingly, we propose the following two-delay model:

$$\begin{aligned}
\frac{dH(t)}{dt} &= s - kH(t)V(t) - \mu H(t), \\
\frac{dI(t)}{dt} &= kH(t-\tau_1)V(t-\tau_1) - \delta I(t), \\
\frac{dD(t)}{dt} &= aI(t-\tau_2) - \beta D(t) - \delta D(t), \\
\frac{dV(t)}{dt} &= \beta D(t) - cV(t).
\end{aligned} \tag{4.3.1}$$

Let $\sigma = \max\{\tau_1, \tau_2\}$. The initial conditions are $H(\theta) = H_0 > 0$, $I(\theta) = I_0 > 0$, $D(\theta) = D_0 > 0$ and $V(\theta) = V_0 > 0$ for $\theta \in [-\sigma, 0]$. It can be shown that the solutions to the system (4.3.1) subject to positive initial condition remain positive. The two-delay system (4.3.1) has the same steady states as the one-delay system (4.1.1), namely, the uninfected steady state $E_u = \left(H^0, I^0, D^0, V^0\right) = \left(\frac{s}{\mu}, 0, 0, 0\right)$ and the infected steady state $E_i = (H^*, I^*, D^*, V^*)$ which exists provided $R_0 > 1$.

4.4 Global Stability of the Two-Delay Model

In this section, we prove the global asymptotic stability of the two steady states for the two-delay model.

Theorem 4.4.1. *The uninfected steady state E_u is globally asymptotically stable when $R_0 \leq 1$.*

Proof. We define a Lyapunov function $L_3(t)$ as follows:

$$\begin{aligned}
L_3(t) &= H^0\left(\frac{H(t)}{H^0} - 1 - \ln\frac{H(t)}{H^0}\right) + I(t) + \frac{\delta}{a}D(t) + \frac{\delta(\beta+\delta)}{a\beta}V(t) \\
&\quad + k\int_{t-\tau_1}^{t} H(\xi)V(\xi)d\xi + \delta\int_{t-\tau_2}^{t} I(\xi)d\xi.
\end{aligned}$$

The derivative of $L_3(t)$ along the solutions of the system (4.3.1) is

$$\begin{aligned}
\frac{dL_3}{dt} &= \left(1 - \frac{H^0}{H}\right)[s - kHV - \mu H] + [kH(t-\tau_1)V(t-\tau_1) - \delta I] + \frac{\delta}{a}[aI(t-\tau_2) - (\beta+\delta)D] \\
&\quad + \frac{\delta(\beta+\delta)}{a\beta}[\beta D - cV] + k[HV - H(t-\tau_1)V(t-\tau_1)] + \delta[I - I(t-\tau_2)] \\
&= s\left[2 - \frac{H}{H^0} - \frac{H^0}{H}\right] + \frac{c\delta(\beta+\delta)}{a\beta}[R_0 - 1]V.
\end{aligned}$$

Now, taking $p_1 = H, p_2 = H^0, q_1 = H^0, q_2 = H$ and using the inequality (4.2.10) for $n = 2$, we obtain

$$2 - \frac{H}{H^0} - \frac{H^0}{H} \leq 0.$$

Thus, when $R_0 \leq 1$ then $\frac{dL_3}{dt} \leq 0$. Let M be the largest invariant set in $\{(H, I, D, V) | \frac{dL_3}{dt} = 0\}$. We observe that $\frac{dL_3}{dt} = 0$ if and only if $H = H^0 = \frac{s}{\mu}, I = 0, D = 0$, and $V = 0$. Thus,

$M = \{E_u\} = \{(\frac{s}{\mu}, 0, 0, 0)\}$. Therefore, by the Lyapunov-LaSalle invariance principle [25, 77], E_u is globally asymptotically stable whenever $R_0 \leq 1$. □

Theorem 4.4.2. *The infected steady state E_i is globally asymptotically stable when $R_0 > 1$.*

Proof. We define a Lyapunov function $L_4(t)$ as follows:

$$\begin{aligned} L_4(t) &= H^*\left(\frac{H(t)}{H^*} - 1 - \ln\frac{H(t)}{H^*}\right) + I^*\left(\frac{I(t)}{I^*} - 1 - \ln\frac{I(t)}{I^*}\right) + \frac{\delta}{a}D^*\left(\frac{D(t)}{D^*} - 1 - \ln\frac{D(t)}{D^*}\right) \\ &\quad + \frac{\delta(\beta+\delta)}{a\beta}V^*\left(\frac{V(t)}{V^*} - 1 - \ln\frac{V(t)}{V^*}\right) + kH^*V^*\int_{t-\tau_1}^{t} G\left(\frac{H(\xi)V(\xi)}{H^*V^*}\right)d\xi \\ &\quad + \delta I^*\int_{t-\tau_2}^{t} G\left(\frac{I(\xi)}{I^*}\right)d\xi \\ &= L_4^1(t) + L_4^2(t) + L_4^3(t), \end{aligned}$$

where

$$\begin{aligned} L_4^1(t) &= H^*\left(\frac{H(t)}{H^*} - 1 - \ln\frac{H(t)}{H^*}\right) + I^*\left(\frac{I(t)}{I^*} - 1 - \ln\frac{I(t)}{I^*}\right) + \frac{\delta}{a}D^*\left(\frac{D(t)}{D^*} - 1 - \ln\frac{D(t)}{D^*}\right) \\ &\quad + \frac{\delta(\beta+\delta)}{a\beta}V^*\left(\frac{V(t)}{V^*} - 1 - \ln\frac{V(t)}{V^*}\right), \\ L_4^2(t) &= kH^*V^*\int_{t-\tau_1}^{t} G\left(\frac{H(\xi)V(\xi)}{H^*V^*}\right)d\xi, \\ L_4^3(t) &= \delta I^*\int_{t-\tau_2}^{t} G\left(\frac{I(\xi)}{I^*}\right)d\xi. \end{aligned}$$

The derivative of $L_4^1(t)$ along the solutions of the system (4.3.1) is

$$\begin{aligned}
\frac{dL_4^1}{dt} &= \left(1-\frac{H^*}{H}\right)\frac{dH}{dt}+\left(1-\frac{I^*}{I}\right)\frac{dI}{dt}+\frac{\delta}{a}\left(1-\frac{D^*}{D}\right)\frac{dD}{dt}+\frac{\delta(\beta+\delta)}{a\beta}\left(1-\frac{V^*}{V}\right)\frac{dV}{dt}\\
&= \left(1-\frac{H^*}{H}\right)[s-kHV-\mu H]+\left(1-\frac{I^*}{I}\right)[kH(t-\tau_1)V(t-\tau_1)-\delta I]\\
&\quad +\frac{\delta}{a}\left(1-\frac{D^*}{D}\right)[aI(t-\tau_2)-(\beta+\delta)D]+\frac{\delta(\beta+\delta)}{a\beta}\left(1-\frac{V^*}{V}\right)[\beta D-cV]\\
&= \left(1-\frac{H^*}{H}\right)[s-kHV-\mu H]+\left(1-\frac{I^*}{I}\right)[kHV-\delta I]\\
&\quad +\frac{\delta}{a}\left(1-\frac{D^*}{D}\right)[aI-(\beta+\delta)D]+\frac{\delta(\beta+\delta)}{a\beta}\left(1-\frac{V^*}{V}\right)[\beta D-cV]\\
&\quad +k\left(1-\frac{I^*}{I}\right)(H(t-\tau_1)V(t-\tau_1)-HV)+\delta\left(1-\frac{D^*}{D}\right)(I(t-\tau_2)-I)\\
&= \mu H^*\left[2-\frac{H}{H^*}-\frac{H^*}{H}\right]+\delta I^*\left[4-\frac{H^*}{H}-\frac{I^*}{I}\frac{HV}{H^*V^*}-\frac{ID^*}{I^*D}-\frac{DV^*}{D^*V}\right]\\
&\quad +k\left(1-\frac{I^*}{I}\right)(H(t-\tau_1)V(t-\tau_1)-HV)+\delta\left(1-\frac{D^*}{D}\right)(I(t-\tau_2)-I)\\
&= \mu H^*\left[2-\frac{H}{H^*}-\frac{H^*}{H}\right]+\delta I^*\left[4-\frac{H^*}{H}-\frac{I^*}{I}\frac{H(t-\tau_1)V(t-\tau_1)}{H^*V^*}-\frac{D^*}{D}\frac{I(t-\tau_2)}{I^*}-\frac{DV^*}{D^*V}\right]\\
&\quad +kH^*V^*\left[\frac{H(t-\tau_1)V(t-\tau_1)}{H^*V^*}-\frac{HV}{H^*V^*}\right]+\delta I^*\left[\frac{I(t-\tau_2)}{I^*}-\frac{I}{I^*}\right].
\end{aligned}$$

Also,

$$\begin{aligned}
\frac{dL_4^2}{dt} &= kH^*V^*\left[\frac{HV}{H^*V^*}-\frac{H(t-\tau_1)V(t-\tau_1)}{H^*V^*}+\ln\frac{H(t-\tau_1)V(t-\tau_1)}{HV}\right],\\
\frac{dL_4^3}{dt} &= \delta I^*\left[\frac{I}{I^*}-\frac{I(t-\tau_2)}{I^*}+\ln\frac{I(t-\tau_2)}{I}\right].
\end{aligned}$$

Therefore, the derivative of $L_4(t)$ along the solutions of the system (4.3.1) is

$$\begin{aligned}
\frac{dL_4}{dt} &= \frac{dL_4^1}{dt}+\frac{dL_4^2}{dt}+\frac{dL_4^3}{dt}\\
&= \mu H^*\left[2-\frac{H}{H^*}-\frac{H^*}{H}\right]+\delta I^*\left[4-\frac{H^*}{H}-\frac{I^*}{I}\frac{H(t-\tau_1)V(t-\tau_1)}{H^*V^*}-\frac{D^*}{D}\frac{I(t-\tau_2)}{I^*}\right.\\
&\quad \left.-\frac{DV^*}{D^*V}+\ln\frac{H(t-\tau_1)V(t-\tau_1)I(t-\tau_2)}{HVI}\right].
\end{aligned}$$

Using $n=2$ in (4.2.10) it follows that

$$2-\frac{H}{H^*}-\frac{H^*}{H}\le 0.$$

Taking $p_1=H^*, p_2=I^*H(t-\tau_1)V(t-\tau_1), p_3=I(t-\tau_2)D^*, p_4=DV^*, q_1=H, q_2=IH^*V^*, q_3=I^*D, q_4=D^*V$ and using (4.2.9) for $n=4$, we obtain

$$4-\frac{H^*}{H}-\frac{I^*}{I}\frac{H(t-\tau_1)V(t-\tau_1)}{H^*V^*}-\frac{D^*}{D}\frac{I(t-\tau_2)}{I^*}-\frac{DV^*}{D^*V}+\ln\frac{H(t-\tau_1)V(t-\tau_1)I(t-\tau_2)}{HVI}\le 0.$$

Thus, we have $\frac{dL_4}{dt} \leq 0$. Let M be the largest invariant set in $\left\{(H, I, D, V) | \frac{dL_4}{dt} = 0\right\}$. We observe that $\frac{dL_4}{dt} = 0$ if and only if $H = H^*, I = I^*, D = D^*, V = V^*$. Thus, $M = \{E_i\}$. Therefore, by the Lyapunov-LaSalle invariance principle [25, 77], E_i is globally asymptotic stable whenever $R_0 > 1$. □

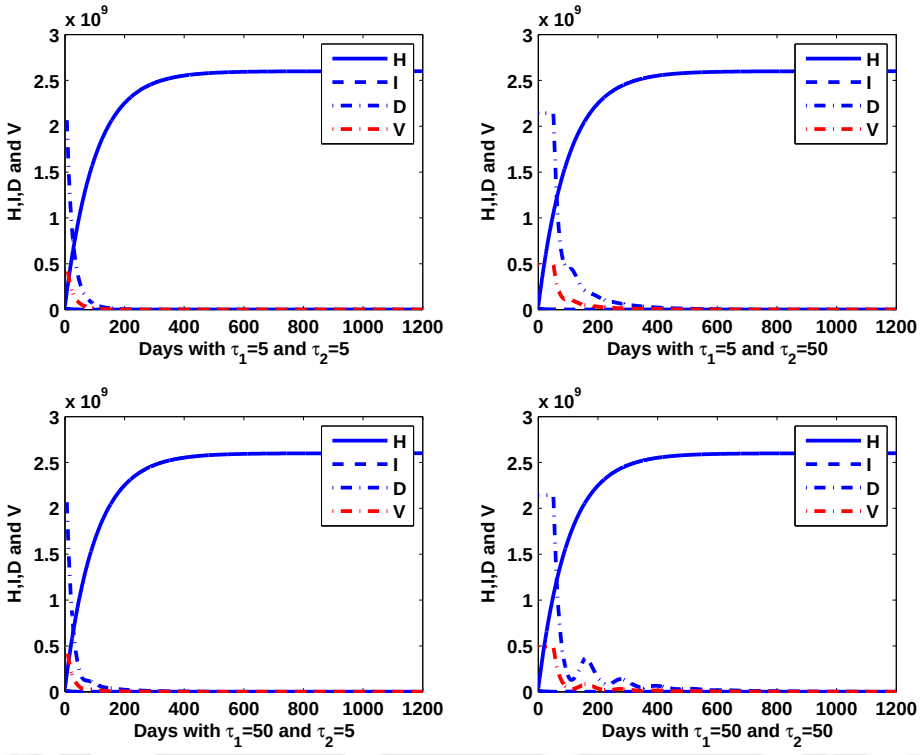

Figure 4.1: Dynamics of the model (4.3.1) when $R_0 = 0.5476 \leq 1$ with four sets of delays $(\tau_1, \tau_2) = \{(5, 5), (5, 50), (50, 5), (50, 50)\}$ in days respectively.

4.5 Numerical Results

In this section, we numerically illustrate and confirm the results of global stability analysis. We first consider the case $R_0 \leq 1$. Accordingly the model parameters used were $s = 2.6 \times 10^7$ cells day^{-1} $k = 3 \times 10^{-13}$ day^{-1} virion^{-1}, $\mu = 0.01$ day^{-1} $\delta = 0.053$ day^{-1}, $a = 150$ day^{-1}, $\beta = 0.87$ day^{-1} and $c = 3.8$ day^{-1} as in the previous chapter, which results in $R_0 = 0.5476 < 1$. For this case, one would expect that the uninfected steady state is asymptotically stable. In fact this holds true when there is one-delay as well two delays. The dynamics of the system (4.3.1) was observed for several time windows as well time delays. For illustrative purpose we present the observations for a duration of 1200 days. We considered several sets of time delays for both the infectivity of the hepatocytes as well as the one arising from the maturation process during the life cycle of the capsids. The

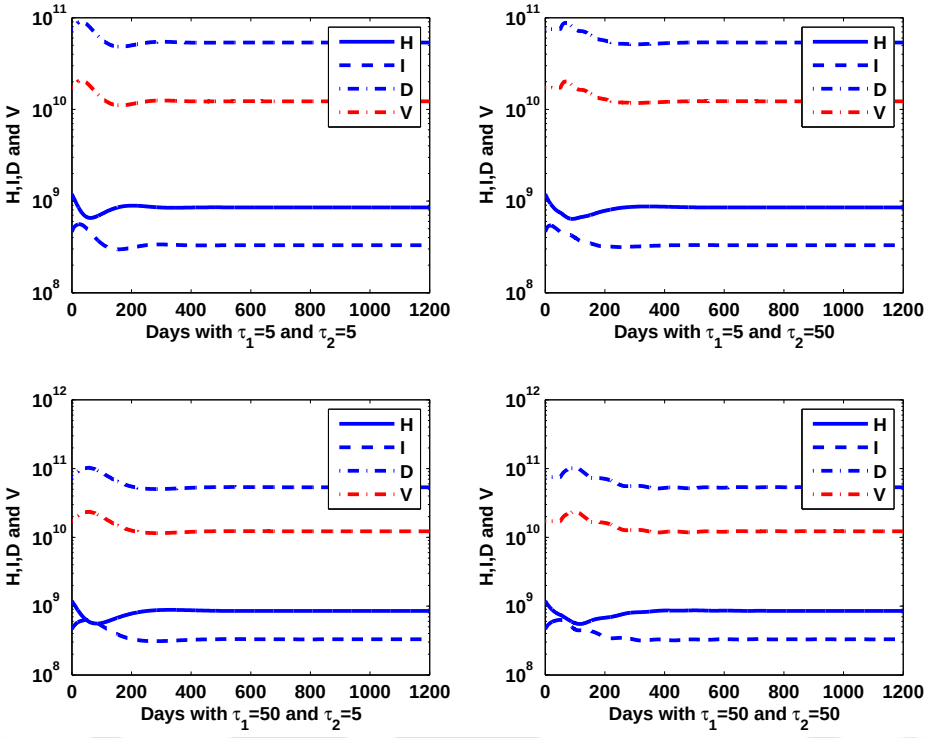

Figure 4.2: Dynamics of the model (4.3.1) when $R_0 = 3.0482 > 1$ with four sets of delays $(\tau_1, \tau_2) = \{(5,5),(5,50),(50,5),(50,50)\}$ in days respectively.

typical length of incubation period for acute HBV could last from $1-6$ months post exposure [84]. Guo et al. [85] studied the molecular pathway of cccDNA formation and reported the detection of the core DNA after $2-4$ days with higher level of capsid DNA being observed after 7 days of tetracycline removal. Taking a cue from these clinical observations, we consider time delays of 5 days and 50 days for our numerical illustration. Accordingly, we chose four sets of time delays (in days), namely, $(\tau_1, \tau_2) = \{(5,5),(5,50),(50,5),(50,50)\}$. In all these cases, it can be seen (from Figure 4.1) that the solutions eventually approach the uninfected steady state, as predicted by the theoretical results in case of $R_0 \leq 1$, resulting in the infection being cleared out. We next consider the scenario when $R_0 > 1$, for which we choose the parameters to be $s = 2.6 \times 10^7$ cells day^{-1} $k = 1.67 \times 10^{-12}$ day^{-1} virion^{-1}, $\mu = 0.01$ day^{-1} $\delta = 0.053$ day^{-1}, $a = 150$ day^{-1}, $\beta = 0.87$ day^{-1} and $c = 3.8$ day^{-1} (as taken in the previous chapter), resulting in $R_0 = 3.0482 > 1$. We again make an observation of the time window of 1200 days with the four sets of time delays considered previously. The evolution of the dynamics (as can be seen in Figure 4.2) shows that the system eventually converges towards the infected steady state and the infection will persist, in absence of therapeutic intervention.

4.6 Conclusion

In this chapter, we studied the global dynamics of a HBV model (with intracellular HBV DNA-containing capsids) by incorporating one and two discrete delays. For the one-delay model, we incorporated the delay in the process of infectivity, that is, the production of productively infected hepatocytes from the uninfected hepatocytes. For the two-delay model, an additional delay term, resulting from the life-cycle induced delay in the production of capsids from infected hepatocytes, was included. The global stability analysis was accomplished through the construction of Lyapunov functions and using the Lyapunov-LaSalle invariance principle and the results were obtained in term of the basic reproduction number. The results for the one-delay model suggests that the delay involved in the production of the productively infected hepatocytes does not induce any periodic oscillation and the occurrence of Hopf bifurcations are also ruled out. The introduction of the second delay was done to make the model formulation more realistic in terms of the life-cycle of the capsids as well as to investigate if the both delays could potentially lead to periodic oscillations and Hopf bifurcations. Interestingly, the two-delay model confirms that the inclusion of the second delay does not alter the dynamics of HBV infection progression and also does not cause any oscillation or bifurcation.

Chapter 5

Combination Therapy and Optimal Controls for HBV Infection

In this chapter, we incorporate the combination therapy of PEG IFN and LMV in the model (3.1.1). We analyze the existence and local stability of the steady states and determine the critical drug efficacy in terms of model parameters. Further, we consider the time dependent drug efficacies and formulate an optimal control problem keeping the biomedical goals in mind. We show the existence of the optimal controls and characterize them using the Pontryagin's maximum principle. We also prove the uniqueness of the optimal controls for a sufficiently small time interval. Finally, the theoretical results obtained are numerically illustrated.

5.1 Mathematical Model

In this section, we extend the model (3.1.1) to include the therapeutic effects of treatment by including the efficacies of PEG IFN and LMV. We denote the levels of uninfected hepatocytes, infected hepatocytes, intracellular HBV DNA-containing capsids and HBV at time t by $H(t)$, $I(t)$, $D(t)$and $V(t)$, respectively and propose the following model :

$$\begin{aligned}
\frac{dH(t)}{dt} &= s-(1-u_1)kH(t)V(t)-\mu H(t),\\
\frac{dI(t)}{dt} &= (1-u_1)kH(t)V(t)-\delta I(t),\\
\frac{dD(t)}{dt} &= (1-u_2)aI(t)-\beta D(t)-\delta D(t),\\
\frac{dV(t)}{dt} &= \beta D(t)-cV(t),
\end{aligned} \tag{5.1.1}$$

with the initial conditions $H(0)=H_0>0$, $I(0)=I_0>0$, $D(0)=D_0>0$ and $V(0)=V_0>0$. Here u_1 and u_2 denote the efficacies of PEG IFN and LMV respectively with $u_i\in(0,1)$ for $i=1,2$. All the parameters of the model (5.1.1) are same as in the Chapter 3. We observe that the term $(1-u_1)$ reflects the efficacy of PEG IFN in blocking the infection of the hepatocytes in the liver.

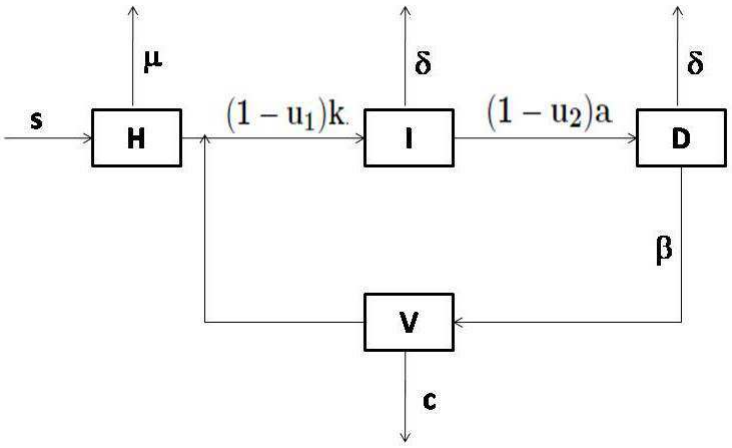

Figure 5.1: Schematic diagram of HBV infection with combination therapy.

Also the factor $(1 - u_2)$ indicates the extent to which the production of intracellular HBV DNA-containing capsids is blocked by as a result of administration of LMV. A schematic representation of the model (5.1.1) is given in Figure 5.1. Also it is reasonable to assume that $\mu \leq \delta$, since $\mu > \delta$ would mean a higher natural death rate of uninfected hepatocytes as compared to infected hepatocytes, thereby significantly diminishing the chance of patient survival due to diminishing levels of uninfected hepatocytes as in the Chapter 3.

5.2 Qualitative Analysis of the Model

5.2.1 Positivity and Boundedness

It can be shown (using vector field analysis) that the solutions to the system (5.1.1) are positive for positive initial conditions. We now examine the boundedness of the solutions to the system (5.1.1) with positive initial conditions [61]. For this purpose we introduce the variable, $X(t) = H(t) + I(t)$. Adding the first two equations of (5.1.1) and using the condition $\mu \leq \delta$, we get

$$\frac{dX}{dt} = s - \mu H - \delta I \leq s - \mu(H + I) \leq s - \mu X.$$

Thus,

$$\limsup_{t \to \infty} X(t) \leq \frac{s}{\mu}.$$

Since $X(t) = H(t) + I(t)$, therefore, we have $\limsup_{t\to\infty} H(t) \leq \frac{s}{\mu}$ and $\limsup_{t\to\infty} I(t) \leq \frac{s}{\mu}$, which implies $H(t) \leq \frac{s}{\mu}$ and $I(t) \leq \frac{s}{\mu}$. The equation for $D(t)$ in (5.1.1) along with $I(t) \leq \frac{s}{\mu}$ gives

$$\begin{aligned} & \frac{dD}{dt} \leq \frac{as(1-u_2)}{\mu} - \beta D - \delta D \\ \Rightarrow \quad & \limsup_{t\to\infty} D(t) \leq \frac{as(1-u_2)}{\mu(\beta+\delta)} \\ \Rightarrow \quad & D(t) \leq \frac{as(1-u_2)}{\mu(\beta+\delta)}. \end{aligned}$$

In a similar way, we obtain

$$\begin{aligned} & \frac{dV}{dt} \leq \frac{a\beta s(1-u_2)}{\mu(\beta+\delta)} - cV \\ \Rightarrow \quad & \limsup_{t\to\infty} V(t) \leq \frac{a\beta s(1-u_2)}{c\mu(\beta+\delta)} \\ \Rightarrow \quad & V(t) \leq \frac{a\beta s(1-u_2)}{c\mu(\beta+\delta)}. \end{aligned}$$

Hence, all the populations in the model (5.1.1) are bounded and we have the following closed and bounded, positively invariant set

$$\mathcal{D} = \left\{(H, I, D, V) \in \mathbb{R}^4_+ : 0 \leq H, I \leq \frac{s}{\mu}, 0 \leq D \leq \frac{as(1-u_2)}{\mu(\beta+\delta)}, 0 \leq V \leq \frac{a\beta s(1-u_2)}{c\mu(\beta+\delta)}\right\}$$

with respect to (5.1.1), where $\mathbb{R}^4_+ = \{(H, I, D, V) : H \geq 0, I \geq 0, D \geq 0, V \geq 0\}$.

5.2.2 Equilibria

The model (5.1.1) admits two steady states that are typical for models in viral dynamics, namely, the uninfected steady state $E_u = \left(\frac{s}{\mu}, 0, 0, 0\right)$ and the infected steady state $E_i = (H^*, I^*, D^*, V^*)$, where

$$H^* = \frac{c\delta(\beta+\delta)}{a\beta k(1-u_1)(1-u_2)}, \; V^* = \left[\frac{a\beta s(1-u_2)}{c\delta(\beta+\delta)} - \frac{\mu}{k(1-u_1)}\right], \; D^* = \left[\frac{c}{\beta}\right] V^* \text{ and } I^* = \left[\frac{\beta+\delta}{a(1-u_2)}\right] D^*.$$

The condition for the existence of the infected steady state E_i is given in terms of the basic reproduction number,

$$R_0 = \frac{a\beta sk(1-u_1)(1-u_2)}{c\delta\mu(\beta+\delta)} > 1.$$

5.2.3 Local Stability Analysis

In order to carry out the local stability analysis of both the steady states, we need the Jacobian, J of the system (5.1.1) given by

$$J = \begin{bmatrix} -(1-u_1)kV - \mu & 0 & 0 & -(1-u_1)kH \\ (1-u_1)kV & -\delta & 0 & (1-u_1)kH \\ 0 & (1-u_2)a & -(\beta+\delta) & 0 \\ 0 & 0 & \beta & -c \end{bmatrix}.$$

We present the stability conditions of E_u and E_i in terms of the following two theorems.

Theorem 5.2.1. *The uninfected steady state E_u is locally asymptotically stable when $R_0 < 1$ and is unstable when $R_0 > 1$.*

Proof. The characteristic equation resulting from J being evaluated at E_u is given by

$$(\lambda+\mu)\left[(\lambda+\delta)(\lambda+c)(\lambda+\beta+\delta)-\frac{a\beta sk(1-u_1)(1-u_2)}{\mu}\right]=0.$$

The eigenvalues are given by $\lambda=-\mu<0$ and the solutions of the following cubic equation

$$\lambda^3+A\lambda^2+B\lambda+C=0,$$

where

$$A=(\beta+2\delta+c),\ B=[(\delta+c)(\beta+\delta)+c\delta] \text{ and } C=\left[\delta(\beta+\delta)c-\frac{a\beta sk(1-u_1)(1-u_2)}{\mu}\right].$$

Two of the conditions of Routh-Hurwitz criterion, namely, $A>0$ and

$$AB-C=(\beta+2\delta+c)\left[(\delta+c)(\beta+\delta)+c\delta\right]-\delta(\beta+\delta)c+\frac{a\beta sk(1-u_1)(1-u_2)}{\mu}>0$$

are satisfied. The last condition of Routh-Hurwitz criterion, $C=\delta(\beta+\delta)c-\frac{a\beta sk(1-u_1)(1-u_2)}{\mu}>0$ is equivalent to $R_0=\frac{a\beta sk(1-u_1)(1-u_2)}{c\delta\mu(\beta+\delta)}<1$. Thus all the conditions of Routh-Hurwitz criterion are satisfied for $R_0<1$ and hence, E_u is locally asymptotically stable for $R_0<1$. In the case of $R_0>1$, at least one of the roots of the characteristic equation will be positive resulting in E_u being unstable. □

Theorem 5.2.2. *The infected steady state E_i is locally asymptotically stable when $R_0 > 1$.*

Proof. The characteristic equation resulting from J being evaluated at E_i is given by

$$\lambda^4+A_3\lambda^3+A_2\lambda^2+A_1\lambda+A_0=0,$$

where

$$A_3=((1-u_1)kV^*+\mu+\beta+2\delta+c),\ A_2=(\delta+c)(\beta+\delta)+c\delta+((1-u_1)kV^*+\mu)(c+\beta+2\delta),$$

$$A_1=[(c+\delta)(\beta+\delta)+c\delta]((1-u_1)kV^*+\mu)+c\delta(\beta+\delta)-(1-u_1)(1-u_2)a\beta kH^*$$

$$\text{and } A_0=c\delta(\beta+\delta)((1-u_1)kV^*+\mu)-(1-u_1)(1-u_2)a\beta\mu kH^*.$$

In order for the roots of the characteristic equation to have negative real parts, the Routh-Hurwitz criterion, namely, $A_3>0$, $A_0>0$, $A_3A_2-A_1>0$ and $(A_3A_2-A_1)A_1-A_3^2A_0>0$ must be satisfied. It can be easily verified that all these four conditions are satisfied provided $R_0>1$. Hence, E_i is locally asymptotically stable for $R_0>1$. □

5.2.4 Critical Drug Efficacy

In the system (5.1.1), the efficacies of PEG IFN and LMV are incorporated through the terms $(1-u_1)$ and $(1-u_2)$ respectively. The values, $u_i = 0$ and $u_i = 1$, reflect completely ineffective and perfectly effective therapy respectively. For brevity, the efficacies of PEG IFN and LMV are combined to obtain a new term to reflect the overall efficacy for this combination therapy and is given by $1-u = (1-u_1)(1-u_2)$ [6, 27]. This choice is motivated by the condition for stability of E_u and E_i. Recalling that the stability criterion for E_u is $R_0 < 1$, which equivalent to

$$\frac{a\beta sk(1-u_1)(1-u_2)}{c\delta\mu(\beta+\delta)} < 1 \quad \Rightarrow \quad (1-u_1)(1-u_2) < \frac{c\delta\mu(\beta+\delta)}{a\beta sk} \Rightarrow 1-u < \frac{c\delta\mu(\beta+\delta)}{a\beta sk}.$$

Similarly the condition $R_0 > 1$, for E_i to be stable is equivalent to

$$\frac{a\beta sk(1-u_1)(1-u_2)}{c\delta\mu(\beta+\delta)} > 1 \quad \Rightarrow \quad (1-u_1)(1-u_2) > \frac{c\delta\mu(\beta+\delta)}{a\beta sk} \Rightarrow 1-u > \frac{c\delta\mu(\beta+\delta)}{a\beta sk}.$$

Thus, there is a transcritical bifurcation point given by

$$1-u \quad = \quad \frac{c\delta\mu(\beta+\delta)}{a\beta sk}.$$

Motivated by this we define the critical efficacy, u_{crit} by

$$u_{crit} \quad = \quad 1-\frac{c\delta\mu(\beta+\delta)}{a\beta sk}.$$

Thus, in order to achieve a successful therapy by way of elimination of HBV, *i.e.,* the uninfected steady state being stable we need $u > u_{crit}$. On the other hand, whenever $u < u_{crit}$, the infected steady state E_i remains stable and the infection persists. Before the initiation of the therapy, the infected steady state obviously exists and $u_1 = 0$, $u_2 = 0$, which means that $R_0 > 1 (\equiv u < u_{crit})$ and the infection persists. The goal is to choose u_1 and u_2 so that the condition $u < u_{crit}$ changes to the condition $u > u_{crit} (\equiv R_0 < 1)$ thereby resulting in a stable uninfected steady state.

5.3 The Optimal Control Problem

In this section, we present an optimal control problem involving the uninfected hepatocytes, infected hepatocytes, intracellular HBV DNA-containing capsids and HBV along with the combination therapy. The problem involves the formulation of an objective functional with the goal of minimizing $I(t)$, $D(t)$ and $V(t)$ as well as the therapeutic cost of the controlled treatment. Accordingly, the objective functional which we seek to minimize is defined by :

$$\mathcal{J}(u_1,u_2) \quad = \quad \frac{1}{2}\int_0^T [Q_2 I^2(t) + Q_3 D^2(t) + Q_4 V^2(t) + R_1 u_1^2(t) + R_2 u_2^2(t)]dt. \qquad (5.3.1)$$

The coefficients Q_2, Q_3, Q_4 are the cost coefficients [43] for $I(t)$, $D(t)$ and $V(t)$, respectively. Also, R_1 and R_2 represent the financial and physiological costs associated with the administration

of PEG IFN and LMV respectively. The coefficients $R_1 > 0$, $R_2 > 0$ reflect the extent of toxicity of the administered drugs. Note that while u_1 and u_2 were taken as constant in the preceding discussion on local stability analysis and critical efficacy, these are now considered as functions of time, since the goal is to determine the optimal treatment strategy over a period of time. The quadratic terms $u_1^2(t)$ and $u_2^2(t)$ reflect the expectation that the side-effects of the drugs are nonlinear [30, 36, 86]. The objective functional is set up so as to encapsulate a balance between therapeutic effectiveness and side-effects. The usage of therapy with the goal of higher efficacy could be limited by the associated physiological and financial costs. The apparent competing nature of the terms is essential to strike a balance between therapeutic efficacy and associated costs [40, 43].

The control set is defined as

$$\mathcal{U} = \{(u_1, u_2) | u_i \text{ is measurable}, a_i \leq u_i \leq b_i, t \in [0, T], \text{for } i = 1, 2\},$$

where $0 < a_i \leq u_i \leq b_i < 1$ for $i = 1, 2$. Here a_i and b_i act as the lower and upper bound on the therapeutic efficacy u_i.

The goal of the problem thus is to determine the optimal control pair, (u_1^*, u_2^*) such that

$$\mathcal{J}(u_1^*, u_2^*) = \min\{\mathcal{J}(u_1, u_2) | (u_1, u_2) \in \mathcal{U}\}$$

subject to state constraints

$$\begin{aligned}
\frac{dH(t)}{dt} &= s - (1 - u_1(t))kH(t)V(t) - \mu H(t), \\
\frac{dI(t)}{dt} &= (1 - u_1(t))kH(t)V(t) - \delta I(t), \\
\frac{dD(t)}{dt} &= (1 - u_2(t))aI(t) - \beta D(t) - \delta D(t), \\
\frac{dV(t)}{dt} &= \beta D(t) - cV(t),
\end{aligned} \tag{5.3.2}$$

with the initial conditions $H(0) = H_0 > 0$, $I(0) = I_0 > 0$, $D(0) = D_0 > 0$ and $V(0) = V_0 > 0$.

5.4 Existence of an Optimal Control Pair

In order to prove the existence of an optimal control pair and uniqueness of the optimality system we need the upper bounds on the state variables [87]. Making use of the relation $H(t) \leq \frac{s}{\mu}$, the upper bounds on the solutions of the state system are obtained. In order to prove this, we observe that the super-solutions $\overline{I}$, $\overline{D}$ and $\overline{V}$ [38] satisfying

$$\begin{aligned}
\frac{d\overline{I}}{dt} &= \frac{ks\overline{V}}{\mu}, \\
\frac{d\overline{D}}{dt} &= a\overline{I}, \\
\frac{d\overline{V}}{dt} &= \beta\overline{D},
\end{aligned}$$

are bounded on a finite time interval. Since this system is linear over a finite time interval and has bounded coefficients, therefore the super-solutions $\overline{I}$, $\overline{D}$ and $\overline{V}$ are uniformly bounded [87].

We now proceed on to the proof of existence of an optimal control pair. We prove the sufficient condition using the result of Fleming and Rishel ([88],Theorem 4.1, Page $68-69$) as used in [87, 38, 34, 89, 90, 91].

Theorem 5.4.1. *Consider the control problem comprising of the objective functional (5.3.1) and the state system (5.3.2). Then there exists an optimal control pair $\overrightarrow{u}^* = (u_1^*, u_2^*) \in \mathcal{U}$ such that*

$$\mathcal{J}(u_1^*, u_2^*) = \min_{(u_1,u_2)\in\mathcal{U}} \mathcal{J}(u_1, u_2),$$

provided the following conditions hold :

1. *The class of all initial conditions with a control pair $\overrightarrow{u} = (u_1, u_2)$ in the admissible control set $\mathcal{U}$ along with the state system (5.3.2) being satisfied is not empty.*
2. *The admissible control set $\mathcal{U}$ is closed and convex.*
3. *The right-hand side of each equation of (5.3.2) is continuous, is bounded above by a sum of the bounded control and the state, and can be written as a linear function of a control pair (u_1, u_2) with coefficients depending on time and state.*
4. *The integrand of (5.3.1) is convex on $\mathcal{U}$ and is bounded below by $-c_0 + c_1(|u_1|^2 + |u_2|^2)$, where $c_0 \geq 0$ and $c_1 > 0$.*

Proof. 1. For the given optimal control problem, we have seen that the system has a bounded solution for an initial condition. Thus, this part is proved.

2. By definition, the admissible control set $\mathcal{U}$ is closed and convex.

3. It can be easily seen that the right-hand side of the each equation of (5.3.2) is continuous and can be written as :

$$\overrightarrow{f}(t, \overrightarrow{x}, \overrightarrow{u}) = \overrightarrow{\varphi}(t, \overrightarrow{x}) + \overrightarrow{\chi}(t, \overrightarrow{x})\overrightarrow{u}.$$

Since the system is bilinear in u_1, u_2 and the solutions of the system (5.3.2) are bounded, we have

$$|\overrightarrow{f}(t, \overrightarrow{x}, \overrightarrow{u})| \leq C(1 + |\overrightarrow{x}| + |\overrightarrow{u}|), \text{ for } 0 \leq t \leq T,$$

where $\overrightarrow{x} = (H, I, D, V)$ and $\overrightarrow{u} = (u_1, u_2)$ and C depends on the coefficients of the state system (5.3.2).

4. For the last part, let L be the integrand of the objective functional. Let $\overrightarrow{x} = (H, I, D, V)$ be the state vector and $\overrightarrow{u} = (u_1, u_2)$ and $\overrightarrow{v} = (v_1, v_2)$ be two control vectors. Then (for $0 < \varepsilon < 1$),

$$\begin{aligned} & L(\overrightarrow{x}, (1-\varepsilon)\overrightarrow{u} + \varepsilon\overrightarrow{v}, t) - [(1-\varepsilon)L(\overrightarrow{x}, \overrightarrow{u}, t) + \varepsilon L(\overrightarrow{x}, \overrightarrow{v}, t)] \\ = & \frac{1}{2}\left[Q_2 I^2(t) + Q_3 D^2(t) + Q_4 V^2(t) + \sum_{i=1}^{2} R_i((1-\varepsilon)u_i + \varepsilon v_i)^2\right] \\ & -\frac{1}{2}\left[Q_2 I^2(t) + Q_3 D^2(t) + Q_4 V^2(t) + \sum_{i=1}^{2} R_i((1-\varepsilon)u_i^2 + \varepsilon v_i^2)\right] \\ = & \frac{1}{2}\left[\sum_{i=1}^{2}\{R_i((1-\varepsilon)u_i + \varepsilon v_i)^2 - ((1-\varepsilon)R_i u_i^2 + \varepsilon R_i v i^2)\}\right] \\ = & -\frac{1}{2}\sum_{i=1}^{2} R_i(1-\varepsilon)\varepsilon(u_i - v_i)^2 \leq 0. \end{aligned}$$

Thus, L is convex on $\mathcal{U}$. Now,

$$\begin{aligned} & \frac{1}{2}[Q_2 I^2(t) + Q_3 D^2(t) + Q_4 V^2(t) + R_1 u_1^2(t) + R_2 u_2^2(t)] \\ \geq & \frac{1}{2}\sum_{i=1}^{2} R_i u_i^2 \geq -c_0 + c_1(|u_1|^2 + |u_2|^2), \end{aligned}$$

where c_0 is any nonnegative real number and $c_1 = \frac{1}{2}\min\{R_1, R_2\}$. Therefore, this part is also satisfied.

Therefore, there exists an optimal control pair $\overrightarrow{u}^* = (u_1^*, u_2^*)$ such that

$$\mathcal{J}(u_1^*, u_2^*) = \min_{(u_1,u_2)\in\mathcal{U}} \mathcal{J}(u_1, u_2).$$

□

5.5 Characterization of Optimal Control

We have already proved the existence of an optimal control pair which minimizes the functional (5.3.1) subject to (5.3.2). We now use Pontryagin's maximum principle to derive the necessary conditions for the optimal control. Accordingly the Lagrangian for this control problem is defined as [38, 92] :

$$\begin{aligned} & \mathcal{L}(H, I, D, V, u_1, u_2, \lambda_1, \lambda_2, \lambda_3, \lambda_4, w_{11}, w_{12}, w_{21}, w_{22}) \\ = & \frac{1}{2}[Q_2 I^2(t) + Q_3 D^2(t) + Q_4 V^2(t) + R_1 u_1^2(t) + R_2 u_2^2(t)] \\ & +\lambda_1[s - (1-u_1(t))kH(t)V(t) - \mu H(t)] + \lambda_2[(1-u_1(t))kH(t)V(t) - \delta I(t)] \\ & +\lambda_3[(1-u_2(t))aI(t) - \beta D(t) - \delta D(t)] + \lambda_4[\beta D(t) - cV(t)] \\ & -w_{11}(t)(b_1 - u_1(t)) - w_{12}(t)(u_1(t) - a_1) - w_{21}(t)(b_2 - u_2(t)) - w_{22}(t)(u_2(t) - a_2), \end{aligned}$$

where $w_{11}(t), w_{12}(t), w_{21}(t), w_{22}(t) \geq 0$ are penalty multipliers satisfying

$$w_{11}(t)(b_1 - u_1) = 0, w_{12}(t)(u_1 - a_1) = 0 \text{ at } u_1^*$$

and

$$w_{21}(t)(b_2 - u_2) = 0, w_{22}(t)(u_2 - a_2) = 0 \text{ at } u_2^*.$$

Using the Pontryagin's maximum principle we obtain the state equations (5.3.2) as well as the co-state or adjoint equations given by :

$$\begin{aligned}
\lambda_1' &= -\frac{\partial \mathcal{L}}{\partial H} = \lambda_1[k(1-u_1)V + \mu] - \lambda_2[k(1-u_1)V], \\
\lambda_2' &= -\frac{\partial \mathcal{L}}{\partial I} = -Q_2 I + \lambda_2[\delta] - \lambda_3[a(1-u_2)], \\
\lambda_3' &= -\frac{\partial \mathcal{L}}{\partial D} = -Q_3 D + \lambda_3[\beta + \delta] - \lambda_4[\beta], \\
\lambda_4' &= -\frac{\partial \mathcal{L}}{\partial V} = -Q_4 V + \lambda_1[k(1-u_1)H] - \lambda_2[k(1-u_1)H] + \lambda_4[c].
\end{aligned} \tag{5.5.1}$$

The adjoint variables satisfy the transversality conditions $\lambda_i(T) = 0$ for $i = 1, 2, 3, 4$. The conditions for determining the optimal controls can be obtained by setting $\frac{\partial \mathcal{L}}{\partial u_i} = 0$, for $i = 1, 2$. That is,

$$\begin{aligned}
\frac{\partial \mathcal{L}}{\partial u_1} &= R_1 u_1(t) + \lambda_1 kHV - \lambda_2 kHV + w_{11}(t) - w_{12}(t) = 0, \\
\frac{\partial \mathcal{L}}{\partial u_2} &= R_2 u_2(t) - \lambda_3 aI + w_{21}(t) - w_{22}(t) = 0.
\end{aligned}$$

Solving these two equations, we obtain the optimal controls

$$\begin{aligned}
u_1^*(t) &= \frac{(\lambda_2 - \lambda_1)kHV - w_{11}(t) + w_{12}(t)}{R_1}, \\
u_2^*(t) &= \frac{\lambda_3 aI - w_{21}(t) + w_{22}(t)}{R_2}.
\end{aligned}$$

Now there are three possible cases for u_1^* resulting from the condition $a_1 \leq u_1 \leq b_1$:

1. When $u_1^*(t) = a_1$, then $w_{11}(t) = 0$. Therefore,

$$a_1 = u_1^*(t) = \frac{(\lambda_2 - \lambda_1)kHV + w_{12}(t)}{R_1}.$$

   Now,

$$R_1 a_1 - (\lambda_2 - \lambda_1)kHV = w_{12}(t) \geq 0 \Rightarrow a_1 \geq \frac{(\lambda_2 - \lambda_1)kHV}{R_1}.$$

2. When $a_1 < u_1^*(t) < b_1$, then $w_{11}(t) = 0$, $w_{12}(t) = 0$. Therefore, we have

$$u_1^*(t) = \frac{(\lambda_2 - \lambda_1)kHV}{R_1}.$$

3. When $u_1^*(t) = b_1$, then $w_{12}(t) = 0$. Therefore,

$$b_1 = u_1^*(t) = \frac{(\lambda_2 - \lambda_1)kHV - w_{11}(t)}{R_1} \Rightarrow R_1 b_1 = (\lambda_2 - \lambda_1)kHV - w_{11}(t)$$
$$\Rightarrow \quad w_{11}(t) = (\lambda_2 - \lambda_1)kHV - R_1 b_1 \geq 0 \Rightarrow b_1 \leq \frac{(\lambda_2 - \lambda_1)kHV}{R_1}.$$

Hence, we obtain

$$u_1^*(t) = \begin{cases} \frac{(\lambda_2-\lambda_1)kHV}{R_1}, & \text{if } a_1 < \frac{(\lambda_2-\lambda_1)kHV}{R_1} < b_1 \\ a_1, & \text{if } \frac{(\lambda_2-\lambda_1)kHV}{R_1} \leq a_1 \\ b_1, & \text{if} \frac{(\lambda_2-\lambda_1)kHV}{R_1} \geq b_1. \end{cases}$$

This can be written in the following simplified form

$$u_1^*(t) = \min\left\{\max\left\{a_1, \frac{(\lambda_2 - \lambda_1)kHV}{R_1}\right\}, b_1\right\}.$$

Similarly, we obtain the following expression for the second optimal control,

$$u_2^*(t) = \min\left\{\max\left\{a_2, \frac{\lambda_3 aI}{R_2}\right\}, b_2\right\}.$$

We summarize the above characterization in the following theorem:

Theorem 5.5.1. *Given the pair of optimal controls (u_1^*, u_2^*) and the existence of solutions of the state system (5.3.2), there exist adjoint variables $\lambda_i,\ i = 1, 2, 3, 4$ which satisfy the adjoint equations (5.5.1) subject to the transversality conditions $\lambda_i(T) = 0$ for $i = 1, 2, 3, 4$.*
Moreover, the characterization of the optimal control pair $u_1^*(t)$ and $u_2^*(t)$ are given by

$$u_1^*(t) = \min\left\{\max\left\{a_1, \frac{(\lambda_2 - \lambda_1)kHV}{R_1}\right\}, b_1\right\}, \tag{5.5.2}$$
$$u_2^*(t) = \min\left\{\max\left\{a_2, \frac{\lambda_3 aI}{R_2}\right\}, b_2\right\}. \tag{5.5.3}$$

5.6 Uniqueness of the Optimality System

As seen from the preceding section, the optimal controls are functions of the state and the adjoint variables. We will prove that the optimality system comprising of (5.3.2) and (5.5.1) has a unique solution. Further, we will prove that the optimal control pair is also unique [34]. Using the uniform boundedness of the state variables, we can show that there exists a $K_i > 0$ such that $|\lambda_i(t)| < K_i T$ on $[0, T]$ for $i = 1, 2, 3, 4$. These bounds (for both state and adjoint variables) will be used in the proof of uniqueness of the solution of the optimality system. The following lemma required in the uniqueness proof of the solution of the optimality system for a small time window, is stated below (without proof) [38, 89].

Lemma 5.6.1. *The function $u^*(\theta) = \min\{\max\{\theta, \alpha\}, \gamma\}$ is Lipschitz continuous in θ, where $\alpha < \gamma$ are some fixed positive constants.*

We now state and prove the following theorem for the uniqueness of the solution of the optimality system.

Theorem 5.6.2. *For a sufficiently small T, the solution of the optimality system is unique.*

Proof. Suppose that $(H, I, D, V, \lambda_1, \lambda_2, \lambda_3, \lambda_4)$ and $(\overline{H}, \overline{I}, \overline{D}, \overline{V}, \overline{\lambda_1}, \overline{\lambda_2}, \overline{\lambda_3}, \overline{\lambda_4})$ are two different solutions of the optimality system. Let $H = e^{\xi t}p_1$, $I = e^{\xi t}p_2$, $D = e^{\xi t}p_3$, $V = e^{\xi t}p_4$, $\lambda_1 = e^{-\xi t}q_1$, $\lambda_2 = e^{-\xi t}q_2$, $\lambda_3 = e^{-\xi t}q_3$, $\lambda_4 = e^{-\xi t}q_4$. Also, let $\overline{H} = e^{\xi t}\overline{p_1}$, $\overline{I} = e^{\xi t}\overline{p_2}$, $\overline{D} = e^{\xi t}\overline{p_3}$, $\overline{V} = e^{\xi t}\overline{p_4}$, $\overline{\lambda_1} = e^{-\xi t}\overline{q_1}$, $\overline{\lambda_2} = e^{-\xi t}\overline{q_2}$, $\overline{\lambda_3} = e^{-\xi t}\overline{q_3}$ and $\overline{\lambda_4} = e^{-\xi t}\overline{q_4}$. Here an appropriate choice of $\xi > 0$ has to be made. Further, let

$$\begin{aligned} u_1^*(t) &= \min\left\{\max\left\{a_1, \frac{(q_2 - q_1)kp_1p_4e^{\xi t}}{R_1}\right\}, b_1\right\}, \\ u_2^*(t) &= \min\left\{\max\left\{a_2, \frac{aq_3p_2}{R_2}\right\}, b_2\right\}, \end{aligned}$$

and

$$\begin{aligned} \overline{u_1}^*(t) &= \min\left\{\max\left\{a_1, \frac{(\overline{q_2} - \overline{q_1})k\overline{p_1}\ \overline{p_4}e^{\xi t}}{R_1}\right\}, b_1\right\}, \\ \overline{u_2}^*(t) &= \min\left\{\max\left\{a_2, \frac{a\overline{q_3}\ \overline{p_2}}{R_2}\right\}, b_2\right\}. \end{aligned}$$

Using lemma (5.6.1), we get

$$\begin{aligned} |u_1^*(t) - \overline{u_1}^*(t)| &\leq \left|\frac{ke^{\xi t}}{R_1}\{p_1p_4(q_2 - q_1) - \overline{p_1}\ \overline{p_4}(\overline{q_2} - \overline{q_1})\}\right| \\ &= \frac{k}{R_1}\left|e^{\xi t}\{p_1p_4(q_2 - q_1) - \overline{p_1}\ \overline{p_4}(\overline{q_2} - \overline{q_1})\}\right|, \end{aligned}$$

and

$$\begin{aligned} |u_2^*(t) - \overline{u_2}^*(t)| &\leq \left|\frac{a}{R_2}(q_3p_2 - \overline{q_3}\ \overline{p_2})\right| \\ &= \frac{a}{R_2}\left|q_3p_2 - \overline{q_3}\ \overline{p_2}\right|. \end{aligned}$$

Substituting $H = e^{\xi t}p_1$ in the first equation of (5.3.2), we obtain

$$p_1' + \xi p_1 = se^{-\xi t} - (1 - u_1^*)kp_1p_4e^{\xi t} - \mu p_1. \tag{5.6.1}$$

Similarly, the other substitutions of $I = e^{\xi t}p_2$, $D = e^{\xi t}p_3$, $V = e^{\xi t}p_4$, $\lambda_1 = e^{-\xi t}q_1$, $\lambda_2 = e^{-\xi t}q_2$,

$\lambda_3 = e^{-\xi t}q_3$, $\lambda_4 = e^{-\xi t}q_4$ result in

$$\begin{aligned}
p_2' + \xi p_2 &= (1-u_1^*)kp_1p_4e^{\xi t} - \delta p_2, && (5.6.2)\\
p_3' + \xi p_3 &= (1-u_2^*)ap_2 - (\beta+\delta)p_3, && (5.6.3)\\
p_4' + \xi p_4 &= \beta p_3 - cp_4, && (5.6.4)\\
-q_1' + \xi q_1 &= -\mu q_1 - (1-u_1^*)kq_1p_4e^{\xi t} + (1-u_1^*)kq_2p_4e^{\xi t}, && (5.6.5)\\
-q_2' + \xi q_2 &= Q_2p_2e^{2\xi t} - \delta q_2 + (1-u_2^*)aq_3, && (5.6.6)\\
-q_3' + \xi q_3 &= Q_3p_3e^{2\xi t} - (\beta+\delta)q_3 + \beta q_4, && (5.6.7)\\
-q_4' + \xi q_4 &= Q_4p_4e^{2\xi t} - (1-u_1^*)kq_1p_1e^{\xi t} + (1-u_1^*)kq_2p_1e^{\xi t} - cq_4. && (5.6.8)
\end{aligned}$$

Again, for the first equation of (5.3.2) we substitute $\overline{H} = e^{\xi t}\overline{p_1}$ to obtain

$$\overline{p_1}' + \xi\overline{p_1} = se^{-\xi t} - (1-\overline{u_1}^*)k\overline{p_1}\,\overline{p_4}e^{\xi t} - \mu\overline{p_1}. \quad (5.6.9)$$

Now, we subtract (pairwise) the equations for H and $\overline{H}$, I and $\overline{I}$, D and $\overline{D}$, V and $\overline{V}$, λ_1 and $\overline{\lambda_1}$, λ_2 and $\overline{\lambda_2}$, λ_3 and $\overline{\lambda_3}$, λ_4 and $\overline{\lambda_4}$. Each of the resulting equations is multiplied by an appropriate difference of functions and integrated over $[0,T]$. Finally, these equations involving integrals are added to obtain the required estimates.

To illustrate this, we subtract the equation (5.6.9) from (5.6.1) to obtain

$$(p_1-\overline{p_1})' + \xi(p_1-\overline{p_1}) = -ke^{\xi t}[(1-u_1^*)p_1p_4 - (1-\overline{u_1}^*)\overline{p_1}\,\overline{p_4}] - \mu(p_1-\overline{p_1}).$$

Multiplying both sides by $(p_1-\overline{p_1})$ and integrating over $[0,T]$, we get

$$\begin{aligned}
&\frac{1}{2}(p_1-\overline{p_1})^2(T) + \xi\int_0^T (p_1-\overline{p_1})^2dt\\
&= -k\int_0^T e^{\xi t}[(1-u_1^*)p_1p_4 - (1-\overline{u_1}^*)\overline{p_1}\,\overline{p_4}](p_1-\overline{p_1})dt - \mu\int_0^T (p_1-\overline{p_1})^2dt\\
&= -k\int_0^T e^{\xi t}(p_1p_4 - \overline{p_1}\,\overline{p_4})(p_1-\overline{p_1})dt + k\int_0^T e^{\xi t}(u_1^*p_1p_4 - \overline{u_1}^*\,\overline{p_1}\,\overline{p_4})(p_1-\overline{p_1})dt\\
&\quad -\mu\int_0^T (p_1-\overline{p_1})^2dt.
\end{aligned}$$

Now,

$$\begin{aligned}
k\int_0^T e^{\xi t}(p_1p_4 - \overline{p_1}\,\overline{p_4})(p_1-\overline{p_1})dt &= k\int_0^T e^{\xi t}[p_1p_4 - p_1\overline{p_4} + p_1\overline{p_4} - \overline{p_1}\,\overline{p_4}](p_1-\overline{p_1})dt\\
&= k\int_0^T e^{\xi t}[p_1(p_4-\overline{p_4}) + \overline{p_4}(p_1-\overline{p_1})](p_1-\overline{p_1})dt\\
&= k\int_0^T e^{\xi t}[p_1(p_1-\overline{p_1})(p_4-\overline{p_4}) + \overline{p_4}(p_1-\overline{p_1})^2]dt\\
&\le C_1e^{\xi T}\int_0^T [(p_1-\overline{p_1})^2 + (p_4-\overline{p_4})^2]dt.
\end{aligned}$$

Further,

$$\begin{aligned}\int_0^T (u_1^* - \overline{u_1}^*)^2 dt &\leq \frac{k^2}{R_1^2}\int_0^T [e^{\xi t}\{p_1p_4(q_2-q_1) - \overline{p_1}\ \overline{p_4}(\overline{q_2}-\overline{q_1})\}]^2 dt \\ &\leq \left(\frac{ke^{\xi T}}{R_1}\right)^2 \int_0^T [p_1^2p_4^2(q_2-q_1)^2 - 2p_1p_4(q_2-q_1)\overline{p_1}\ \overline{p_4}(\overline{q_2}-\overline{q_1}) \\ &\quad +\overline{p_1}^2\ \overline{p_4}^2(\overline{q_2}-\overline{q_1})^2]dt \\ &\leq C_2\left(\frac{ke^{\xi T}}{R_1}\right)^2 \int_0^T [(q_1-\overline{q_1})^2 + (q_2-\overline{q_2})^2]dt.\end{aligned}$$

Also,

$$\begin{aligned}& k\int_0^T e^{\xi t}(u_1^*p_1p_4 - \overline{u_1}^*\ \overline{p_1}\ \overline{p_4})(p_1-\overline{p_1})dt \\ =\ & k\int_0^T e^{\xi t}[(u_1^*-\overline{u_1}^*)p_1p_4 + \overline{u_1}^*(p_1p_4 - \overline{p_1}\ \overline{p_4})](p_1-\overline{p_1})dt \\ \leq\ & C_3e^{3\xi T}\int_0^T [(p_1-\overline{p_1})^2 + (p_4-\overline{p_4})^2 + (q_1-\overline{q_1})^2 + (q_2-\overline{q_2})^2]dt.\end{aligned}$$

The constants C_1, C_2 and C_3 obtained above are dependent on the system coefficients as well as the bounds on state and adjoint variables.

Therefore, we have

$$\begin{aligned}& \frac{1}{2}(p_1-\overline{p_1})^2(T) + \xi\int_0^T (p_1-\overline{p_1})^2 dt \\ \leq\ & C_1'\int_0^T (p_1-\overline{p_1})^2 dt + C_2'e^{3\xi T}\int_0^T [(p_1-\overline{p_1})^2 + (p_4-\overline{p_4})^2 + (q_1-\overline{q_1})^2 + (q_2-\overline{q_2})^2]dt.\end{aligned}$$

Obviously the constants C_1' and C_2' also depend on the system coefficients and the upper bounds of state and adjoint variables.

Now, substituting $\overline{\lambda_1} = e^{-\xi t}\overline{q_1}$ in the first equation of (5.5.1), we get

$$-\overline{q_1}' + \xi\overline{q_1} = -\mu\overline{q_1} - (1-\overline{u_1}^*)k\overline{q_1}\ \overline{p_4}e^{\xi t} + (1-\overline{u_1}^*)k\overline{q_2}\ \overline{p_4}e^{\xi t}. \tag{5.6.10}$$

Subtracting equation (5.6.10) from equation (5.6.5), we obtain

$$\begin{aligned}-(q_1-\overline{q_1})' + \xi(q_1-\overline{q_1}) &= -\mu(q_1-\overline{q_1}) - [(1-u_1^*)kq_1p_4e^{\xi t} - (1-\overline{u_1}^*)k\overline{q_1}\ \overline{p_4}e^{\xi t}] \\ &\quad +[(1-u_1^*)kq_2p_4e^{\xi t} - (1-\overline{u_1}^*)k\overline{q_2}\ \overline{p_4}e^{\xi t}].\end{aligned}$$

Multiplying this equation by $(q_1 - \overline{q_1})$ and integrating over $[0, T]$, we get

$$\begin{aligned}
&\frac{1}{2}(q_1 - \overline{q_1})^2(0) + \xi \int_0^T (q_1 - \overline{q_1})^2 dt \\
= \; & -\mu \int_0^T (q_1 - \overline{q_1})^2 dt - k \int_0^T e^{\xi t}[(1 - u_1^*)kq_1p_4 - (1 - \overline{u_1}^*)k\overline{q_1}\ \overline{p_4}](q_1 - \overline{q_1})dt \\
& + k \int_0^T e^{\xi t}[(1 - u_1^*)kq_2p_4 - (1 - \overline{u_1}^*)k\overline{q_2}\ \overline{p_4}](q_1 - \overline{q_1})dt \\
= \; & -\mu \int_0^T (q_1 - \overline{q_1})^2 dt - k \int_0^T e^{\xi t}[q_1p_4 - \overline{q_1}\ \overline{p_4}](q_1 - \overline{q_1})dt \\
& + k \int_0^T e^{\xi t}[u_1^*q_1p_4 - \overline{u_1}^*\ \overline{q_1}\ \overline{p_4}](q_1 - \overline{q_1})dt + k \int_0^T e^{\xi t}[q_2p_4 - \overline{q_2}\ \overline{p_4}](q_1 - \overline{q_1})dt \\
& - k \int_0^T e^{\xi t}[u_1^*q_2p_4 - \overline{u_1}^*\ \overline{q_2}\ \overline{p_4}](q_1 - \overline{q_1})dt.
\end{aligned}$$

Now,

$$\begin{aligned}
& k \int_0^T e^{\xi t}[q_1p_4 - \overline{q_1}\ \overline{p_4}](q_1 - \overline{q_1})dt \\
= \; & k \int_0^T e^{\xi t}[q_1(p_4 - \overline{p_4}) + \overline{p_4}(q_1 - \overline{q_1})](q_1 - \overline{q_1})dt \\
= \; & k \int_0^T e^{\xi t}[q_1(p_4 - \overline{p_4})(q_1 - \overline{q_1}) + \overline{p_4}(q_1 - \overline{q_1})^2]dt \\
\leq \; & C_4e^{\xi T} \int_0^T [(p_4 - \overline{p_4})^2 + (q_1 - \overline{q_1})^2]dt.
\end{aligned}$$

Also,

$$\begin{aligned}
& k \int_0^T e^{\xi t}[u_1^*q_1p_4 - \overline{u_1}^*\ \overline{q_1}\ \overline{p_4}](q_1 - \overline{q_1})dt \\
= \; & k \int_0^T e^{\xi t}[(u_1^* - \overline{u_1}^*)q_1p_4 - \overline{u_1}^*(q_1p_4 - \overline{q_1}\ \overline{p_4})](q_1 - \overline{q_1})dt \\
\leq \; & C_5e^{3\xi T} \int_0^T [(p_4 - \overline{p_4})^2 + (q_1 - \overline{q_1})^2 + (q_2 - \overline{q_2})^2]dt.
\end{aligned}$$

Further,

$$\begin{aligned}
& k \int_0^T e^{\xi t}[q_2p_4 - \overline{q_2}\ \overline{p_4}](q_1 - \overline{q_1})dt \\
= \; & k \int_0^T e^{\xi t}[q_2(p_4 - \overline{p_4}) + \overline{p_4}(q_2 - \overline{q_2})](q_1 - \overline{q_1})dt \\
= \; & k \int_0^T e^{\xi t}[q_2(p_4 - \overline{p_4})(q_1 - \overline{q_1}) + \overline{p_4}(q_1 - \overline{q_1})(q_2 - \overline{q_2})]dt \\
\leq \; & C_6e^{\xi T} \int_0^T [(p_4 - \overline{p_4})^2 + (q_1 - \overline{q_1})^2 + (q_2 - \overline{q_2})^2]dt.
\end{aligned}$$

Again,

$$\begin{aligned} & k\int_0^T e^{\xi t}[u_1^* q_2 p_4 - \overline{u_1}^*\ \overline{q_2}\ \overline{p_4}](q_1-\overline{q_1})dt \\ = \ & k\int_0^T e^{\xi t}[(u_1^*-\overline{u_1}^*)q_2p_4 + \overline{u_1}^*(q_2p_4 - \overline{q_2}\ \overline{p_4})](q_1-\overline{q_1})dt \\ \leq \ & C_7 e^{3\xi T}\int_0^T [(p_4-\overline{p_4})^2 + (q_1-\overline{q_1})^2 + (q_2-\overline{q_2})^2]dt. \end{aligned}$$

The constants C_4, C_5, C_6 and C_7 are dependent on the system coefficients as well as the bounds on state and adjoint variables.

Therefore, we have

$$\begin{aligned} \frac{1}{2}(q_1-\overline{q_1})^2(0) + \xi\int_0^T (q_1-\overline{q_1})^2 dt \ \leq \ & C_3'\int_0^T (q_1-\overline{q_1})^2 dt \\ & + C_4' e^{3\xi T}\int_0^T [(p_4-\overline{p_4})^2 + (q_1-\overline{q_1})^2 + (q_2-\overline{q_2})^2]dt. \end{aligned}$$

Obviously the constants C_3' and C_4' also depend on the system coefficients and the bounds on the state and adjoint variables.

We can derive the integral equations and their estimates for the remaining six state and adjoint variables. Combining all the eight of these estimates, we get

$$\begin{aligned} & \frac{1}{2}(p_1-\overline{p_1})^2(T) + \frac{1}{2}(p_2-\overline{p_2})^2(T) + \frac{1}{2}(p_3-\overline{p_3})^2(T) + \frac{1}{2}(p_4-\overline{p_4})^2(T) + \\ & \frac{1}{2}(q_1-\overline{q_1})^2(0) + \frac{1}{2}(q_2-\overline{q_2})^2(0) + \frac{1}{2}(q_3-\overline{q_3})^2(0) + \frac{1}{2}(q_4-\overline{q_4})^2(0) \\ & + \xi\int_0^T [(p_1-\overline{p_1})^2 + (p_2-\overline{p_2})^2 + (p_3-\overline{p_3})^2 + (p_4-\overline{p_4})^2 \\ & + (q_1-\overline{q_1})^2 + (q_2-\overline{q_2})^2 + (q_3-\overline{q_3})^2 + (q_4-\overline{q_4})^2]dt \\ \leq \ & (\widetilde{C_1} + \widetilde{C_2}e^{3\xi T})\int_0^T [(p_1-\overline{p_1})^2 + (p_2-\overline{p_2})^2 + (p_3-\overline{p_3})^2 \\ & + (p_4-\overline{p_4})^2 + (q_1-\overline{q_1})^2 + (q_2-\overline{q_2})^2 + (q_3-\overline{q_3})^2 + (q_4-\overline{q_4})^2]dt. \end{aligned}$$

Thus, from the above equation, we conclude that

$$\begin{aligned} & (\xi - \widetilde{C_1} - \widetilde{C_2}e^{3\xi T})\int_0^T [(p_1-\overline{p_1})^2 + (p_2-\overline{p_2})^2 + (p_3-\overline{p_3})^2 \\ & + (p_4-\overline{p_4})^2 + (q_1-\overline{q_1})^2 + (q_2-\overline{q_2})^2 + (q_3-\overline{q_3})^2 + (q_4-\overline{q_4})^2]dt \leq 0, \end{aligned}$$

where $\widetilde{C_1}$ and $\widetilde{C_2}$ are dependent on the system coefficients as well as the bounds on state and adjoint variables.

If we choose ξ such that $\xi > \widetilde{C_1} + \widetilde{C_2}$ and $T < \frac{1}{3\xi}\ln\left(\frac{\xi-\widetilde{C_1}}{\widetilde{C_2}}\right)$, then $p_i = \overline{p_i}$ and $q_i = \overline{q_i}$ for $i = 1, 2, 3, 4$. Hence, the solution of the optimality system is unique for T sufficiently small. □

Therefore, the unique optimal controls u_1^* and u_2^* are characterized in terms of the unique solution of the optimality system.

5.7 Numerical Results

In this section, we numerically analyze the various results for the pharmacokinetic model, as well as the consequence of application of optimal combination therapy of PEG IFN and LMV. We first examine the impact of efficacies u_1 and u_2 (of PEG IFN and LMV respectively) on the basic reproduction number R_0. Recall that the infection clears out (persists) whenever $R_0 < 1$ (> 1), which is equivalent to $u > u_{crit}$ ($u < u_{crit}$). The parameter values used here are $s = 2.6 \times 10^7$ cells day^{-1} $k = 1.67 \times 10^{-12}$ day^{-1} virion^{-1}, $\mu = 0.01$ day^{-1} $\delta = 0.053$ day^{-1}, $a = 150$ day^{-1}, $\beta = 0.87$ day^{-1} and $c = 3.8$ day^{-1}. While most of the parameters were obtained from [7], s and μ are from [27]. Prior to the initiation of treatment $R_0 = 3.0482 > 1$, and $u_1 = 0, u_2 = 0$. The goal is to keep increasing u_1 and u_2 such that R_0 is driven to a value less than 1. In this case u_1 and u_2 must be chosen so that $u\,(= 1 - (1 - u_1)(1 - u_2)) > u_{crit} = 0.6719$. We illustrate this by a surface plot and a contour plot in Figure 5.2. One can easily observe that for $u_1 = 0$ and $u_2 = 0$ the value of R_0 attains its maximum value of 3.0482. We increase u_1 and u_2 from 0 to 1 in increments of 0.1 and observe that the value of R_0 gradually decreases and eventually tends towards 0 (corresponding to $u_1 = 1, u_2 = 1$). This clearly reflects the impact of the efficacies in terms of clearance of the infection.

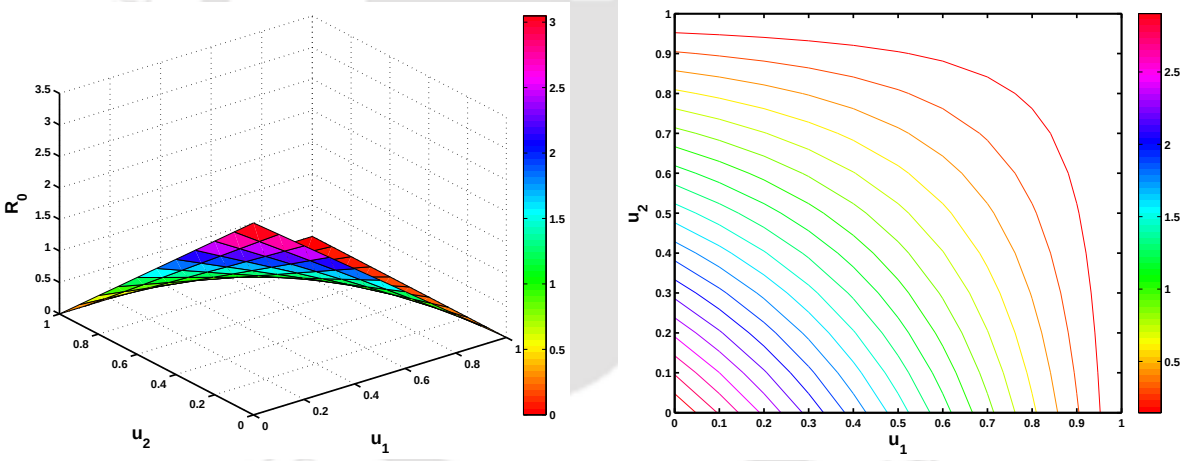

(a) Surface plot of R_0 (b) Contour plot of R_0

Figure 5.2: Surface and contour plot of R_0 for various values of u_1 and u_2.

We simulated the dynamics of the system as a result of administration of the combination therapy. Recall that the parameter values (without treatment) chosen are for $R_0 > 1$. In Figure 5.3, we fix the efficacy of PEG IFN as $u_1 = 0.5$ and consider four different efficacies of LMV, namely, $u_2 = 0.2, 0.5, 0.7, 0.9$. For $u_2 = 0.2$, the combination efficacy, $u = 0.6$, which is less than the critical efficacy $u_{crit} = 0.6719$. In this case, the levels of uninfected hepatocytes, intracellular HBV DNA-containing capsids and virions show some signs of decline over a period of 200 days as

can be seen in Figure 5.3. But if the simulation is run for a longer time period, then we can see that despite the initial signs of patient recovery, the levels of all three will rebound and eventually move towards the infected steady state. Further, for $u_2 = 0.5, 0.7, 0.9$, the combination efficacy u is always greater than the critical efficacy u_{crit} *i.e.,* $R_0 < 1$. For these cases, the levels of I, D and V show a gradual decline over the period of 200 days and simulation for a longer period will confirm that the populations tend towards the levels for the uninfected steady state, *i.e.,* $E_u = \left(2.6 \times 10^9, 0, 0, 0\right)$. We observe that this decline is biphasic in nature in case of D and V with a more rapid decline in the first phase of a couple of days followed by a slower decline, which is consistent with clinical results [6]. We observe similar results by fixing $u_2 = 0.5$ and varying the values of $u_1 = 0.2, 0.5, 0.7, 0.9$. These results are presented in Figure 5.4. We note that in this case also there is a biphasic decline that is observed in the behavior of HBV.

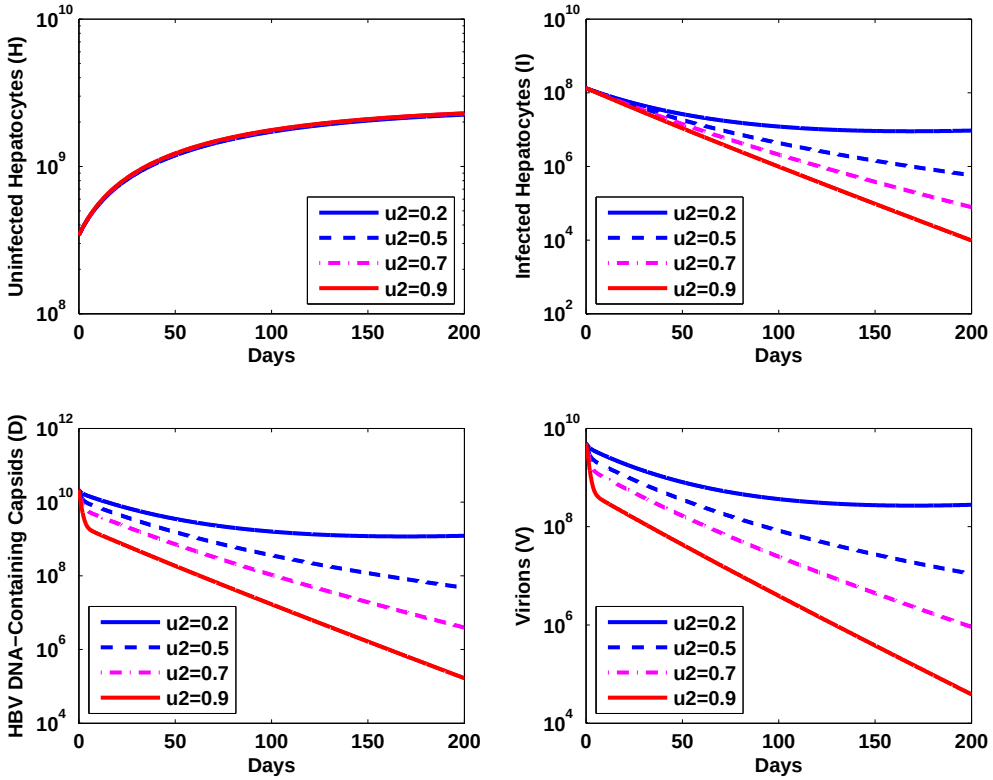

Figure 5.3: Dynamics of the uninfected & infected hepatocytes, intracellular HBV DNA-containing capsids and HBV for various values of u_2 with $u_1 = 0.5$.

Interruptions in treatment can happen due to a variety of reasons such as side effects and financial constraints for a continued long term treatment [36]. To illustrate one such scenario, we consider four sets of combination therapy (u_1, u_2) as $(0.5, 0.5)$, $(0.5, 0.8)$, $(0.8, 0.5)$ and $(0.8, 0.8)$ for a period of 50 days. For these four pairs of (u_1, u_2), $u > u_{crit}$. Once the treatment period of 50 days is over, we observed the dynamics of the system for another 50 days starting from the levels

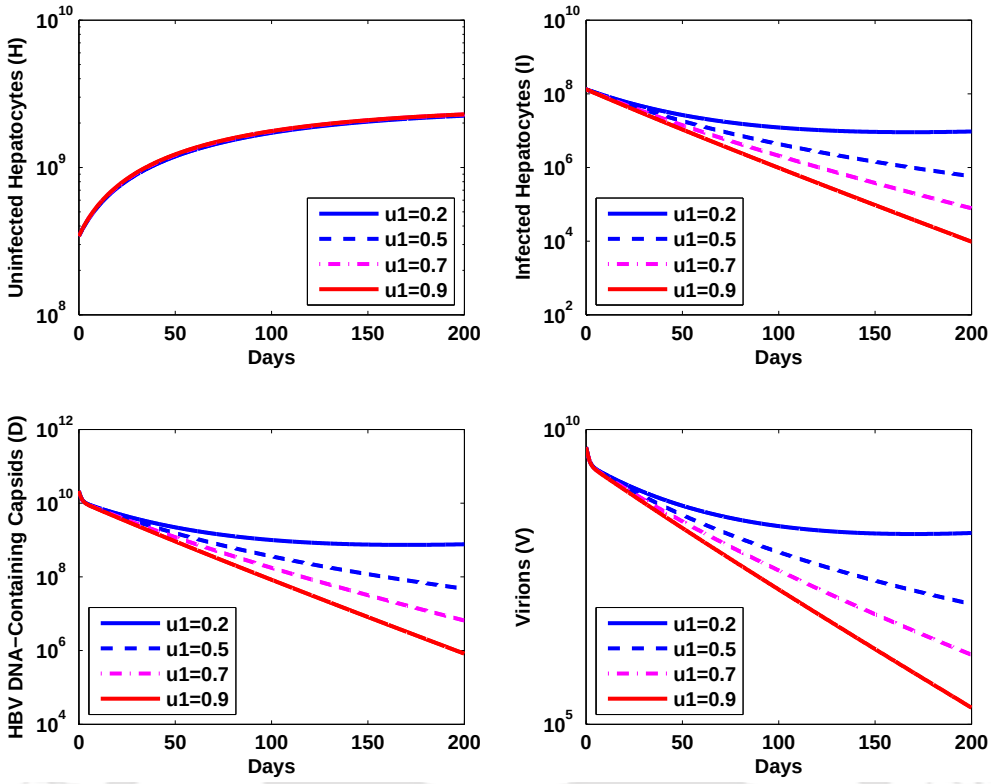

Figure 5.4: Dynamics of the uninfected & infected hepatocytes, intracellular HBV DNA-containing capsids and HBV for various values of u_1 with $u_2 = 0.5$

at the cessation of treatment after 50 days. We see in Figure 5.5, as to how the viral load declines in a biphasic manner. The decline is significant (approximately 10^3 folds). The discontinuation of treatment after 50 days results in the rebound of the levels of HBV virions. It can be seen that the viral load on an average is lower with this on-off therapeutic protocol as compared to the scenario when no treatment is administered over the entire period of 100 days.

The optimal control problem comprising of the state equations, co-state equations and the optimal controls (equations (5.3.2,5.5.1,5.5.2,5.5.3)) is solved using the following algorithm [29].

1. Initial guesses, $u_1^{(0)}$ and $u_2^{(0)}$ are made for u_1 and u_2 respectively.

2. Using this, a solution $(H^{(0)}, I^{(0)}, D^{(0)}, V^{(0)})$ of (5.3.2) is obtained using the Runge-Kutta 4 method.

3. Substituting the values of control and state variables in (5.5.1) we obtain a final time problem which is solved using Runge-Kutta 4 method.

4. The updated values $u_1^{(1)}$ and $u_2^{(1)}$ are obtained using (5.5.2,5.5.3). Steps 1-3 are repeated until a convergence criterion is satisfied.

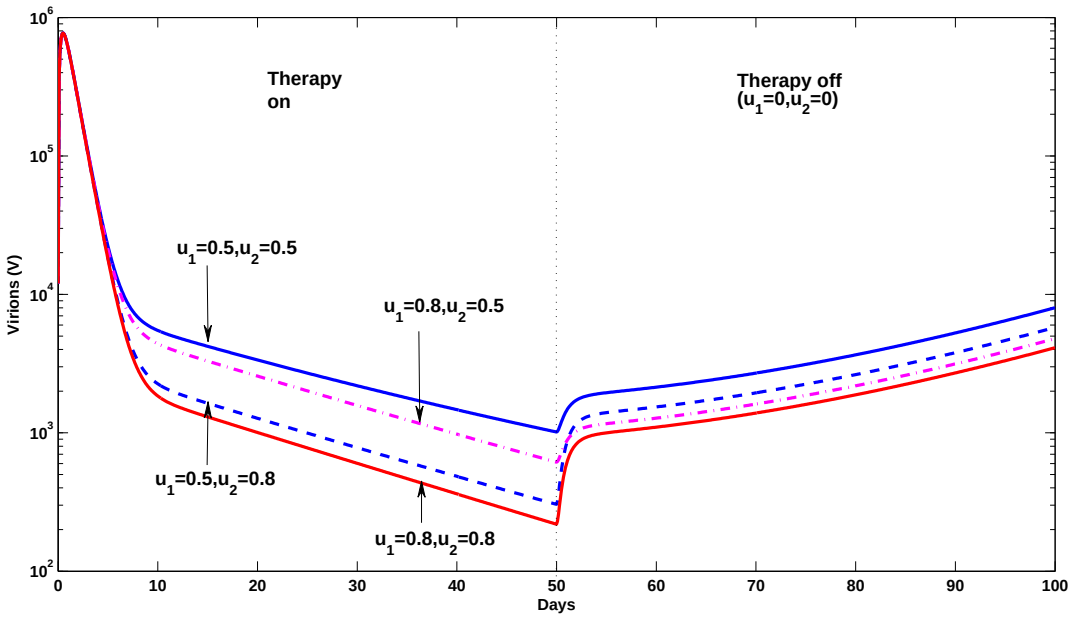

Figure 5.5: Pattern of viral load with an on-off treatment with the treatment being administered for 50 days and then the treatment being interrupted for the next 50 days.

For the purpose of this work we take the minimum and maximum control to be $a_i = 0.01$ and $b_i = 0.99$, $i = 1, 2$. The initial condition for the state variables at the time of commencement of the therapy is taken to be $(8.5 \times 10^7, 3 \times 10^2, 5.3 \times 10^6, 1.2 \times 10^4)$. The optimal control pair $\overrightarrow{u}^* = (u_1^*, u_2^*)$ is obtained for a period of 50 days [43]. The cost coefficients that were introduced in the definition of the objective functional (5.3.1) were set at $Q_2 = 10^{-5}$, $Q_3 = 10^{-5}$, $Q_4 = 10^{-5}$, $R_1 = 5000$ and $R_2 = 5000$ [43]. We observe (in Figure 5.6) that the optimal efficacy of PEG IFN is at the maximum for a period of about three days after which it shows a steep decline. A similar pattern is observed for the case of LMV, except that the maximal efficacy is the optimal one for a period of about six days. The subsequent fall in the efficacy level of LMV is less rapid as compared to that of PEG IFN. It is seen that the viral load increases slightly after the initiation of therapy which requires the efficacy to be the maximum. However, this drops after about three days, which coincides with the drop of efficacy levels of PEG IFN from its maximum. A similar observation can be seen in case of HBV DNA-containing capsids. It also coincides with the first phase decline in the infected hepatocyte level. However, even after three days, the levels of I, D and V are not close to the uninfected steady state. Since the efficacy of PEG IFN is significantly diminished after three days, the role of LMV becomes more crucial in achieving the reduction of these levels. As such the optimal efficacy of LMV remains at its peak until the time when these levels fall to low levels. It can be seen here that the simultaneous drop of LMV efficacy and complete decline of I,

D, V happens after about six days, with the relatively lower level therapeutic efficacy resulting in prevention of any relapse.

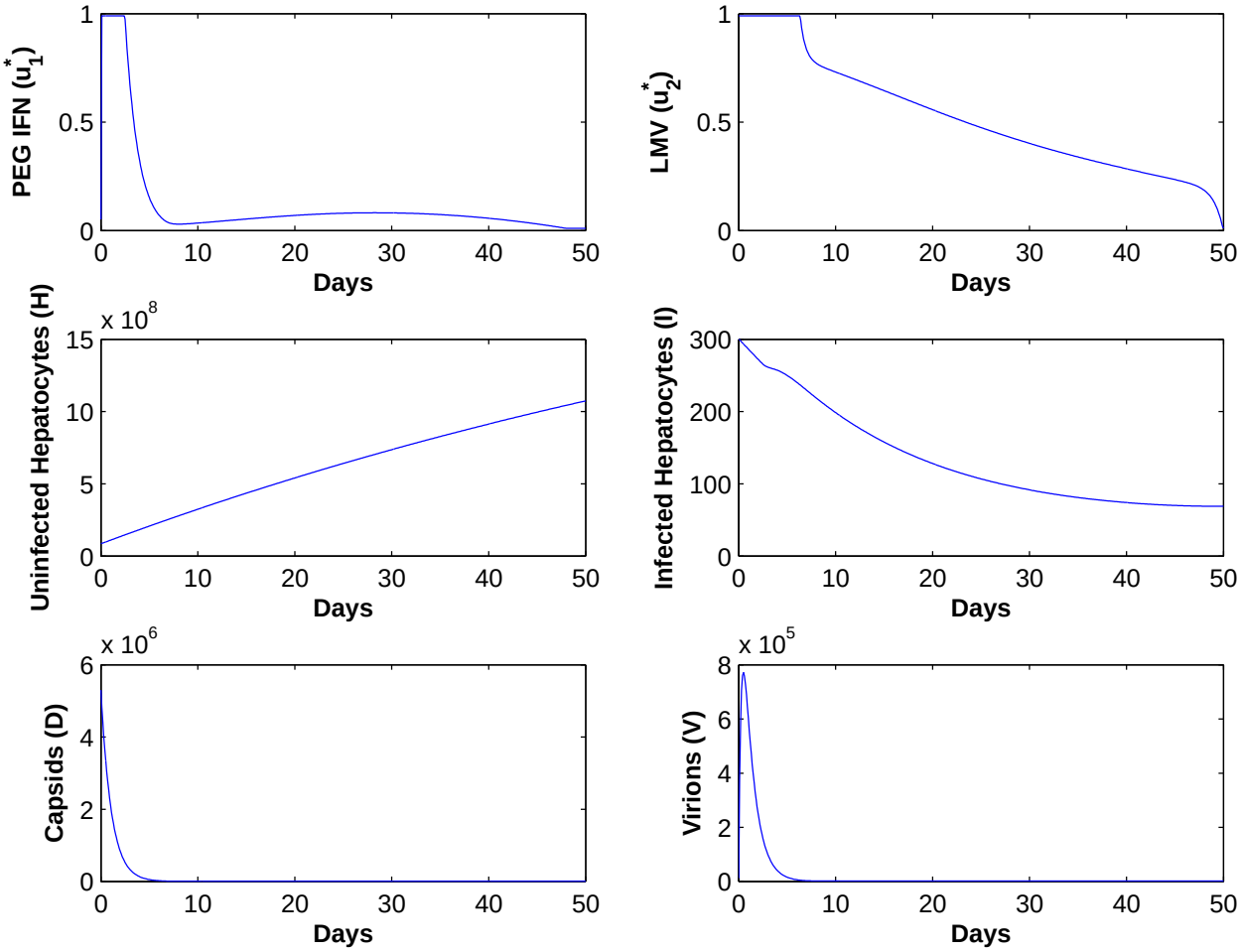

Figure 5.6: Optimal therapeutic efficacy for the combination treatment and the consequent dynamics.

5.8 Conclusion

In this chapter, we presented a model for HBV infection where the patient is subjected to the combination therapy of PEG IFN and LMV. We undertook the local stability analysis for the uninfected and the infected steady states of the model and obtained a critical efficacy in terms of model parameters. A combination efficacy of both PEG IFN and LMV was defined in such a way that the clearance or persistence of infection depends on whether this combination efficacy is greater than or less than the critical efficacy.

We then formulated an optimal control problem with the objective of minimizing the levels of infected hepatocytes, intracellular HBV DNA-containing capsids and HBV as well as the thera-

peutic cost of the combination treatment. We proved the existence and uniqueness of the optimal controls using techniques from control theory such as Pontryagin's maximum principle. The problem was solved using numerical techniques. The key finding is that the optimal efficacy of LMV has to be at the maximum permissible level for almost double the time as in the case of PEG IFN for a treatment period of fifty days.

The determination of the critical efficacy and the optimal efficacy would be of great use for the biomedical community in designing individual treatment protocols. Robust methods of determination of patient parameters is the key to the success of this approach, since the optimal theory is dependent on these parameters and this could lead to great improvements and optimization of drug dosage administered to patients.

Chapter 6

The HBV Infection Model with Diffusion

In this chapter, a diffusion driven model for HBV infection is presented and analyzed. To incorporate diffusion, the spatial mobility of both the HBV and the HBV DNA-containing capsids is taken into account. The conditions for global stability of the continuous model is established in terms of the basic reproduction number. Furthermore, a discretized version of the model is presented. The analysis of this model is accomplished through the principle of dynamic consistency (DC) applied for a discretized version of the spatial model [93]. Numerical instability (NI) is essentially a result of additional parameters (such as temporal and spatial grid sizes for spatiotemporal models) resulting from the discretization process, over and above the model parameters. The variation of these parameters could result in solutions of the discretized system which are not solutions of the original system and such solutions are termed as NI. The phenomenon of NI can potentially be restricted or even eliminated through the approach of DC whose definition is system specific and could vary from one model to another. Mickens [93] demonstrated how DC can be achieved through the use of non-standard finite difference (NSFD) schemes. The NSFD schemes were pioneered by Mickens through a series of works [93] and the interested reader may refer to the works of Mickens [94, 95, 96]. Finally, the results are numerically illustrated for the dynamics and stability of the various populations in addition to demonstrating the advantages of the usage of NSFD method over the standard finite difference (SFD) scheme.

6.1 Mathematical Model

The model presented and analyzed in this chapter is based on the model that was studied in the Chapter 3. In this chapter, we analyze a diffusion driven model to capture the mobility of both the capsids as well as the virions [45, 49, 50, 54]. Accordingly, we let $H(\mathbf{x},t)$, $I(\mathbf{x},t)$, $D(\mathbf{x},t)$ and $V(\mathbf{x},t)$ denote the densities of the uninfected hepatocytes, infected hepatocytes, intracellular HBV

DNA-containing capsids and the virions at position $\mathbf{x}$ and at time t, respectively. We propose the following model with diffusion as:

$$\begin{aligned}
\frac{\partial H}{\partial t} &= s - \mu H(x,t) - kH(x,t)V(x,t), \\
\frac{\partial I}{\partial t} &= kH(x,t)V(x,t) - \delta I(x,t), \\
\frac{\partial D}{\partial t} &= d_D \Delta D + aI(x,t) - (\beta+\delta)D(x,t), \\
\frac{\partial V}{\partial t} &= d_V \Delta V + \beta D(x,t) - cV(x,t).
\end{aligned} \tag{6.1.1}$$

Here, $d_D > 0$ and $d_V > 0$ are the diffusion coefficients of capsids and virions, respectively with Δ being the Laplacian operator, that is, $\Delta = \sum_{i=1}^{n} \frac{\partial^2}{\partial x_i^2}$ where n is the number of spatial dimensions of the domain Ω. In the current work we restrict ourselves to only one spatial dimension [45]. The initial conditions for the model (6.1.1) are

$$H(x,0) = H_0(x) > 0, I(x,0) = I_0(x) > 0, D(x,0) = D_0(x) > 0, V(x,0) = V_0(x) > 0 \text{ in } \overline{\Omega},$$

with the no-flux boundary conditions given by

$$\frac{\partial D}{\partial \nu} = 0, \frac{\partial V}{\partial \nu} = 0 \text{ on } \partial\Omega \times (0, +\infty),$$

where $\partial\Omega$ is the boundary of the domain Ω and $\frac{\partial}{\partial \nu}$ is the outward normal derivative on $\partial\Omega$. The homogeneous Neumann boundary conditions imply that capsids and virions do not move across the boundary $\partial\Omega$. It can be shown that the solutions of the system (6.1.1) are positive. The basic reproduction number R_0 of the non-diffusive model (3.1.1) in the Chapter 3 was shown to be

$$R_0 = \frac{a\beta sk}{c\delta\mu(\beta+\delta)}.$$

The model (6.1.1) admits two steady states, namely, the uninfected steady state, $E_u = \left(H^0, I^0, D^0, V^0\right) = \left(\frac{s}{\mu}, 0, 0, 0\right)$ and the infected steady state, $E_i = (H^*, I^*, D^*, V^*)$ where

$$H^* = \frac{c\delta(\beta+\delta)}{a\beta k}, \; V^* = \left[\frac{a\beta s}{c\delta(\beta+\delta)} - \frac{\mu}{k}\right], \; D^* = \left[\frac{c}{\beta}\right] V^* \text{ and } I^* = \left[\frac{\beta+\delta}{a}\right] D^*.$$

While there is no existential condition for the uninfected steady state E_u, it can be seen that the infected steady state, E_i, exists provided $R_0 > 1$.

6.2 Global Stability for the Continuous Model

In this section, we study the global stability of the uninfected and the infected steady states by using the method of construction of Lyapunov functions developed in [52]. For this purpose, we

note that the function $G(u) = u - 1 - \ln u \geq 0$ for $u > 0$ with $G(u) = 0$ iff $u = 1$. Also we note that for $P_i, Q_i > 0$ with $\prod_{i=1}^{n} P_i = \prod_{i=1}^{n} Q_i$, the relation,

$$n - \sum_{i=1}^{n} \frac{P_i}{Q_i} \leq 0 \tag{6.2.1}$$

holds. These two points will be used in Sections 6.2 and 6.4.

Theorem 6.2.1. *The uninfected steady state E_u is globally asymptotically stable provided $R_0 \leq 1$.*

Proof. We first define the function

$$G_1(t) = H^0 G\left(\frac{H(t)}{H^0}\right) + I(t) + \frac{\delta}{a} D(t) + \frac{\delta(\beta+\delta)}{a\beta} V(t).$$

Then, the derivative of $G_1(t)$ with respect to t is

$$\frac{dG_1}{dt} = s\left[2 - \frac{H}{H^0} - \frac{H^0}{H}\right] + \frac{c\delta(\beta+\delta)}{a\beta}(R_0 - 1)V.$$

Now, we define a Lyapunov function as follows:

$$L_1 = \int_\Omega G_1 dx.$$

Calculating the time derivative of L_1 along the positive solutions of model (6.1.1), we obtain

$$\frac{dL_1}{dt} = \int_\Omega \left[s\left\{2 - \frac{H}{H^0} - \frac{H^0}{H}\right\} + \frac{c\delta(\beta+\delta)}{a\beta}(R_0 - 1)V \right] dx.$$

Using the relation (6.2.1), we get

$$2 - \frac{H}{H^0} - \frac{H^0}{H} \leq 0.$$

It is clear that $R_0 \leq 1$ ensures $\frac{dL_1}{dt} \leq 0$. Therefore, by Lyapunov-LaSalle invariance theorem, E_u is globally asymptotically stable provided $R_0 \leq 1$. □

Theorem 6.2.2. *The infected steady state E_i is globally asymptotically stable provided $R_0 > 1$.*

Proof. We first define the function

$$G_2(t) = H^* G\left(\frac{H(t)}{H^*}\right) + I^* G\left(\frac{I(t)}{I^*}\right) + \frac{\delta}{a} D^* G\left(\frac{D(t)}{D^*}\right) + \frac{\delta(\beta+\delta)}{a\beta} V^* G\left(\frac{V(t)}{V^*}\right).$$

Then, the derivative of $G_2(t)$ with respect to t is

$$\frac{dG_2}{dt} = \mu H^*\left[2 - \frac{H}{H^*} - \frac{H^*}{H}\right] + \delta I^*\left[4 - \frac{H^*}{H} - \frac{I^* H V}{I H^* V^*} - \frac{I D^*}{I^* D} - \frac{D V^*}{D^* V}\right].$$

Now, we define a Lyapunov function as follows:

$$L_2 = \int_\Omega G_2 dx.$$

Calculating the time derivative of L_2 along the positive solutions of model (6.1.1), we obtain

$$\begin{aligned}\frac{dL_2}{dt} = & \int_\Omega \left[\mu H^* \left\{2 - \frac{H}{H^*} - \frac{H^*}{H}\right\} + \delta I^* \left\{4 - \frac{H^*}{H} - \frac{I^*HV}{IH^*V^*} - \frac{ID^*}{I^*D} - \frac{DV^*}{D^*V}\right\}\right] dx \\ & -\frac{\delta}{a} D^* d_D \int_\Omega \frac{|\nabla D|^2}{D^2} dx - \frac{\delta(\beta+\delta)}{a\beta} V^* d_V \int_\Omega \frac{|\nabla V|^2}{V^2} dx.\end{aligned}$$

Using the relation (6.2.1), we get

$$\begin{aligned} 2 - \frac{H}{H^*} - \frac{H^*}{H} &\leq 0, \\ 4 - \frac{H^*}{H} - \frac{I^*HV}{IH^*V^*} - \frac{ID^*}{I^*D} - \frac{DV^*}{D^*V} &\leq 0.\end{aligned}$$

Hence, $\frac{dL_2}{dt} \leq 0$. Therefore, by Lyapunov-LaSalle invariance theorem, E_i is globally asymptotically stable provided it exists, that is, $R_0 > 1$. □

6.3 Non-standard Finite Difference Scheme

We now consider the model (6.1.1) in the spatial domain $\Omega = [p, q]$ where $p, q \in \mathbb{R}$. Let the spatial domain be divided into N subintervals of equal length Δx, that is, $\Delta x = (q-p)/N$. Also, let the length of uniform time intervals be Δt. The n-th spatial and the m-th temporal grid points are given by $x_n = p + n\Delta x$, $n = 0, 1, \ldots, N$ and $t_m = m\Delta t$, $m = 0, 1, \ldots$. The values of $H(x,t)$, $I(x,t)$, $D(x,t)$ and $V(x,t)$ at the discretized spatio-temporal point (x_n, t_m) are given by $H(x_n, t_m)$, $I(x_n, t_m)$, $D(x_n, t_m)$ and $V(x_n, t_m)$ and denoted by H_n^m, I_n^m, D_n^m and V_n^m, respectively. Accordingly the NSFD scheme [54] for the model (6.1.1) are given by

$$\begin{aligned}\frac{H_n^{m+1} - H_n^m}{\Delta t} &= s - \mu H_n^{m+1} - k H_n^{m+1} V_n^m, \\ \frac{I_n^{m+1} - I_n^m}{\Delta t} &= k H_n^{m+1} V_n^m - \delta I_n^{m+1}, \\ \frac{D_n^{m+1} - D_n^m}{\Delta t} &= d_D \frac{D_{n+1}^{m+1} - 2D_n^{m+1} + D_{n-1}^{m+1}}{(\Delta x)^2} + a I_n^{m+1} - (\beta+\delta) D_n^{m+1}, \\ \frac{V_n^{m+1} - V_n^m}{\Delta t} &= d_V \frac{V_{n+1}^{m+1} - 2V_n^{m+1} + V_{n-1}^{m+1}}{(\Delta x)^2} + \beta D_n^{m+1} - c V_n^{m+1},\end{aligned} \tag{6.3.1}$$

where $n = 0, 1, \ldots, N$ and $m = 0, 1, \ldots$. The discretized initial and boundary conditions are given by

$$H_n^0 = H_0(x_n),\ I_n^0 = I_0(x_n),\ D_n^0 = D_0(x_n),\ V_n^0 = V_0(x_n) \text{ for } n = 0, 1, \ldots, N, \tag{6.3.2}$$

and

$$D_{-1}^m = D_0^m,\ D_{N+1}^m = D_N^m,\ V_{-1}^m = V_0^m,\ V_{N+1}^m = V_N^m \text{ for } m = 0, 1, \ldots, \tag{6.3.3}$$

respectively. One can verify that the NSFD discretized system (6.3.1) has the same two steady states as that of the continuous model (6.1.1), namely, the uninfected (E_u) and the infected (E_i) steady states. The positivity of the solutions of the discretized system (6.3.1) can be proved using the M-matrix theory [54]. A real square matrix is an M-matrix if the off-diagonal entries are non-positive, the diagonal entries are positive and it has strict diagonal dominance [54]. Consequently, the M-matrix is non-singular and hence invertible with the entries of the inverse matrix being positive real numbers [54].

Theorem 6.3.1. *For any $\Delta x > 0$ and $\Delta t > 0$, the solutions of the discretized system (6.3.1) are positive, that is, $H^m > 0,\ I^m > 0,\ D^m > 0,\ V^m > 0$ for all $m = 0, 1, \ldots$.*

Proof. The system (6.3.1) can be written as

$$\begin{aligned} H_n^{m+1} &= \frac{s\Delta t + H_n^m}{1 + \mu\Delta t + k\Delta t V_n^m}, \\ I_n^{m+1} &= \frac{I_n^m + k\Delta t H_n^{m+1} V_n^m}{1 + \delta\Delta t}, \\ AD^{m+1} &= D^m + a\Delta t I^{m+1}, \\ BV^{m+1} &= V^m + \beta\Delta t D^{m+1}. \end{aligned} \tag{6.3.4}$$

Here, the square matrices A and B of dimension $(N+1)\times(N+1)$ are given by

$$A = \begin{bmatrix} a_1 & a_2 & 0 & \ldots & 0 & 0 & 0 \\ a_2 & a_3 & a_2 & \ldots & 0 & 0 & 0 \\ 0 & a_2 & a_3 & \ldots & 0 & 0 & 0 \\ \vdots & \vdots & \vdots & \ddots & \vdots & \vdots & \vdots \\ 0 & 0 & 0 & \ldots & a_3 & a_2 & 0 \\ 0 & 0 & 0 & \ldots & a_2 & a_3 & a_2 \\ 0 & 0 & 0 & \ldots & 0 & a_2 & a_1 \end{bmatrix}, \tag{6.3.5}$$

and

$$B = \begin{bmatrix} b_1 & b_2 & 0 & \ldots & 0 & 0 & 0 \\ b_2 & b_3 & b_2 & \ldots & 0 & 0 & 0 \\ 0 & b_2 & b_3 & \ldots & 0 & 0 & 0 \\ \vdots & \vdots & \vdots & \ddots & \vdots & \vdots & \vdots \\ 0 & 0 & 0 & \ldots & b_3 & b_2 & 0 \\ 0 & 0 & 0 & \ldots & b_2 & b_3 & b_2 \\ 0 & 0 & 0 & \ldots & 0 & b_2 & b_1 \end{bmatrix}. \tag{6.3.6}$$

The off-diagonal and the diagonal entries of A and B are given by $a_1 = 1 + d_D\lambda + (\beta+\delta)\Delta t$, $a_2 = -d_D\lambda$, $a_3 = 1 + 2d_D\lambda + (\beta+\delta)\Delta t$, $b_1 = 1 + d_V\lambda + c\Delta t$, $b_2 = -d_V\lambda$, $b_3 = 1 + 2d_V\lambda + c\Delta t$, where

$\lambda = \frac{\Delta t}{(\Delta x)^2}$. Also $Z^m = \begin{pmatrix} Z_0^m & Z_1^m & \dots & Z_{N-1}^m & Z_N^m \end{pmatrix}^\top$ where $Z = H, I, D$ and V. Since $a_2, b_2 < 0$ and $a_1, a_3, b_1, b_3 > 0$ and there is strict diagonal dominance therefore we conclude that both A and B qualify as M-matrices. Thus, A and B are non-singular. Consequently the third and the fourth equation of (6.3.4) can be rearranged as

$$D^{m+1} = A^{-1}(D^m + a\Delta t I^{m+1}), \tag{6.3.7}$$

and

$$V^{m+1} = B^{-1}(V^m + \beta\Delta t D^{m+1}), \tag{6.3.8}$$

respectively. Assuming that $H^m > 0$, $I^m > 0$, $D^m > 0$ and $V^m > 0$, we conclude from the first and second equation of (6.3.4) that $H^{m+1} > 0$ and $I^{m+1} > 0$ respectively. Using these along with the fact that A^{-1} and B^{-1} being inverses of M-matrices have all entries as positive, we conclude from (6.3.7) and (6.3.8) that $D^{m+1} > 0$ and $V^{m+1} > 0$. Thus the result follows from the method of induction. □

6.4 Global Stability for the Discrete Model

In this section, global asymptotic stability of the steady states E_u and E_i of the discretized system (6.3.1) are proved by constructing the appropriate Lyapunov functions [54].

Theorem 6.4.1. *For any $\Delta x > 0$ and $\Delta t > 0$, the uninfected steady state E_u is globally asymptotically stable provided $R_0 \le 1$.*

Proof. We first define the following discretized Lyapunov function

$$L^m = \sum_{n=0}^{N} \frac{1}{\Delta t}\left[H^0\left(\frac{H_n^m}{H^0} - 1 - \ln\frac{H_n^m}{H^0}\right) + I_n^m + \frac{\delta}{a}D_n^m + \frac{\delta(\beta+\delta)}{a\beta}V_n^m(1+c\Delta t)\right]. \tag{6.4.1}$$

Recall that the function $G(u) = u - 1 - \ln(u) \ge 0$ for all $u > 0$ and $G(u) = 0$ iff $u = 1$. Then using the property of $G(u)$ we see that $L^m \ge 0$ with the equality holding iff $\frac{H_n^m}{H^0} = 1$, that is, $H_n^m = H^0$, $I_n^m = 0$, $D_n^m = 0$ and $V_n^m = 0$ for all $n = 0, 1, \dots, N$. Now,

$$\begin{aligned} L^{m+1} - L^m &= \sum_{n=0}^{N} \frac{1}{\Delta t}\left[H_n^{m+1} - H_n^m + H^0 \ln\frac{H_n^m}{H_n^{m+1}} + I_n^{m+1} - I_n^m + \frac{\delta}{a}(D_n^{m+1} - D_n^m)\right. \\ &\quad \left. + \frac{\delta(\beta+\delta)}{a\beta}(1+c\Delta t)(V_n^{m+1} - V_n^m)\right]. \end{aligned} \tag{6.4.2}$$

Since $\ln u \le u - 1$ for $u > 0$, therefore,

$$\begin{aligned} L^{m+1} - L^m &\le \sum_{n=0}^{N}\left[\frac{1}{\Delta t}\left\{(H_n^{m+1} - H_n^m)\left(1 - \frac{H^0}{H_n^{m+1}}\right) + (I_n^{m+1} - I_n^m) + \frac{\delta}{a}(D_n^{m+1} - D_n^m)\right.\right. \\ &\quad \left.\left. + \frac{\delta(\beta+\delta)}{a\beta}(V_n^{m+1} - V_n^m)\right\} + \frac{c\delta(\beta+\delta)}{a\beta}(V_n^{m+1} - V_n^m)\right]. \end{aligned} \tag{6.4.3}$$

Then using system (6.3.1), $H^0 = \frac{s}{\mu}$ and $R_0 = \frac{a\beta sk}{c\delta\mu(\beta+\delta)}$, we obtain

$$\begin{aligned}
L^{m+1} - L^m \leq & \sum_{n=0}^{N} \left[(s - \mu H_n^{m+1} - k H_n^{m+1} V_n^m) \left(1 - \frac{H^0}{H_n^{m+1}}\right) + (k H_n^{m+1} V_n^m - \delta I_n^{m+1}) \right. \\
& + \frac{\delta}{a} \left(d_D \frac{D_{n+1}^{m+1} - 2D_n^{m+1} + D_{n-1}^{m+1}}{(\Delta x)^2} + a I_n^{m+1} - (\beta+\delta) D_n^{m+1} \right) \\
& + \frac{\delta(\beta+\delta)}{a\beta} \left(d_V \frac{V_{n+1}^{m+1} - 2V_n^{m+1} + V_{n-1}^{m+1}}{(\Delta x)^2} + \beta D_n^{m+1} - c V_n^{m+1} \right) \\
& \left. + \frac{c\delta(\beta+\delta)}{a\beta} (V_n^{m+1} - V_n^m) \right] \\
= & \sum_{n=0}^{N} \left[s \left(2 - \frac{H_n^{m+1}}{H^0} - \frac{H^0}{H_n^{m+1}}\right) + \frac{c\delta(\beta+\delta)}{a\beta} V_n^m (R_0 - 1) \right] \\
& + \frac{\delta}{a} \left[d_D \frac{D_{N+1}^{m+1} - D_N^{m+1}}{(\Delta x)^2} + d_D \frac{D_0^{m+1} - D_{-1}^{m+1}}{(\Delta x)^2} \right] \\
& + \frac{\delta(\beta+\delta)}{a\beta} \left[d_V \frac{V_{N+1}^{m+1} - V_N^{m+1}}{(\Delta x)^2} + d_V \frac{V_0^{m+1} - V_{-1}^{m+1}}{(\Delta x)^2} \right] \\
= & \sum_{n=0}^{N} \left[s \left(2 - \frac{H_n^{m+1}}{H^0} - \frac{H^0}{H_n^{m+1}}\right) + \frac{c\delta(\beta+\delta)}{a\beta} V_n^m (R_0 - 1) \right]. \qquad (6.4.4)
\end{aligned}$$

Using the relation (6.2.1), we get

$$2 - \frac{H_n^{m+1}}{H^0} - \frac{H^0}{H_n^{m+1}} \leq 0.$$

The equality holds only when $H_n^{m+1} = H^0$. Hence, for $R_0 \leq 1$, we have

$$L^{m+1} - L^m \leq 0. \qquad (6.4.5)$$

Since this holds for $m = 0, 1, \ldots$, therefore the sequence $\{L^m\}_m$ is monotonically decreasing which means that $\lim_{m\to+\infty} L^m = \overline{L}$ for some constant $\overline{L} \geq 0$. Arguing on the lines of [54] it can be shown that

$$\lim_{m\to+\infty} H_n^m = H^0, \lim_{m\to+\infty} I_n^m = 0, \lim_{m\to+\infty} D_n^m = 0, \lim_{m\to+\infty} V_n^m = 0,$$

for all $n = 0, 1, \ldots, N$ and when $R_0 \leq 1$. Hence E_u is globally asymptotically stable provided $R_0 \leq 1$. □

Theorem 6.4.2. *For any $\Delta x > 0$ and $\Delta t > 0$, the infected steady state E_i is globally asymptotically stable provided $R_0 > 1$.*

Proof. We define the following discretized Lyapunov function

$$\hat{L}^m = \sum_{n=0}^{N} \frac{1}{\Delta t}\left[H^* g\left(\frac{H_n^m}{H^*}\right) + I^* g\left(\frac{I_n^m}{I^*}\right) + \frac{\delta}{a} D^* g\left(\frac{D_n^m}{D^*}\right) + \left\{\frac{\delta(\beta+\delta)}{a\beta} V^* + \delta I^* \Delta t\right\} g\left(\frac{V_n^m}{V^*}\right)\right]. \tag{6.4.6}$$

Recall that the function $G(u) = u - 1 - \ln(u) \geq 0$ for all $u > 0$ and $G(u) = 0$ iff $u = 1$. The Lyapunov function $\hat{L}^m \geq 0$ for all $m = 0, 1, \ldots,$ with equality holding iff $H_n^m = H^*$, $I_n^m = I^*$, $D_n^m = D^*$, $V_n^m = V^*$ for all $n = 0, 1, \ldots, N$. Now,

$$\begin{aligned}\hat{L}^{m+1} - \hat{L}^m = \sum_{n=0}^{N} \frac{1}{\Delta t}\Bigg[&H^*\left(\frac{H_n^{m+1} - H_n^m}{H^*} + \ln\left(\frac{H_n^m}{H_n^{m+1}}\right)\right) + I^*\left(\frac{I_n^{m+1} - I_n^m}{I^*} + \ln\left(\frac{I_n^m}{I_n^{m+1}}\right)\right) \\ &+ \frac{\delta}{a} D^*\left(\frac{D_n^{m+1} - D_n^m}{D^*} + \ln\left(\frac{D_n^m}{D_n^{m+1}}\right)\right) + \left(\frac{\delta(\beta+\delta)}{a\beta} V^* + \delta I^* \Delta t\right) \\ &\left(\frac{V_n^{m+1} - V_n^m}{V^*} + \ln\left(\frac{V_n^m}{V_n^{m+1}}\right)\right)\Bigg].\end{aligned} \tag{6.4.7}$$

Using $\ln u \leq u - 1,\ u > 0$, we obtain

$$\begin{aligned}\hat{L}^{m+1} - \hat{L}^m \leq \sum_{n=0}^{N} \frac{1}{\Delta t}\Bigg[&(H_n^{m+1} - H_n^m)\left(1 - \frac{H^*}{H_n^{m+1}}\right) + (I_n^{m+1} - I_n^m)\left(1 - \frac{I^*}{I_n^{m+1}}\right) + \\ &\frac{\delta}{a}(D_n^{m+1} - D_n^m)\left(1 - \frac{D^*}{D_n^{m+1}}\right) + \frac{\delta(\beta+\delta)}{a\beta}(V_n^{m+1} - V_n^m)\left(1 - \frac{V^*}{V_n^{m+1}}\right) \\ &+\delta I^* \Delta t\left(\frac{V_n^{m+1} - V_n^m}{V^*} + \ln\left(\frac{V_n^m}{V_n^{m+1}}\right)\right)\Bigg].\end{aligned} \tag{6.4.8}$$

Using the expressions for $H^*,\ I^*,\ D^*,\ V^*$ along with system (6.3.1) and discrete boundary condi-

tions (6.3.3), we get

$$\begin{aligned}
\hat{L}^{m+1}-\hat{L}^{m} \leq & \sum_{n=0}^{N}\Bigg[(s-\mu H_n^{m+1}-kH_n^{m+1}V_n^m)\left(1-\frac{H^*}{H_n^{m+1}}\right)+(kH_n^{m+1}V_n^m-\delta I_n^{m+1})\left(1-\frac{I^*}{I_n^{m+1}}\right)\\
&+\frac{\delta}{a}\left(d_D\frac{D_{n+1}^{m+1}-2D_n^{m+1}+D_{n-1}^{m+1}}{(\Delta x)^2}+aI_n^{m+1}-(\beta+\delta)D_n^{m+1}\right)\left(1-\frac{D^*}{D_n^{m+1}}\right)+\\
&\frac{\delta(\beta+\delta)}{a\beta}\left(d_V\frac{V_{n+1}^{m+1}-2V_n^{m+1}+V_{n-1}^{m+1}}{(\Delta x)^2}+\beta D_n^{m+1}-cV_n^{m+1}\right)\left(1-\frac{V^*}{V_n^{m+1}}\right)+\\
&\delta I^*\left(\frac{V_n^{m+1}-V_n^m}{V^*}+\ln\left(\frac{V_n^m}{V_n^{m+1}}\right)\right)\Bigg]\\
= & \sum_{n=0}^{N}\Bigg[\mu H^*\left(2-\frac{H_n^{m+1}}{H^*}-\frac{H^*}{H_n^{m+1}}\right)+\delta I^*\left(4-\frac{H^*}{H_n^{m+1}}-\frac{H_n^{m+1}V_n^mI^*}{I_n^{m+1}H^*V^*}-\frac{I_n^{m+1}D^*}{I^*D_n^{m+1}}-\right.\\
&\left.\frac{D_n^{m+1}V^*}{D^*V_n^{m+1}}+\ln\left(\frac{V_n^m}{V_n^{m+1}}\right)\right)\Bigg]+\sum_{n=0}^{N}\frac{\delta}{a}\left(d_D\frac{D_{n+1}^{m+1}-2D_n^{m+1}+D_{n-1}^{m+1}}{(\Delta x)^2}\right)\left(1-\frac{D^*}{D_n^{m+1}}\right)\\
&+\sum_{n=0}^{N}\frac{\delta(\beta+\delta)}{a\beta}\left(d_V\frac{V_{n+1}^{m+1}-2V_n^{m+1}+V_{n-1}^{m+1}}{(\Delta x)^2}\right)\left(1-\frac{V^*}{V_n^{m+1}}\right)\\
= & \sum_{n=0}^{N}\Bigg[\mu H^*\left(2-\frac{H_n^{m+1}}{H^*}-\frac{H^*}{H_n^{m+1}}\right)-\delta I^*\left(g\left(\frac{H^*}{H_n^{m+1}}\right)+g\left(\frac{H_n^{m+1}V_n^mI^*}{I_n^{m+1}H^*V^*}\right)+\right.\\
&\left.g\left(\frac{I_n^{m+1}D^*}{I^*D_n^{m+1}}\right)+g\left(\frac{D_n^{m+1}V^*}{D^*V_n^{m+1}}\right)\right)\Bigg]-\frac{\delta}{a}d_DD^*\sum_{n=0}^{N-1}\frac{(D_{n+1}^{m+1}-D_n^{m+1})^2}{(\Delta x)^2D_{n+1}^{m+1}D_n^{m+1}}\\
&-\frac{\delta(\beta+\delta)}{a\beta}d_VV^*\sum_{n=0}^{N-1}\frac{(V_{n+1}^{m+1}-V_n^{m+1})^2}{(\Delta x)^2V_{n+1}^{m+1}V_n^{m+1}}. \qquad (6.4.9)
\end{aligned}$$

Using the relation (6.2.1), we get

$$2-\frac{H_n^{m+1}}{H^*}-\frac{H^*}{H_n^{m+1}}\leq 0.$$

Since $G(u)\geq 0, \forall u>0$, we have $\hat{L}^{m+1}-\hat{L}^m\leq 0, \forall m=0,1,\ldots$. Therefore, $\lim_{m\to+\infty}\hat{L}^m=\tilde{L}$ for some constant $\tilde{L}\geq 0$, which gives $\lim_{m\to+\infty}(\hat{L}^{m+1}-\hat{L}^m)=0$. Using this relation along with expressions (6.4.8) and (6.4.9), we have $\lim_{m\to+\infty}H_n^m=H^*$ for $n=0,1,\ldots,N$ (arguing similar to [54]). Using system (6.3.1), it can be further proved that $\lim_{m\to+\infty}I_n^m=I^*$, $\lim_{m\to+\infty}D_n^m=D^*$, $\lim_{m\to+\infty}V_n^m=V^*$ hold for $n=0,1,\ldots,N$. This completes the proof. □

Thus, using the Theorem 6.4.1 and 6.4.2, we conclude that the discretized system (6.3.1) exhibits dynamic consistency with the continuous system (6.1.1) vis-a-vis the global asymptotic stability of both the uninfected and the infected steady states.

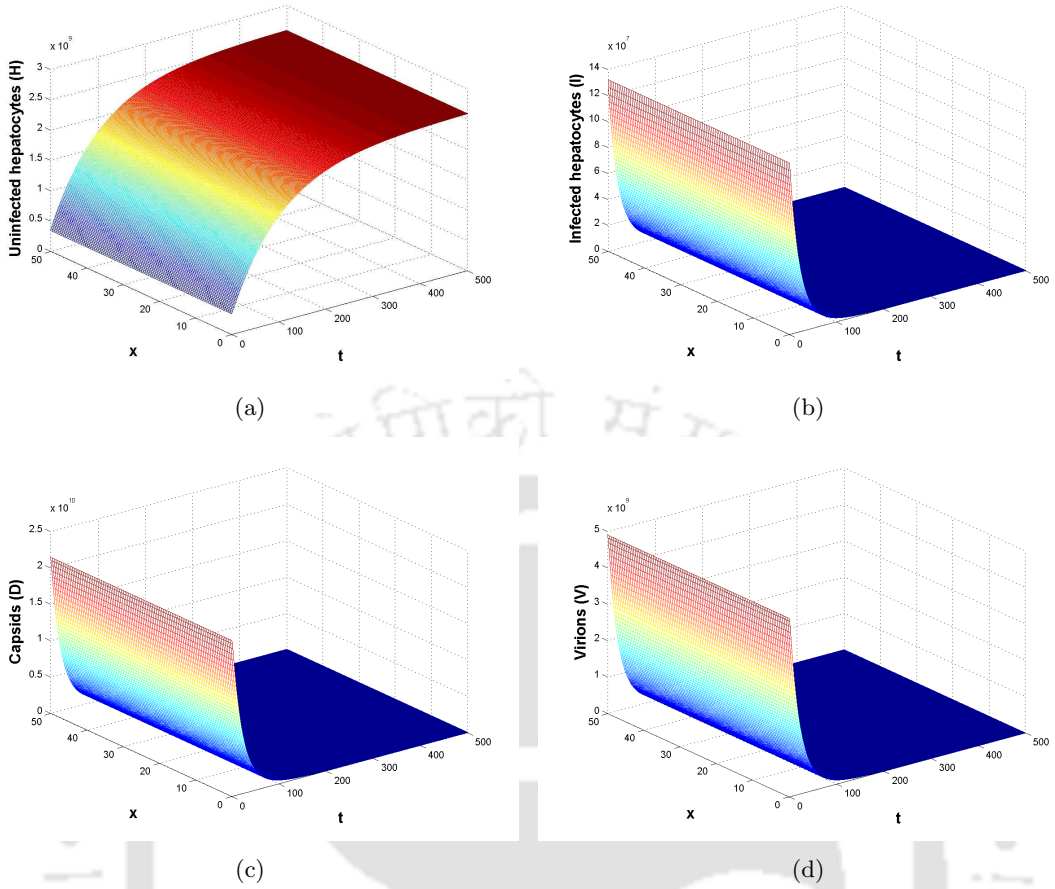

Figure 6.1: Dynamics of the populations when $R_0 = 0.5476 < 1$.

6.5 Numerical Results

In this section, we present the numerical illustration and validation of the theoretical results obtained in the preceding sections. For this purpose, we first numerically illustrate the results for global stability for both the steady states. Accordingly, we use two sets of system parameters, one corresponding to $R_0 < 1$ (when E_u is globally asymptotically stable for both the continuous and discretized models) and the other for $R_0 > 1$ (when E_i is globally asymptotically stable for both the continuous and discretized models). The numerical implementation is carried out using the NSFD scheme described in Section 6.3. For the purpose of illustration of both the scenarios, we choose the diffusion coefficients as $d_D = 0.1$ mm^{2}day^{-1} and $d_V = 0.1$ mm^{2}day^{-1}. The one-dimensional spatial domain is taken as $\Omega = [0, 50]$ and the simulation carried out for a time window of 500 days. The grid sizes used in the spatial and temporal directions are $\Delta x = 0.5$ and $\Delta t = 1$ respectively. The parameter set $s = 2.6 \times 10^7$ cells day^{-1} $k = 3 \times 10^{-13}$ day^{-1} virion^{-1}, $\mu = 0.01$ day^{-1} $\delta = 0.053$ day^{-1}, $a = 150$ day^{-1}, $\beta = 0.87$ day^{-1} and $c = 3.8$ day^{-1} [1, 7, 27] results in $R_0 = 0.5476 < 1$. Thus, in

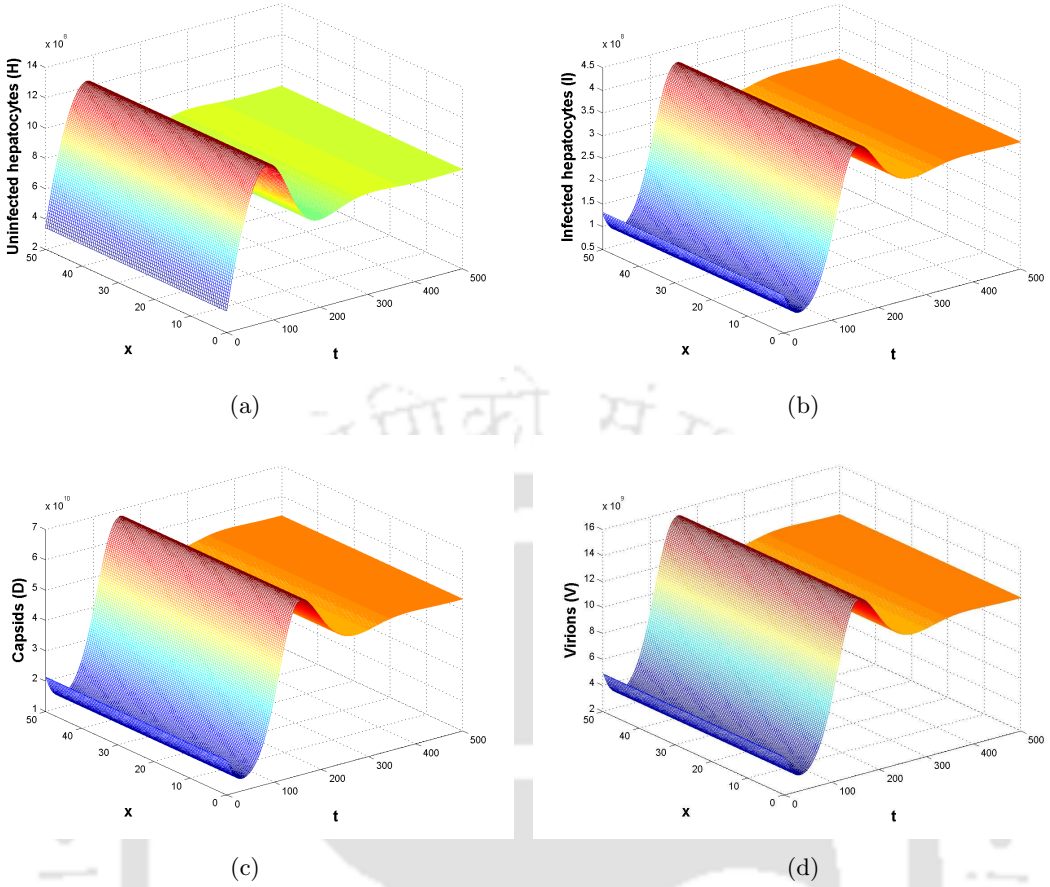

Figure 6.2: Dynamics of the populations when $R_0 = 3.0482 > 1$.

this case, the uninfected steady state E_u is globally asymptotically stable. It can be observed from Figure 6.1 that this is indeed the case and the system eventually approaches the uninfected steady state $E_u = (2.6 \times 10^9, 0, 0, 0)$. For the other scenario, all the parameter values are identical with the exception of $k = 1.67 \times 10^{-12}$ day^{-1} virion^{-1} [7] which renders $R_0 = 3.0482 > 1$. In this case, the infected steady state is stable as can be observed numerically in Figure 6.2, where the state variables approach the infected steady state $E_i = (8.53 \times 10^8, 3.3 \times 10^8, 5.36 \times 10^{10}, 1.23 \times 10^{10})$. For both the sets of simulations the initial condition is uniformly taken to be 40% of E_i at all the spatial points. We have also shown that the global asymptotically stable results are dependent only on the parameters of the non-diffusive system and independent of the choices of the diffusion coefficients d_D and d_V. This is also illustrated by way of numerical simulations. For illustrative purpose we only show the case for $R_0 > 1$ using the corresponding parameter values used above. We also restrict ourselves to demonstrating the dynamics of virions (V) only. We choose four different combinations of (d_D, d_V), namely, $(0.1, 0.1)$, $(0.1, 10)$, $(10, 0.1)$ and $(10, 10)$. We see from Figure 6.3, that the evolution of the dynamics of V for all the four combinations of (d_D, d_V) are

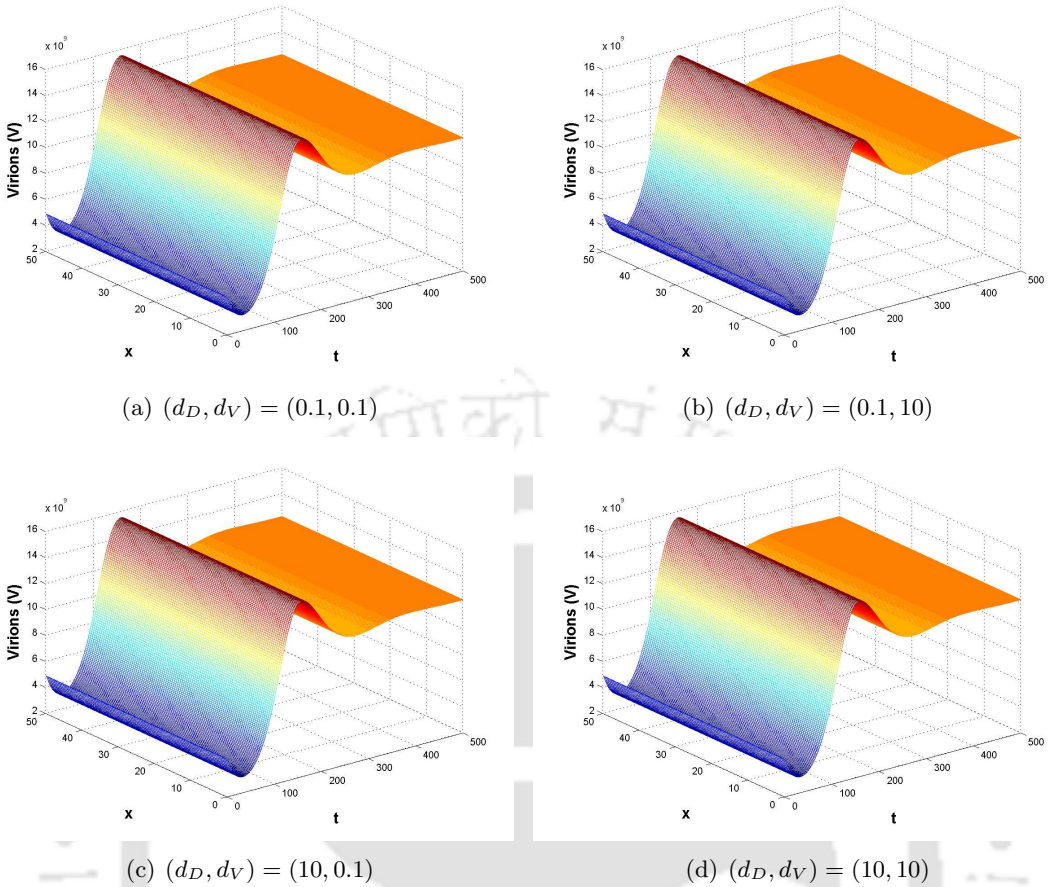

(a) $(d_D, d_V) = (0.1, 0.1)$ (b) $(d_D, d_V) = (0.1, 10)$

(c) $(d_D, d_V) = (10, 0.1)$ (d) $(d_D, d_V) = (10, 10)$

Figure 6.3: Dynamics of virions (V) when $R_0 = 3.0482 > 1$ for four different sets of (d_D, d_V).

very similar to each other in the long run. Similar results can be observed for the other variables H, I and D and are not presented here.

We now compare the NSFD scheme with a standard finite difference (SFD) scheme using the same discrete boundary conditions. This comparison is carried out to illustrate the advantage of the NSFD method over the SFD scheme outlined below,

$$\begin{aligned}
\frac{H_n^{m+1} - H_n^m}{\Delta t} &= s - \mu H_n^m - k H_n^m V_n^m, \\
\frac{I_n^{m+1} - I_n^m}{\Delta t} &= k H_n^m V_n^m - \delta I_n^m, \\
\frac{D_n^{m+1} - D_n^m}{\Delta t} &= d_D \frac{D_{n+1}^m - 2D_n^m + D_{n-1}^m}{(\Delta x)^2} + a I_n^m - (\beta + \delta) D_n^m, \\
\frac{V_n^{m+1} - V_n^m}{\Delta t} &= d_V \frac{V_{n+1}^m - 2V_n^m + V_{n-1}^m}{(\Delta x)^2} + \beta D_n^m - c V_n^m.
\end{aligned} \tag{6.5.1}$$

We again examine the case for $R_0 > 1$. We choose the diffusion coefficients to be $d_D = 0.25$ and $d_V = 0.1$ along with the domain $\Omega = [0, 50]$, time window of 100 days and grid size of

$\Delta x = 0.5$, $\Delta t = 0.4$. The initial conditions used is $H(x,0) = 10^9$, $I(x,0) = 100 \times \exp(-x)$, $D(x,0) = 100 \times \exp(-x)$ and $V(x,0) = 100 \times \exp(-x)$ where the exponential form of the initial condition for I, D and V is motivated by [45, 54]. The dynamics for all the four variables under both the schemes, namely, the NSFD scheme (6.3.1) and the SFD scheme (6.5.1) are given in Figure 6.4. The left hand side of the figures clearly show that the positivity of the solutions of the model (6.1.1) is preserved under the NSFD scheme, but fails to preserve the positivity under the SFD scheme, as is evident from the right hand side figures of Figure 6.4. Also we would like to note that even if we simulate the NSFD scheme for a much longer period of time than 100 days it is observed that the stability of E_i is preserved.

6.6 Conclusion

A spatiotemporal model for HBV infection propagation is proposed and analyzed under the assumption that the HBV DNA-containing capsids and virions exhibit Fickian diffusion, whereas the hepatocytes, both uninfected as well as infected do not exhibit any such spatial mobility. A non-diffusive HBV infection model is extended to incorporate this diffusivity through a reaction-diffusion model. The uninfected and infected steady states are shown to be globally asymptotically stable provided the basic reproduction number $R_0 \leq 1$, and $R_0 > 1$, respectively. The continuous model is discretized using a NSFD scheme and results for global stability are obtained in terms of R_0, similar to the continuous model. More specifically, the number of steady states and the conditions for their stability are identical in case of both the continuous and discrete models. Another crucial observation, regarding the advantage of the NSFD scheme is that the positivity of solutions of the continuous model is preserved, independent of the initial condition as well as the grid sizes. Finally, numerical illustrations are provided to support the theoretical findings.

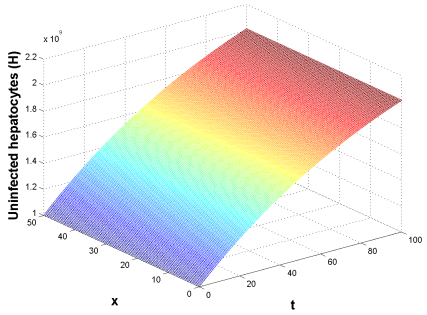

(a) NSFD Scheme

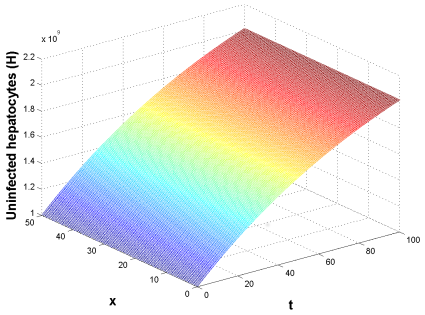

(b) SFD Scheme

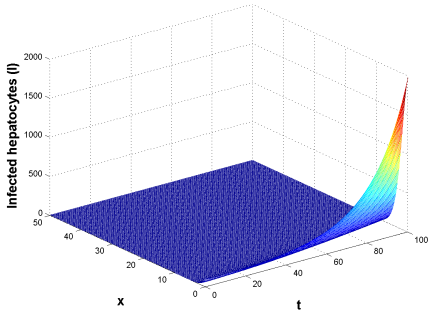

(c) NSFD Scheme

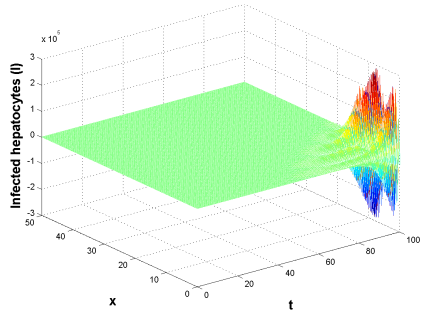

(d) SFD Scheme

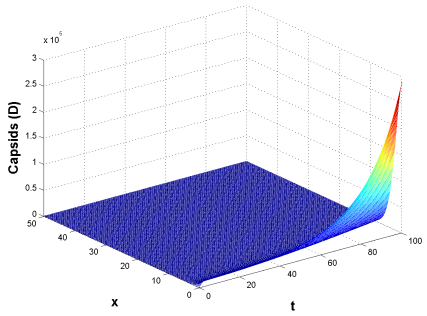

(e) NSFD Scheme

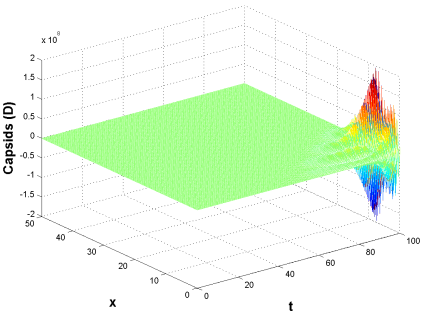

(f) SFD Scheme

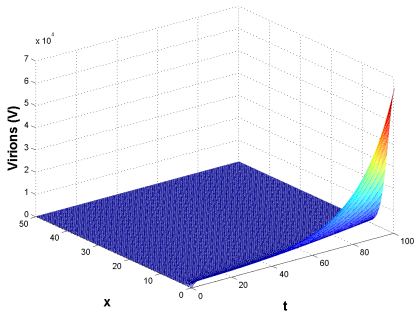

(g) NSFD Scheme

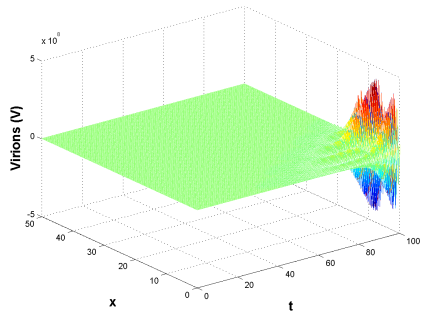

(h) SFD Scheme

Figure 6.4: Graphs of the numerical solutions of the NSFD Scheme and the SFD Scheme when $R_0 = 3.0482 > 1$.

Chapter 7

Conclusion and Future Directions

In this study, we have proposed and analyzed several mathematical models for in vivo dynamics of hepatitis B virus (HBV) infection.

In Chapter 2, we have examined a mathematical model for HBV infection proposed by Murray et al. [7], which incorporates the dynamics of infected hepatocytes, the number of intracellular HBV DNA-containing capsids and the virions with the homeostatic mechanism of the liver. We have analyzed the stability of the uninfected and infected steady states and obtained the conditions for stability in terms of the basic reproduction number R_0. We have modified the model by incorporating a delay in the production of intracellular HBV DNA-containing capsids from infected hepatocytes to see if this delay have any effect on the dynamics. It was shown that this delay does not affect the local stability of the system.

In Chapter 3, we have extended the model by incorporating an equation for the uninfected hepatocytes in the model instead of taking into account the homeostatic mechanism of the liver and analyzed the dynamics of the HBV infection. We have proved the conditions for local and global stability of both the uninfected and infected steady states in terms of the basic reproduction number.

In Chapter 4, we have incorporated time lags in the extended model to encompass the intracellular delay in the production of the productively infected hepatocytes and in the production of the matured capsids to find whether these delays have any effect on the overall dynamics of the system. Two models, one with a one-delay and the other with two-delays were analyzed for global properties in terms of the basic reproduction number. By constructing the appropriate Lyapunov functions, it was shown that the uninfected (infected) steady state is globally asymptotically stable when the basic reproduction number is less than or equal to (more than) one for both the one-delay and two-delay models.

In Chapter 5, a model for combination therapy of pegylated interferon and lamivudine was presented. A critical drug efficacy in terms of the parameters of the model comprising of coupled

ordinary differential equations was obtained. The dynamics of viral load was greatly impacted by the relation of the efficacies of the individual drugs vis-a-vis the critical efficacy. A control problem was formulated and solved numerically to obtain the optimal therapeutic regimen keeping in mind both biomedical goals and cost constraints.

In Chapter 6, a diffusion driven model for HBV infection, taking into account the spatial mobility of both the HBV and the HBV DNA-containing capsids was presented. The global stability for the continuous model was discussed in terms of the basic reproduction number. The analysis was further carried out on a discretized version of the model. A non-standard finite difference (NSFD) scheme was introduced and the global stability properties of the discretized model were studied. The results were numerically illustrated for the dynamics and stability of the various populations in addition to demonstrating the advantages of the usage of NSFD method over the standard finite difference (SFD) scheme.

Some of the possible future directions of this work are briefly outlined below.

1. Sampling Based Analysis:

   A sampling based analysis of the model will be carried out. A large number of parameters will be generated using the Latin hypercube sampling [97]. The sample parameters will be generated from a multivariate normal distribution with a specified mean vector $\mathbf{m}$ and covariance matrix $\mathbf{\Sigma}$ [98],

   $$\phi_{\mathbf{m},\mathbf{\Sigma}} = \frac{1}{(2\pi)^{d/2}\,|\mathbf{\Sigma}|^{1/2}} \exp\left(-\frac{1}{2}(\mathbf{x}-\mathbf{m})^{\top}\mathbf{\Sigma}^{-1}(\mathbf{x}-\mathbf{m})\right).$$

   This is due to the fact that specific patient based data is not available, but the distribution parameters for patient data are publicly available. The parameter sets generated will then be used to check for consistency (in terms of percentages with uninfected and infected steady states being locally and globally stable) with response rates in case of actual patients.

2. Modeling Liver Cirrhosis and HCC:

   We plan to incorporate long term dynamics of HBV to encapsulate the full course of HBV infection and the likelihood of development of liver cirrhosis and HCC. These long term conditions are random in nature and will be modelled by stochastic birth and death process as well as mutation (on the lines of [68]). The change in the number of cancerous cells $C(t)$ at time t for all the three process will be modelled as a combination of a random number $\mathcal{P}(\lambda)$ generated from a Poisson distribution with parameter λ and a random number generated from a standard normal distribution $\mathcal{N}(0,1)$.

Bibliography

[1] S.M. Ciupe, R.M. Ribeiro, P.W. Nelson & A.S. Perelson, Modeling the mechanisms of acute hepatitis B virus infection. *Journal of Theoretical Biology*, 247(1): 23-35, 2007.

[2] S.M. Ciupe, R.M. Ribeiro, P.W. Nelson, G. Dusheiko & A.S. Perelson, The role of cells refractory to productive infection in acute hepatitis B viral dynamics. *Proceedings of the National Academy of Sciences of the United States of America*, 104(12): 5050-5055, 2007.

[3] S.A. Whalley, J.M. Murray, D. Brown, G.J.M. Webster, V.C. Emery, G.M. Dusheiko & A.S. Perelson, Kinetics of acute hepatitis B virus infection in humans. *The Journal of Experimental Medicine*, 193(7): 847-853, 2001.

[4] R.M. Ribeiro, A. Lo & A.S. Perelson, Dynamics of hepatitis B virus infection. *Microbes and Infection*, 4(8): 829-835, 2002.

[5] S. Lewin, T. Walters & S. Locarnini, Hepatitis B treatment: rational combination chemotherapy based on viral kinetic and animal model studies. *Antiviral Research*, 55(3): 381-396, 2002.

[6] H. Dahari, E. Shudo, R.M. Ribeiro & A.S. Perelson, Modeling complex decay profiles of hepatitis B virus during antiviral therapy. *Hepatology*, 49(1): 32-38, 2009.

[7] J.M. Murray, R.H. Purcell & S.F. Wieland, The half-life of hepatitis B virions. *Hepatology*, 44(5): 1117-1121, 2006.

[8] T. Asselah, O. Lada, R. Moucari, M. Martinot, N. Boyer & P. Marcellin, Interferon therapy for chronic hepatitis B. *Clinics In Liver Disease*, 11(4): 839-849, 2007.

[9] S.W. Schalm, J. Heathcote, J. Cianciara, G. Farrell, M. Sherman, B. Willems, A. Dhillon, A. Moorat, J. Barber & D.F. Gray, Lamivudine and alpha interferon combination treatment of patients with chronic hepatitis B infection: a randomised trial. *Gut*, 46(4): 562-568, 2000.

[10] A. Severini, X.Y. Liu, J.S. Wilson & D.L. Tyrrell, Mechanism of inhibition of duck hepatitis B virus polymerase by (-)-beta-L-2',3'-dideoxy-3'-thiacytidine. *Antimicrobial Agents and Chemotherapy*, 39(7): 1430-1435, 1995.

[11] F. Zoulim, Mechanism of viral persistence and resistance to nucleoside and nucleotide analogs in chronic Hepatitis B virus infection. *Antiviral Research*, 64(1): 1-15, 2004.

[12] M.A. Nowak, S. Bonhoeffer, A.M. Hill, R. Boehme, H.C. Thomas & H. McDade, Viral dynamics in hepatitis B virus infection. *Proceedings of the National Academy of Sciences of the United States of America*, 93(9): 4398-4402, 1996.

[13] L. Min, Y. Su & Y. Kuang, Mathematical analysis of a basic virus infection model with application to HBV infection. *Rocky Mountain Journal of Mathematics*, 38(5): 1573-1585, 2008.

[14] K. Wang, A. Fan & A. Torres, Global properties of an improved hepatitis B virus model. *Nonlinear Analysis: Real World Applications*, 11(4): 3131-3138, 2010.

[15] S.A. Gourley, Y. Kuang & J.D. Nagy, Dynamics of a delay differential equation model of hepatitis B virus infection. *Journal of Biological Dynamics*, 2(2): 140-153, 2008.

[16] S. Hews, S. Eikenberry, J.D. Nagy & Y. Kuang, Rich dynamics of a hepatitis B viral infection model with logistic hepatocyte growth. *Journal of Mathematical Biology*, 60(4): 573-590, 2010.

[17] J. Li, K. Wang & Y. Yang, Dynamical behaviors of an HBV infection model with logistic hepatocyte growth. *Mathematical and Computer Modelling*, 54(1-2): 704-711, 2011.

[18] S. Eikenberry, S. Hews, J.D. Nagy & Y. Kuang, The dynamics of a delay model of hepatitis B virus infection with logistic hepatocyte growth. *Mathematical Biosciences and Engineering*, 6(2): 283-299, 2009.

[19] X. Chen, L. Min, Y. Zheng, Y. Kuang & Y. Ye, Dynamics of acute hepatitis B virus infection in chimpanzees. *Mathematics and Computers in Simulation*, 96: 157-170, 2014.

[20] Y. Yu, J.J. Nieto, A. Torres & K. Wang, A viral infection model with a nonlinear infection rate. *Boundary Value Problems*, 2009(Article ID 958016): 19 pages, 2009.

[21] S.-H. Cheng, L. Mai, F.-Q. Zhu, X.-F. Pan, H.-X. Sun, H. Cao, X. Shu, W.-M. Ke, G. Li & Q.-H. Xu, Influence of chronic HBV infection on superimposed acute hepatitis E. *World Journal of Gastroenterology*, 19(35): 5904-5909, 2013.

[22] F. Zoulim, Does occult HBV infection have an impact on the evolution of chronic hepatitis C ? *Journal of Hepatology*, 59(4): 646-647, 2013.

[23] M.A. Nowak & C.R.M. Bangham, Population dynamics of immune responses to persistent viruses. *Science*, 272(5258): 74-79, 1996.

[24] J. Pang, J. Cui & J. Hui, The importance of immune responses in a model of hepatitis B virus. *Nonlinear Dynamics*, 67(1): 723-734, 2012.

[25] J. Wang & X. Tian, Global stability of a delay differential equation of hepatitis B virus infection with immune response. *Electronic Journal of Differential Equations*, 2013(94): 1-11, 2013.

[26] S.R. Lewin, R.M. Ribeiro, T. Walters, G.K. Lau, S. Bowden, S. Locarnini & A.S. Perelson, Analysis of hepatitis B viral load decline under potent therapy: complex decay profiles observed. *Hepatology*, 34(5): 1012-1020, 2001.

[27] H. Dahari, A. Lo, R.M. Ribeiro & A.S. Perelson, Modeling hepatitis C virus dynamics: Liver regeneration and critical drug efficacy. *Journal of Theoretical Biology*, 247(2): 371-381, 2007.

[28] A.U. Neumann, N.P. Lam, H. Dahari, D.R. Gretch, T.E. Wiley, T.J. Layden & A.S. Perelson, Hepatitis C viral dynamics in vivo and the antiviral efficacy of interferon-alpha therapy. *Science*, 282: 103-107, 1998.

[29] S. Lenhart & J.T. Workman, Optimal control applied to biological models. *Chapman and Hall/CRC*, 2007.

[30] G.W. Swan, Role of optimal control theory in cancer chemotherapy. *Mathematical Biosciences*, 101(2): 237-284, 1990.

[31] J.M. Murray, Some optimal control problems in cancer chemotherapy with a toxicity limit. *Mathematical Biosciences*, 100(1): 49-67, 1990.

[32] J.M. Murray, Optimal control for a cancer chemotherapy problem with general growth and loss functions. *Mathematical Biosciences*, 98(2): 273-287, 1990.

[33] L.G. de Pillis, W. Gu, K.R. Fister, T. Head, K. Maples, A. Murugan, T. Neal & K. Yoshida, Chemotherapy for tumors: An analysis of the dynamics and a study of quadratic and linear optimal controls. *Mathematical Biosciences*, 209(1): 292-315, 2007.

[34] K.R. Fister & J.C. Panetta, Optimal control applied to competing chemotherapeutic cell-kill strategies. *SIAM Journal of Applied Mathematics*, 63(6): 1954-1971, 2003.

[35] I.Y.S. Chavez, R. Morales-Menendez & S.O.M. Chapa, Glucose optimal control system in diabetes treatment. *Applied Mathematics and Computation*, 209(1): 19-30, 2009.

[36] S. Nanda, H. Moore & S. Lenhart, Optimal control of treatment in a mathematical model of chronic myelogenous leukemia. *Mathematical Biosciences*, 210(1): 143-156, 2007.

[37] D. Kirschner, S. Lenhart & S. Serbin, Optimal control of the chemotherapy of HIV. *Journal of Mathematical Biology*, 35(7): 775-792, 1997.

[38] H.R. Joshi, Optimal control of an HIV immunology model. *Optimal Control Applications and Methods*, 23(4): 199-213, 2002.

[39] B.M. Adams, H.T. Banks, M. Davidian, H.-D. Kwon, H.T. Tran, S.N. Wynne & E.S. Rosenberg, HIV dynamics: modeling, data analysis, and optimal treatment protocols. *Journal of Computational and Applied Mathematics*, 184(1): 10-49, 2005.

[40] R.F. Stengel, Mutation and control of the human immunodeficiency virus. *Mathematical Biosciences*, 213(2): 93-102, 2008.

[41] S.P. Chakrabarty & H.R. Joshi, Optimally controlled treatment strategy using interferon and ribavirin for hepatitis C. *Journal of Biological Systems*, 17(1): 97-110, 2009.

[42] S.P. Chakrabarty, Optimal efficacy of ribavirin in the treatment of hepatitis C. *Optimal Control Applications and Methods*, 30(6): 594-600, 2009.

[43] G. Pachpute & S.P. Chakrabarty, Dynamics of hepatitis C under optimal therapy and sampling based analysis. *Communications in Nonlinear Science and Numerical Simulation*, 18(8): 2202-2212, 2013.

[44] N.K. Martin, A.B. Pitcher, P. Vickerman, A. Vassall & M. Hickman, Optimal control of hepatitis C antiviral treatment programme delivery for prevention amongst a population of injecting drug users. *PLoS ONE*, 6(8): e22309, 2011.

[45] K. Wang & W. Wang, Propagation of HBV with spatial dependence. *Mathematical Biosciences*, 210(1): 78-95, 2007.

[46] N.F. Britton, Essential Mathematical Biology. *Springer-Verlag, London*, 2003.

[47] G.A. Funk, V.A.A. Jansen, S. Bonhoeffer & T. Killingback, Spatial models of virus-immune dynamics. *Journal of Theoretical Biology*, 233(2): 221-236, 2005.

[48] S.A. Gourley & J.W.H. So, Dynamics of a food-limited population model incorporating nonlocal delays on a finite domain. *Journal of Mathematical Biology*, 44(1): 49-78, 2002.

[49] K. Wang, W. Wang & S. Song, Dynamics of an HBV model with diffusion and delay. *Journal of Theoretical Biology*, 253(1): 36-44, 2008.

[50] R. Xu & Z. Ma, An HBV model with diffusion and time delay. *Journal of Theoretical Biology*, 257(3): 499-509, 2009.

[51] W. Shaoli, F. Xinlong & H. Yinnian, Global asymptotical properties for a diffused HBV infection model with CTL immune response and nonlinear incidence. *Acta Mathematica Scientia*, 31(5): 1959-1967, 2011.

[52] K. Hattaf & N. Yousfi, Global stability for reaction-diffusion equations in biology. *Computers and Mathematics with Applications*, 66(8): 1488-1497, 2013.

[53] K. Hattaf & N. Yousfi, A generalized HBV model with diffusion and two delays. *Computers and Mathematics with Applications*, 69(1): 31-40, 2015.

[54] W. Qin, L. Wang & X. Ding, A non-standard finite difference method for a hepatitis B virus infection model with spatial diffusion. *Journal of Difference Equations and Applications*, 20(12): 1641-1651, 2014.

[55] D.T. Dimitrov & H.V. Kojouharov, Positive and elementary stable nonstandard numerical methods with applications to predatorprey models. *Journal of Computational and Applied Mathematics*, 189(1-2): 98-108, 2006.

[56] L.I.W. Roeger, Dynamically consistent discrete Lotka-Volterra competition models derived from nonstandard finite-difference schemes. *Discrete and Continuous Dynamical Systems Series B*, 9: 415-429, 2008.

[57] S.M. Moghadas, M.E. Alexander, B.D. Corbett & A.B. Gumel, A positivity-preserving Mickens-type discretization of an epidemic model. *Journal of Difference Equations and Applications*, 9(11): 1037-1051, 2003.

[58] D. Ding, Q. Ma & X. Ding, A non-standard finite difference scheme for an epidemic model with vaccination. *Journal of Difference Equations and Applications*, 19(2): 179-190, 2013.

[59] D. Ding & X. Ding, Dynamic consistent non-standard numerical scheme for a dengue disease transmission model. *Journal of Difference Equations and Applications*, 20(3): 492-505, 2014.

[60] P.K. Srivastava, M. Banerjee & P. Chandra, Modeling the drug therapy for HIV infection. *Journal of Biological Systems*, 17(2): 213-223, 2009.

[61] P.K. Srivastava & P. Chandra, Modeling the dynamics of HIV and CD4+ T cells during primary infection. *Nonlinear Analysis: Real World Applications*, 11(2): 612-618, 2010.

[62] L. Cai, X. Li, M. Ghosh & B. Guo, Stability analysis of an HIV/AIDS epidemic model with treatment. *Journal of Computational and Applied Mathematics*, 229(1): 313-323, 2009.

[63] H.I. Freedman, S. Ruan & M. Tang M, Uniform persistence and flows near a closed positively invariant set. *Journal of Dynamics and Differential Equations*, 6(4): 583-600, 1994.

[64] G. Butler, H.I. Freedman & P. Waltman, Uniformly persistent systems. *Proceedings of the American Mathematical Society*, 96(3): 425-430, 1986.

[65] S. Busenberg & P. van den Driessche, Analysis of a disease transmission model in a population with varying size. *Journal of Mathematical Biology*, 28(3): 257-270, 1990.

[66] S. Banerjee, Immunotherapy with interleukin-2: A study based on mathematical modeling. *International Journal of Applied Mathematics and Computer Science*, 18(3): 389-398, 2008.

[67] S. Banerjee & R.R. Sarkar RR, Delay-induced model for tumor-immune interaction and control of malignant tumor growth. *Bio Systems*, 91(1): 268-288, 2008.

[68] S.P. Chakrabarty & J.M. Murray, Modelling hepatitis C virus infection and the development of hepatocellular carcinoma. *Journal of Theoretical Biology*, 305: 24-29, 2012.

[69] P.K. Srivastava, M. Banerjee & P. Chandra, A primary infection model for HIV and immune response with two discrete time delays. *Differential Equations and Dynamical Systems*, 18(4): 385-399, 2010.

[70] M.Y. Li & J.S. Muldowney, A geometric approach to global-stability problems. *SIAM Journal on Mathematical Analysis*, 27(4): 1070-1083, 1996.

[71] L. Wang & M.Y. Li, Mathematical analysis of the global dynamics of a model for HIV infection of CD4+ T cells. *Mathematical Biosciences*, 200(1): 44-57, 2006.

[72] M.Y. Li & L. Wang, A criterion for stability of matrices. *Journal of Mathematical Analysis and Applications*, 225(1): 249-264, 1998.

[73] Y. Li & J.S. Muldowney, On Bendixson's criterion. *Journal of Differential Equations*, 106(1): 27-39, 1993.

[74] S. Banerjee, R. Keval & S. Gakkhar, Modeling the dynamics of Hepatitis C virus with combined antiviral drug therapy: Interferon and Ribavirin. *Mathematical Biosciences*, 245(2): 235-248, 2013.

[75] A.V.M. Herz, S. Bonhoeffer, R.M. Anderson, R.M. May & M.A. Nowak, Viral dynamics in vivo: Limitations on estimates of intracellular delay and virus decay. *Proceedings of the National Academy of Sciences af the United States of America*, 93(14): 7247-7251, 1996.

[76] T. Kajiwara, T. Sasaki & Y. Takeuchi, Construction of Lyapunov functionals for delay differential equations in virology and epidemiology. *Nonlinear Analysis: Real World Applications*, 13(4): 1802-1826, 2012.

[77] G. Huang, W. Ma & Y. Takeuchi, Global properties for virus dynamics model with Beddington-DeAngelis functional response. *Applied Mathematics Letters*, 22(11): 1690-1693, 2009.

[78] P.W. Nelson & A.S. Perelson, Mathematical analysis of delay differential equation models of HIV-1 infection. *Mathematical Biosciences*, 179(1): 73-94, 2002.

[79] M.Y. Li & H. Shu, Impact of intracellular delays and target-cell dynamics on in vivo viral infections. *SIAM Journal on Applied Mathematics*, 70(7): 2434-2448, 2010.

[80] R. Xu, Global dynamics of an HIV-1 infection model with distributed intracellular delays. *Computers and Mathematics with Applications*, 61(9): 2799-2805, 2011.

[81] A. Korobeinikov, Global properties of basic virus dynamics models. *Bulletin of Mathematical Biology*, 66(4): 879-883, 2004.

[82] K.A. Pawelek, S. Liu, F. Pahlevani & L. Rong, A model of HIV-1 infection with two time delays: Mathematical analysis and comparison with patient data. *Mathematical Biosciences*, 235(1): 98-109, 2012.

[83] X. Wang, A. Elaiw & X. Song, Global properties of a delayed HIV infection model with CTL immune response. *Applied Mathematics and Computation*, 218(18): 9405-9414, 2012.

[84] T.J. Liang, Hepatitis B: The virus and disease. *Hepatology*, 49(5): S13-S21, 2009.

[85] H. Guo, D. Jiang, T. Zhou, A. Cuconati, T.M. Block & J.-T. Guo, Characterization of the intracellular deproteinized relaxed circular DNA of hepatitis B virus: An intermediate of covalently closed circular DNA formation. *Journal of Virology*, 81(22): 12472-12484, 2007.

[86] B.M. Adams, H.T. Banks, H.-D. Kwon & H.T. Tran, Dynamic multidrug therapies for HIV: Optimal and STI control approaches. *Mathematical Bioscience and Engineering*, 1(2): 223-241, 2004.

[87] K.R. Fister, S. Lenhart & J.S. McNally, Optimizing chemotherapy in an HIV model. *Electronic Journal of Differential Equations*, 1998(32): 1-12, 1998.

[88] W.H. Fleming & R.W. Rishel, Deterministic and stochastic optimal control. *Springer-Verlag*, 1975.

[89] W. Garira, S.D. Musekwa & T. Shiri, Optimal control of combined therapy in a single strain HIV-1 model. *Electronic Journal of Differential Equations*, 2005(52): 1-22, 2005.

[90] S.P. Chakrabarty & S. Banerjee, A control theory approach to cancer remission aided by an optimal therapy. *Journal of Biological Systems*, 18(1): 75-91, 2010.

[91] T. Burden, J. Ernstberger & K.R. Fister, Optimal control applied to immunotherapy. *Discrete and Continous Dynamical Systems Series B*, 4(1): 135-146, 2004.

[92] D.E. Kirk, Optimal control theory: an introduction. *Dover Publications*, 2004.

[93] R.E. Mickens, Dynamic consistency: a fundamental principle for constructing nonstandard finite difference schemes for differential equations. *Journal of Difference Equations and Applications*, 11(7): 645-653, 2005.

[94] R.E. Mickens, Nonstandard Finite Difference Models of Differential Equations. *World Scientific, River Edge, New Jersey*, 1994.

[95] R.E. Mickens, Applications of Nonstandard Finite Difference Scheme. *World Scientific, River Edge, New Jersey*, 2000.

[96] R.E. Mickens, Advances in the Applications of Nonstandard Finite Difference Schemes. *World Scientific, River Edge, New Jersey*, 2005.

[97] G. Pachpute & S.P. Chakrabarty, Analysis of hepatitis C viral dynamics using Latin hypercube sampling. *Communications in Nonlinear Science and Numerical Simulation*, 17(12): 5125-5130, 2012.

[98] P. Glasserman, Monte Carlo methods in financial engineering. *Springer*, 2004.

List of Accepted or Communicated Papers

Based on the work in this thesis, the following research articles have been accepted or communicated.

1. Kalyan Manna & Siddhartha P. Chakrabarty, "Dynamics and analysis of a model for chronic hepatitis B infection", accepted in *Journal of Interdisciplinary Mathematics*.

2. Kalyan Manna & Siddhartha P. Chakrabarty, "Chronic hepatitis B infection and HBV DNA-containing capsids: Modeling and analysis", *Communications in Nonlinear Science and Numerical Simulation*, 22(1-3): 383-395, 2015.

3. Kalyan Manna & Siddhartha P. Chakrabarty, "Global stability of one and two discrete delay models for chronic hepatitis B infection with HBV DNA-containing capsids", *Computational and Applied Mathematics*, (DOI: 10.1007/s40314-015-0242-3), 2015.

4. Kalyan Manna & Siddhartha P. Chakrabarty, "Combination therapy of pegylated interferon and lamivudine and optimal controls for chronic hepatitis B infection", *Communicated*.

5. Kalyan Manna & Siddhartha P. Chakrabarty, "Global stability and a non-standard finite difference scheme for a diffusion driven HBV model with capsids", *Journal of Difference Equations and Applications*, 21(10): 918-933, 2015.